University of Windsor

Scholarship at UWindsor

Electronic Theses and Dissertations

Theses, Dissertations, and Major Papers

2002

Electrical conduction in dielectric films.

Riazuddin R. Shaikh
University of Windsor

Recommended Citation

INFORMATION TO USERS

This manuscript has been reproduced from the microfilm master. UMI films the text directly from the original or copy submitted. Thus, some thesis and dissertation copies are in typewriter face, while others may be from any type of computer printer.

The quality of this reproduction is dependent upon the quality of the copy submitted. Broken or indistinct print, colored or poor quality illustrations and photographs, print bleedthrough, substandard margins, and improper alignment can adversely affect reproduction.

In the unlikely event that the author did not send UMI a complete manuscript and there are missing pages, these will be noted. Also, if unauthorized copyright material had to be removed, a note will indicate the deletion.

Oversize materials (e.g., maps, drawings, charts) are reproduced by sectioning the original, beginning at the upper left-hand corner and continuing from left to right in equal sections with small overlaps.

ELECTRICAL CONDUCTION IN DIELECTRIC FILMS

By

Riaz R Shaikh

A Thesis
Submitted to the Faculty of Graduate Studies and Research Through
the Department of Electrical and Computer Engineering
in Partial Fulfillment of the Requirements
for the Degree of
Master of Applied Science
at the University of Windsor

Windsor, Ontario, Canada
2002

0-612-75805-2

Canada

961999

ABSTRACT.

Polyimides as a class of polymers have excellent electrical, mechanical and chemical properties, which makes them ideal for use as insulators.

This dissertation deals with the studies of charge storage, decay and conduction currents in polyimide and polyimide-FEP fluoropolymer dielectric materials. These studies would fill and complement the available electrical data and provide design data for the polyimide user.

Absorption and Desorption currents are studied for polyimide (HN500 Film) and polyimide – FEP fluoropolymer (150FN019 Film) under the influence of varying parameters such as field, temperature and electrode material. The conduction currents were also studied over a temperature range of 200 ^{0}C and fields up to 100KVcm^{-1}. Attempts were then made to identify basic mechanisms that govern the absorption and the conduction currents in these materials.

The results on polyimide (HN500 Film) shows that the charging and discharging follow a mirror image of each other for temperatures up to 90 ^{0}C and are dissimilar for all other temperature ranges investigated. The low frequency dielectric loss peaks are seen to move to higher frequencies possibly due to dipolar processes.

Ionic jump distances were evaluated from the results of conduction current and are found to be increasing with temperature with a value in the range of 5-9 nm. Ionic conduction seems to be the operative mechanism when viewed in the light of the available conduction theories. The resistivity is found to be decreasing from 5.59 x 10^{16} Ω cm at 90 ^{0}C to 3.31 x 10^{12} Ω cm at 200 ^{0}C.

The results on polyimide –FEP fluoropolymer (150FN019 Film) shows that the charging and discharging currents are dissimilar for all the temperature ranges investigated. The low frequency dielectric loss factor in polyimide–FEP fluoropolymer gives two curves, for regime 0 $\leq$ T $\leq$ 120 ^{0}C and 120 $\leq$ T $\leq$ 200 ^{0}C. For temperatures up to 90 ^{0}C one broad peak is observed at frequency around 3 x 10^{-4} Hz. For temperatures (>120 ^{0}C) the magnitude of the

loss factor increases by an order of magnitude and no peaks are observed suggesting an interfacial polarization.

The activation energy of 0.76 eV and the ionic jump distance in the range 19-28 nm have been evaluated from analysis of the conduction currents. The resistivity is calculated and is found to be decreasing from 1.29×10^{17} Ω cm at 90 ^{0}C to 5.25×10^{12} Ω cm at 200 ^{0}C.

ACKNOWLEDGEMENTS

TABLE OF CONTENTS

List of Tables

List of Figures

Chapter 1

INTRODUCTION

1.1   AN OVERVIEW

The highly aromatic nature of the polyimide polymer contributes to its extremely good thermal and radiation resistance. In addition it has excellent electrical as well as mechanical properties and is chemically stable. These polyimidies have found increasing applications as insulating material in transformers, motors and generators since the last two decades. In present day polyimide is projected as the most important polymer having the potential for the microelectronics applications because of its good electric properties, high temperature stability, relatively good planarization and easy processing.

These polymer materials have the capability to store charges when they are under the influence of applied electric field. It is important to know the amount of the charges that are stored under different temperature and electric field and rate of decay of the charge. The conduction current due to the applied electric field and discharging current flowing after removal of applied voltage are of to be taken into consideration in designing if it is used as insulators. This dissertation is concerned with the study of the charge storage/decay that govern the conduction currents in polyimide and polyimide-FEP fluoropolymer dielectric material.

1.2   SCOPE OF WORK AND OBJECTIVE

This study is concerned with the mechanisms that govern the absorption and the conduction current in polyimides. The studies considered are outlined below

1)   The charging and discharging currents in polyimide film (Kapton® HN500 Film) are studied under the influence of various parameters such as field, temperature and electrode materials. The low frequency dielectric loss (ε'') is obtained using Hamons approximation. The conduction currents are also studied and the process examined in the light of available conduction mechanisms.

2)   The charging and discharging currents in polyimide –FEP fluoropolymer film (Kapton®150FN019 Film) are studied and the influences of various parameters of field,

field, temperature and electrode material are noted. The conduction currents and low frequency dielectric loss are also studied.

The objective of this dissertation is to study basic mechanisms of conduction and decay in polyimides. These studies fill and complement the available electrical data in the literature, provide design data for the polyimide user and provide insight into reliability concerns arising due to their use in VLSI processes.

The two reliability concerns affecting their use in VLSI processes is the charging of the polyimide /silicon dioxide surface leading to the inversion of the underlying silicon surface and the corrosion of metal electrodes. An integrated circuit is designed such that the metal polyimide oxide silicon (MPOS) capacitor in the field region does not form an inversion layer in the semiconductor. However, if the polyimide is more conductive than the oxide then charge can be transported through the polyimide to the polyimide/oxide interface, which could lead to surface inversion [1,2]. The electrochemical corrosion reaction has been studied by Smith [3]. Polyimide conductivity i.e. bulk, ionic or surface/interface conductivity is thought to be as one of the potential mechanism that causes device failure [4].

The ratio of dielectric constant to loss factor is known as the dissipation factor (tanδ). The dielectric constant and dissipation factor of the material is a function of temperature, water content, impurity and frequency of applied field. These properties of the materials should be studied and relations must be known in the operating range. It has also been shown that the signal is distorted at the interfaces due to the impedance mismatch. The signal propagation delay time constant is roughly given by $\varepsilon^{1/2}/C$ [5] where C is the speed of the light. Thus it is seen clearly that the whole dielectric spectrum of an insulating material and the fundamental processes are vital considerations for the design purposes.

1.3   ORGANIZATION OF THESIS

Chapter 2 reviews and provides insight into some of fundamental theories of charging, discharging, conduction currents and the theory of dielectric loss.

In **Chapter 3** the experimental techniques and details of experiment are discussed. The sample preparation, the thermal protocol and the experimental arrangements are also discussed.

In **Chapter 4** the results of charging and discharging currents in polyimide (HN500 Film) and the low frequency dielectric loss are discussed under the influence of field, temperature and electrode materials.

In **Chapter 5** the results of conduction current in polyimide (HN500 Film) are studied for electric field strength up to 10 MVm^{-1} and the processes thought to be occurring are evaluated and put forward in the light of available conduction theory.

In **Chapter 6** the results of charging and discharging currents and the low frequency dielectric loss factor for polyimide–FEP fluoropolymer (150FN019 Film) are discussed.

Chapter 7 presents the results of conduction current in polyimide–FEP fluoropolymer (150FN019 Film) for field up to $10MVm^{-1}$ and the process is examined in the light of Schottky emissions, Poole-Frenkel effect and ionic hopping theories.

Chapter 8 summaries the conclusions and includes suggestions for future work.

Appendix 1 summarizes the properties of the materials investigated and their applications.

Appendix 2 compares the properties of polyimide (HN500 Film) and polyimide-FEP fluoropolymer (150FN019 Film) with some inorganic dielectrics.

References are listed at the end.

Chapter 2

FUNDAMENTAL PROCESSES

Polymeric materials are unique because of the range of the structural forms that can be synthesized and the way in which changes can be made in the structure in the local or general way. In contrast to metals in which the electrical field response is one of electronic conduction, polymers responds in a more varied way. For example, polarization phenomena resulting from distortion and alignment of the molecules under the influence of applied field become apparent. In summary, the response of polymers to an electric field can be separated into dielectric properties and bulk conductive properties. The fundamental parameters representing dielectric properties are dielectric constant representing polarization and dielectric loss representing relaxation phenomena. The parameters characterizing bulk conductive properties are dielectric strength representing breakdown and conductivity representing electrical conduction.

2.1   CHARGING AND DISCHARGING CURRENTS

The current, which flows in the external circuit upon application of step voltage to a dielectric material decays with time until steady state is achieved. This current has been termed variously as charging, resorption current [6-9]. If the step voltage is removed and the electrodes short circuited a discharging or absorption current flows and decay with time as t^{-n} according to the power law [10,11,12]

$$I(t) = A(T) t^n \qquad (2.1)$$

Where $I(t)$ is the current at time t, t is the time after application or removal of the external voltage, $A(t)$ is the temperature dependent factor and n is the decay constant.

A number of mechanisms have been proposed to explain this behaviour, the most important of which are

(1)   Dipolar orientation

(2)   Electrode polarization

(3)   Charge injection leading to trapped space charge

(4)   Hopping of charge carriers from one localised state to other

(5)   Tunnelling of charge from the electrodes in empty traps

2.1.1   Concept of Dielectric Polarization

Dielectric polarization arises due to the existence of atomic and molecular forces and appears whenever charges in a material are displaced with respect to one another under the influence of electric field. In a capacitor, the negative charges within the dielectric are displaced toward the positive electrode, while the positive charge shift in the opposite direction. As charges are not free to move in an insulator, restoring forces are activated which either do work, or cause work to be done on the system i.e. energy transferred. On charging a capacitor, the polarization effect opposing the applied electric field draws charges on to the electrode, storing energy. On discharge, this energy is released. As a result of the above interaction certain materials that possess easily polarisable charges will greatly influence the degree of charge that can be stored in the capacitor. The proportional increase in the storage ability of the dielectric with respect to vacuum is defined as the dielectric constant of the material.

The degree of polarization P is related to the dielectric constant ε and the electric field strength is given by [13]

$$P = \varepsilon_0 \, (\varepsilon - 1) \, E \qquad\qquad (2.2)$$

Where P = degree of polarization, ε_0 is the permittivity of free space, ε is the dielectric constant and E is the electric field strength.

The total polarization of a dielectric arises from four sources of charge displacement

a) Electronic Polarization

b) Ionic Polarization

c) Orientational Polarization

d) Interfacial Polarization

The total contribution of polarization to the dielectric constant is therefore a summation of the above

$$P_{total} = P_e + P_i + P_d + P_s \qquad\qquad (2.3)$$

Where P_e is electronic polarization, P_i is the Ionic polarization, P_d is the orientational polarization and P_s is the Interfacial polarization.

a) Electronic Polarization

This effect is common to all materials as it involves distortion of the centre of charge symmetry of the basic atom. Under the influence of an applied field the nucleus of an atom and the negative charge centre of the electron shift creating a dipole. This polarization is small despite the vast number of atoms within the material because the moment arm of the dipoles is very short in the order of nanometer.

b) Ionic Polarization

Ionic displacement is common in ceramic materials, which consists of crystal lattice occupied by cations and anions. Under the influence of an applied electric field dipole moments are created by shifting of these ions towards their respective polarity of the field. The displacement or moment arm of the dipoles can be relatively large in comparison to the electronic displacement and therefore can give rise to a high dielectric constant in some ceramics

c) Orientational Polarization

If the molecules already possess a permanent dipole moment, the moment will tend to be aligned by the applied field to give a net polarization in that direction. The dipoles with out the field are pointing in all directions and continually jumping from one orientation to another as a result of thermal agitation The polarization develops, when the field is applied is relatively small, the resulting net orientations favouring the direction of applied filed .The tendency to revert to random orientations opposes the tendency of the field to align the dipoles and thus allows for polarization to vary in proportion of the applied field. If an electric field E is applied, the orientation polarization will grow to an equilibrium value at which the rate of polarization produced by the field is equal to the rate at which it is opposed by the thermal agitation. The average moment per dipole in the direction of electric field is given by [14]

$$\mu_o = \mu^2 E / KT \tag{2.4}$$

Where μ is the dipole moment, E is the electric field, K is the Boltzman constant and T is the temperature. Therefore the polarizability due to the orientational polarization (α_0) is given by

$$\alpha_0 = \mu^2 / 3KT \tag{2.5}$$

The rate at which the electric field produces polarization from the randomly oriented dipoles is independent of the polarization already created, whereas the rate at which the polarization is destroyed by the random thermal motion must be proportional to the polarization. If τ is the relaxation time of orientation polarization and P is the instantaneous value of polarization then it can be established

$$dP/dt = - P/\tau \qquad (2.6)$$

Integrating the above equation with the condition that the final value of P is Ps [14] we get

$$P = Ps \, [1\text{-exp} \, (\text{-}t/\tau)]$$

$$(2.7)$$

Where Ps is the equilibrium polarization

The relaxation time of orientation polarization varies for the different kinds of polymers.

d) Interfacial Polarization

Electronic, atomic and orientational polarization occurs due to the charges that are locally bound in atoms, molecules, or the structure of the solid. But in addition, charge carriers exists that can migrate for some distance through the dielectric. When the charge are impended in their motion, either because they are trapped in the material or at an interface space charge and microscopic field distortion results. In general, a material is always likely to have regions of nonuniformity and small amount of impurities. Free charge carriers migrating through these regions may be trapped by or pile up against a defect. This effect will create a localised accumulation of charge and give rise to dipole moment. In any case when the structural inhomogeneities between the materials of different dielectric constant and conductivities are present, interfacial polarization is expected to occur.

2.1.2   Electrode Polarization

The process of electrode polarization or blocking also leads to current decay with time. As the carriers of one or both signs are prevented from leaving the specimen and pile up in front of the drain electrode space charge sets up a reverse field which tend to inhibit further charge flow. This effect is very complicated and the current may exhibit a wide variety of time dependence depending on the precise conditions at the electrodes [15,16,17].

2.1.3 Charge injection leading to space charge effect

Under charge injection conditions the result is that the field is reduced at the source electrode and enhanced at the drain. If the source can provide an unlimited supply of carriers at zero field one obtain the full space charge limited decay. The more usual case is that the rate of supply of carrier depends on the field and that some significant trapping takes place in the bulk. So the current density at the source electrode will decrease with time as the field falls. The result is that the current falls as t^{-n} under these conditions [18,19,20]

2.1.4 Hopping of Charge carriers

The trapped carriers in the neutral potential wells occasionally jump from one equilibrium position to another on being thermally activated.

2.1.5 Tunnelling

At high fields the width of potential barrier decreases. As a result the probability of finding an electron on the other side of the potential barrier by quantum mechanical tunnelling increases. The tunnelling process is independent of temperature and the tunnelling current is given by equation

$$I = (e^2 V/h^2 d)(2m^*\phi)^{1/2} \exp [-4\pi d(2m^*\phi)^{1/2}/h] \qquad (2.8)$$

Where I is the tunnelling current, e is the electron charge, V is the voltage, h is the Planks constant, d is the thickness of the film, m^* is the effective mass of charge carrier and ϕ is the potential barrier at the electrode-polymer interface. The experimental results at low temperature do not agree with the theoretically expected tunnelling current curve. Miyoshi and Chino [21] concluded that tunnelling is predominant phenomena in films less than 50-120 nm or at low voltages.

2.2 ELECTRICAL CONDUCTION

The electrical conductivity measurement involves a simple measurement of current as a function of time, temperature, ambient atmosphere and potential. Attempts are then made to relate the conduction to the physical processes thought to occur in the polymer. It has been found that electrical conductivity increases with temperature is a function of time and may vary with the electrical field. Often electrode effects, non-linear current voltage characteristics, changes in time are seen and behavior is often history dependent.

2.2.1 The Charge Carriers

The electrical conductivity of the polymers increases exponentially with increasing temperature. This can be interpreted in terms of classical semiconductor theory to indicate that the intrinsic charge carrier creation occurs as described by conventional Solid-state physics.

a) Intrinsic Charge –Carrier Generation

Materials are often classified on the basis of their electrical properties. They can be classified as metals, semiconductors or insulators depending on the way in which their electrical resistivity changes with temperature. With metals the resistivity increases with temperature, with semiconductors and insulators the resistivity decreases with temperature. This classification can be effectively explained with the help of the band model. In real solids the highest filled band is called the valence band, the lowest empty band is called the conduction band and the difference in energy between them is called the forbidden energy gap. If the energy band is partially filled with electrons the material is metallic and there is no forbidden energy gap. For the filled band below a small forbidden energy gap the material is semiconductor. If the energy gap is large it is an insulator. Intrinsic conduction in semiconductor arises by the excitation of an electron across the forbidden energy gap

b) Impurity Conduction

The band theory states that the for each electron that is excited to the conduction band from the ground state a vacancy is created in the valence band This vacancy is called hole.

Conduction can occur by means of electrons moving in the conduction band or by means of electrons moving to the vacancies in the ground state. If an electron donor or an acceptor is introduced in the host matrix the conduction increases due to the presence of the impurity.

2.2.2   Localized States

In case of polymer, the condition of regular spacing of like atoms only applies to simplest carbon-Hydrogen polymers such as polymethylene, polyacetylenes etc. Breakdowns in local structure or dipoles in the chain will impact the system energetics. Many polymers consist of both crystalline and non-crystalline regions. It is convenient to think of semi crystalline polymers as a continuous matrix of an amorphous polymer in which the properties are modified by the crystalline regions that act as sites for reinforcing the amorphous matrix. The effect of crystallinity is to lower the conductivity. If the conduction is ionic, ion mobility will be lower through the crystalline region, if electronic, it will be faster but the crystalline – amorphous interface may act as trapping sites a phenomenon like the Maxwell-Wagner interfacial polarization. Wholly amorphous polymer can exist in two states depending upon the temperature. At low temperatures they are hardy glassy materials .At a temperature referred to the glass transition temperature they undergo a transition to a rubber-like state. Thus localized states i.e. states forming extended band like states can be envisioned associated with structure of the polymer. Escape from these local states may be purely thermal it may depend on the local environment and specific molecular motions. The local states may assist in de trapping

2.2.3   Injection Processes

Electrons are emitted from the electrons or generated under the influence of the light (photo-conduction). Electrons in the metal are free to move throughout the bulk of the solid. However when they reach the surface they are subjected to the constraints imposed by the non-continuity of the solid. In order to move beyond the surface they require excess energy. If instead of vacuum a dielectric is placed the potential barrier will be modified and electrons will be emitted

Such process can be represented by the equations

$$M^+ + P \longrightarrow M + P^+ \quad \text{at the cathode} \tag{2.9}$$

$$M^- + P \longrightarrow M + P^- \quad \text{at the anode} \tag{2.10}$$

Where M represents electrode and P the Polymer

There are three ways in which the energy required to escape from the metal may be supplied

1) By thermal methods in a process known as thermionic emission

2) By the application of high electric field in field emission

3) By the photon absorption at sufficiently short wavelength

Mechanisms 1 and 3 may be modified by the Schottky effect, which arises from the field dependent lowering of the potential barrier to injection. Poole-Freenkel effect mechanism is based on the same lowering of the barrier height within the dielectric. For this mechanism t o occur the polymer must contain donor or acceptors. At high fields the width of the potential barrier decreases .As a result the probability of finding an electron on the other side of the potential barrier by quantum mechanical tunneling increases. The tunneling current is independent of the temperature.

2.2.4 Steady State Conduction

The steady state current density is given by

$$J = e n \mu E \tag{2.11}$$

Where J is the current density, e is the charge, n is the number of charge carriers, μ is the mobility of the charge carriers and E is the electric field. This means that the charge flux is constant across the sample. However the number of charge carriers and their drift velocity is sensitive to the electrical environment. An ohmic electrode is an electrode that has no potential barrier to the injection and is capable of providing an infinite supply of charge carriers. The deviation from the ohms law arises because the charge is unable to move uniformly within the solid. These accumulated charges build up adjacent to the ohmic electrode so the field distribution changes and gives the space charge limited currents. A great deal of literature is available space limited current [23,24]. This analysis explains the nonlinear current-voltage characteristics

If the applied potential is sufficiently low the conduction is ohmic. If at some higher potential the solid is unable to transport all the charges the current becomes non linear in the voltage .If there are traps in solid the space charge limited currents may decrease by several orders of the magnitude. The current density in case of trap limiting parameter is given by the Childs law for an insulator with shallow traps and is given by

$$J = 9 \, n_{eff \, exp} \, [-E_T/KT] \, \epsilon\mu V^2/8d^3N \qquad (2.12)$$

Where J is the current density, $n_{eff \, is}$ the density of states in the conduction band, and E_T is the energy, T is the temperature, ϵ is the dielectric constant, μ is the mobility, V is the voltage, d is the thickness of the film and N is the density of traps.

As the traps fill the current approach the trap filled limit of the trap-limited Child's law region of the current- voltage curve .At this point the there is a tremendous increase of the current as the last traps of current are filled

2.2.5 Ionic Conduction

Ionic conductivity has been accounted for the conductivity of many polymers and deviations from the ohms law can also be explained in terms of ionic conductivity. The polymers that contain ions (ionomers) groups capable of ionizing or to which ionic materials have been added; the presence of moisture plays an important role as water may act as source of ions. The deviations from the ohms law and the slopes of I vs. E have been used to calculate the jump distances. Jump distances in the range of 8- 20 nm have been calculated by Ambroski [24] for poly (ethylene terephalate) and for Foss and Danhauser [25] for polypropylene. Deviations from ohms law to field assisted ionic disassociation have also been discussed by Barker and Thomas [26] who concluded that this effect was important only at high fields (> than $10^6 Vcm^{-1}$)

2.3 THEORY OF DIELECTRIC LOSS

It has been established that the charging/discharging current can be used to obtain the low frequency dielectric loss (ϵ'') and the dielectric relaxations, which occur in the low frequency range [27,28]. The discharging current decay is given by the equation $\phi(t) = t^{-n}$ The complex dielectric constant of material is given by

$$\varepsilon^* \quad = \varepsilon' - j\,\varepsilon'' \qquad\qquad (2.13)$$

Where ε^* is the complex dielectric constant, ε' is dielectric constant and ε'' is dielectric loss factor.

The theoretical equations for ε' and ε'' in terms of current produced by the application of a step voltage [27,28] are

$$\varepsilon'(\omega) \quad = 1/C_a\,[C0 + {}_0\!\int^\infty \phi(t))\,\cos\omega t\,dt] \qquad\qquad (2.14)$$

$$\varepsilon''(\omega) \quad = 1/C_a\,[G0/\omega + {}_0\!\int^\infty_. \phi(t))\,\sin\omega t\,dt] \qquad\qquad (2.15)$$

Where C_0 is the capacitance of sample at high frequencies, C_a is the capacitance of sample if sample replaced by air, G is steady state dc conductance, ω is the angular frequency, $2\pi f$ and $\phi(t)$ is the current flowing in the sample after applying unit voltages at t =0 and is called as the decay function of the dielectric

$\phi(t)$ does not include the steady state conduction current from which G_0 is calculated and thus $\phi(\infty)$ is zero. $\phi(t)$ can be approximated over a wide range of values by equation.

$$\phi(t) = \beta C_0 t^{-n} \qquad\qquad (2.16)$$

Where β and n are constant for a material.

Putting the value $\phi(t)$ in equations we get [60]

$$\varepsilon'(\omega) = C_0/\,C_a\,[1 + \beta\omega^{n-1}\,\Gamma(1-n)\,\cos\,\{(1-n)\pi\}/2] \qquad\qquad (2.17)$$

$$\varepsilon''(\omega) = 1/C_a\,[G0/\omega + \beta\,C_0\omega^{n-1}\,\Gamma(1-n)\,\cos\,n\pi/2] \qquad\qquad (2.18)$$

The equation (2.16) holds good for 0<n<1 and equation (2.17) for 0<n<2

Hamon [29] expressed the charging current $\phi(t_l)$ at a particular time t_l as

$$\varepsilon'' \quad = [G_o + \phi(\,t_l)]/\,\omega\,C_a \text{ and } \omega \text{ and } t_l \text{ are related}$$

With $\qquad \omega t = [\Gamma(1-n)\,\cos\,n\pi/2]^{-1/n} \qquad\qquad (2.19)$

The right side of the equation is almost independent of n in the range of 0.3 < n < 1.2 and taking a 3% accuracy the mean value can be taken as 0.63 .To an approximate accuracy the above equation can now be written as

$$\varepsilon'' \approx \{Go + \phi(\,0.63/\omega)\}/\omega\,C_a \qquad\qquad (2.20)$$

If i (t) is defined as the total charging current as a function of time after the application of the step voltage V, i.e. the sum of the charging current and the conduction current and is expressed as

$$i(t)/V = G_o + \phi(t) \tag{2.21}$$

and the equations can now be transformed to a to

$$\varepsilon'' = I(0.63/\omega)/\omega\, C_aV. \tag{2.22}$$

The above equation can also be expressed as

$$\varepsilon'' = I\,(0.1/f)/2\pi f\, C_aV \tag{2.23}$$

Hamon [29] also provided a detailed analysis and showed that even if $\phi(t)$ departs considerably from equation (2.16) the approximation holds good .The above has also been confirmed by Baird [30]

In addition to the restriction for the value of n the superposition principle must also hold good. The anomalous charging and the discharging currents are reversible and proportional to applied voltage. The charging current also includes the steady state direct conduction current so often the discharging current is used in order to offset the affect of the conduction current contribution.

<div align="right">**Chapter 3**</div>

EXPERIMENTAL TECHNIQUES

The experimental step up and procedures that have been are used during the course of this work are described here. Also a brief description of the instruments used for the analysis is described.

The charging, discharging and conduction currents involve measurement of currents as a function of time. In theory, the transformation of the absorption currents from time domain to frequency domain would involve the current to be measured from zero to infinity, however, this is not possible and we truncate the experiments at a point where we assume that time ceases to contribute to ε' and ε''. The lowest frequency at which ε' and ε'' are evaluated depends on the longest duration at which the currents are measured.

3.1 SAMPLE PREPARATION AND ELECTRODES

Sample preparation and electrodes can play a critical role in determining the electrical parameters. In case of polymers the presence of residual solvent, changes in the crystalline /amorphous ratio, the sample cooling rate and the ambient atmosphere all play an important role in the electrical behavior.

Before commencement of experiments, samples were heat treated for 12 hours at 200 ^{0}C to remove the moisture and improve the reproducibility of the results. Formation of the electrode is of paramount importance. In laying down the conductive material the surface of the sample should not be chemically changed and care should be taken to avoid gaps between electrodes and the sample. The most efficient way of doing this is by the vacuum depositing of the electrodes on the sample. During the course of the experiments we have used aluminum foil and conductive silver paint as electrode material. The currents in the polyimide sample range from nanoamperes to tens of femtoamperes (10^{-15}A) over the course of the experiment. The measurement of such small currents is hampered by electrical noise. Making all wires as short as possible and fixing them securely to the ground minimized mechanical noise arising from the changes in system capacitance. In order to minimize the low-level spurious leakage

High voltage electrode

Sample

Thermocouple

Guard Ring

Current measuring
electrode
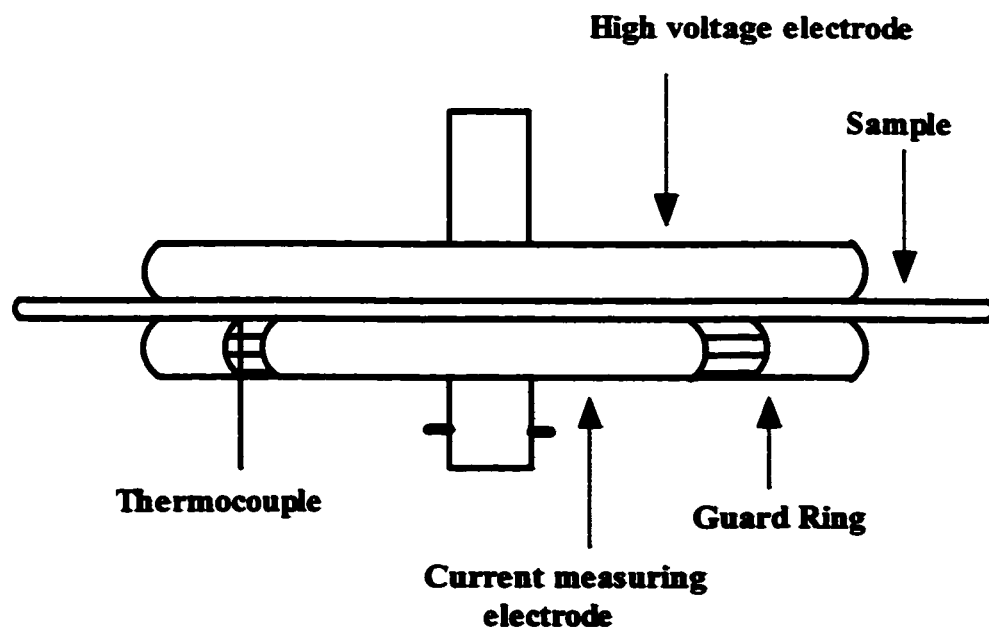
Fig. 3.1   **Three Terminal Electrode Assembly.**

currents, a three terminal electrode system as shown in the fig 3.1 [31,32] is used. This three terminal arrangement eliminates the fringing effect and improves the results tremendously.

3.2 APPARATUS USED FOR MEASUREMENT

The experimental arrangements consists of a High Voltage Direct Current Generator, Tenney Junior Environmental Chamber, Keithley 617 C Electrometer and Data Acquisition System An overview of the instrument specifications is given below.

3.2.1 High Voltage D.C Generator

Brandenburg model 2307R was used for high voltage direct current generation. The voltage ranges from 0 to 5KV at 1 mA.

3.2.2 Tenney Junior Environmental chamber

The Tenney Junior environmental chamber is equipped with a Honeywell's UDC 2000 Mini-Pro universal digital controller. It is used to monitor and control temperature control. It offers precise temperature control, reliability and long life. It is accurate up to 0.1° C. It is also equipped with an over temperature safety and a timer

3.2.3 Keithley 617 C Electrometer

The Keithley model 617c electrometer is a highly sensitive instrument designed to measure voltage, current, charge and resistance. The measuring range of model 617C is between 10mV to 200V for voltage measurement, 0.1fA to 20mA in the current mode. The very high input impedance and the extremely low input offset current allow accurate current measurement. It has a 5 digit display and a standard IEEE-488 interface along with a both preamp and 2V full analog outputs on the rear panel. It has an internal buffer that can store over 100 readings that are accessible from either the front panel or over the IEEE-488 bus. The following are the specifications on the current measuring ranges.
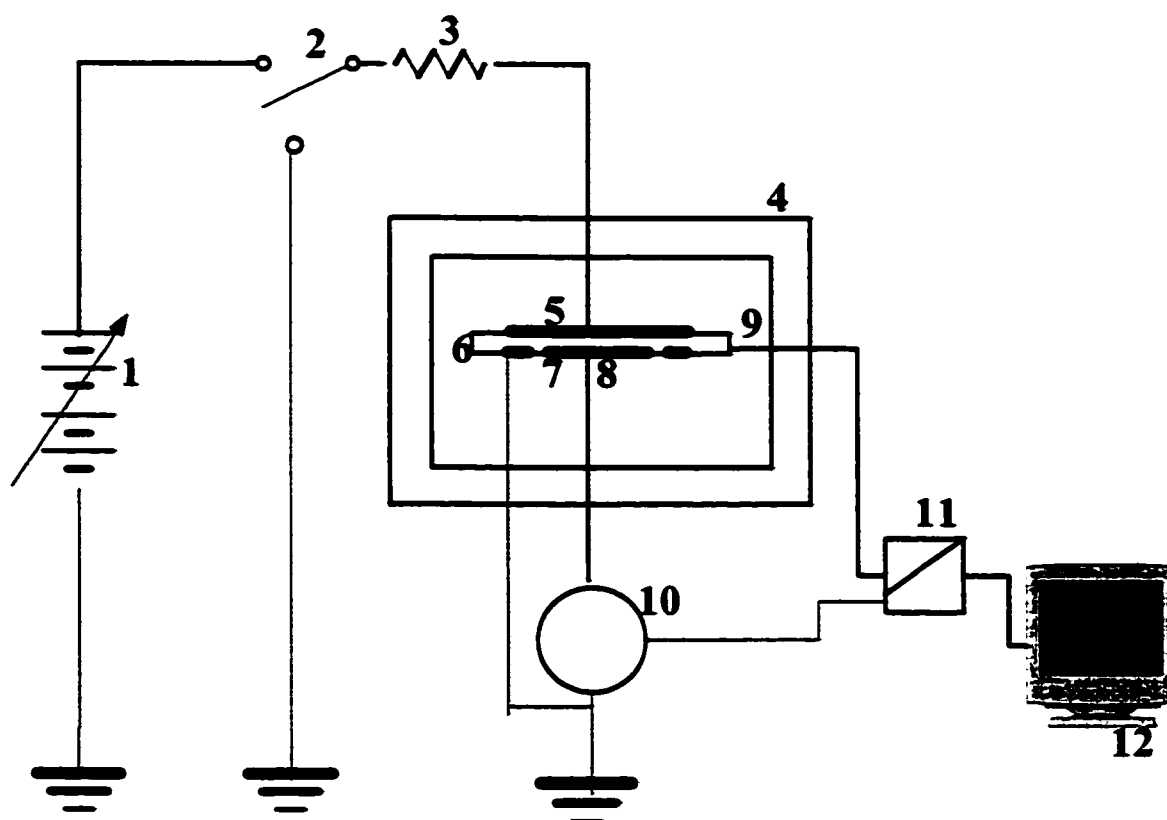
1) Brandenburg Variable D.C Power Supply
2) Two Way Switch
3) Tenney Jr.Environmental Chamber
4) High Voltage Electrode
5) Sample
6) Guard Ring
7) Measuring Electrode
8) Thermocouple
9) Keithley617c Electrometer
11) DT301 series board

Fig. 3.2   Experimental setup for the study of Charging and Discharging currents.
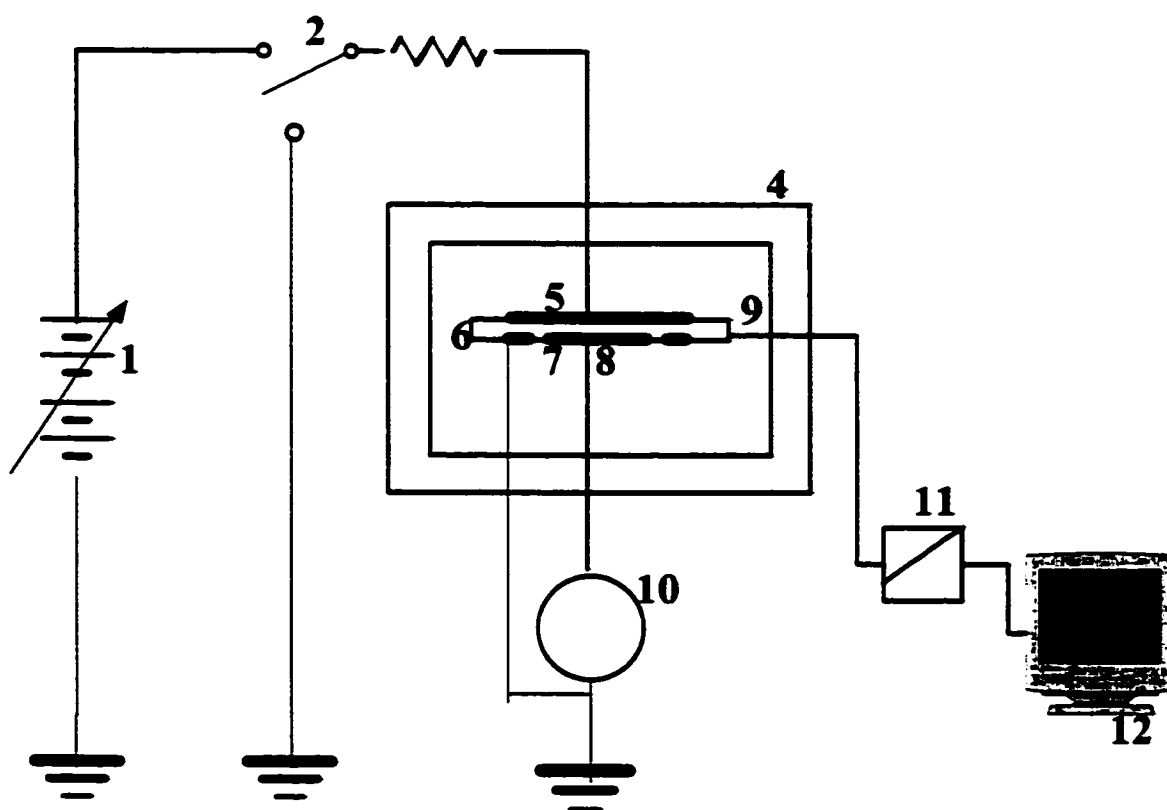
1) Brandenburg Variable D.C Power Supply
2) Two Way Switch
3) Tenney Jr.Environmental Chamber
4) High Voltage Electrode
5) Sample
6) Guard Ring
7) Measuring Electrode
8) Thermocouple
9) Keithley617c Electrometer
11) DT301 series board

Fig. 3.3   Experimental set up for the study of Conduction current.

<u>**Table: 3.1[33]**</u>

Range	Resolution	Accuracy 18⁰-28⁰C ±(% rdg + counts)	Temperature coefficient 0⁰ -18⁰C, 28⁰-50⁰C ±(% rdg + counts) / ⁰C
2pA	100aA	1.6 + 66	0.15 + 8
20pA	1fA	1.6 + 7	0.15 + 1
200pA	10fA	1.6+1	0.15 + 0.1
2nA	100fA	0.25 + 5	0.015 +3
20nA	1pA	0.25 + 1	0.015 + 0.3
200nA	10pA	0.25 + 1	0.015 +0.1
2μA	100pA	0.15 + 4	0.005 + 3
20μA	1nA	0.15 + 1	0.005 + 0.3
200μA	10nA	0.15 + 1	0.006 + 0.1

3.2.4 Data Acquisition System

The data acquisition system consists of a DT300 series board, STP300 screw terminal panel, DT300 series software driver and Labtech software

a) DT301 series board

The DT 300 series is a family of multifunctional data acquisition boards for the PCI bus [34]. The DT series consists of boards DT301, DT302, DT304, DT332 and DT334.The key features of DT301 series board that is used for data acquisition are listed below

Analog Input – 8 D channels

Analog Input Frequency – 225 KHz

Analog Input - ± 0 –10V

Digital I/0 – 23

Counter/timers- 6

Analog resolution – 12 bits

Accuracy – 0.01 of % reading

b) STP300 Screw Terminal Panel

The STP 300 screw terminal panel is used for the connected the instrument signals to the DT301 board .All analog inputs are connected through the STP300 screw terminal panel. A

differential configuration is adapted to measure the currents from the keithely since the measured signal constitutes a low level signal (1V) and this configuration reduces noise.

c) DT301 Series Software

The DT301 series software consists of the device drivers and data acquisition software

d) Labtech Software

Labtech is an ANSI C graphical programming language, which helps to create complete data acquisition and control applications. The block diagram of the process is created using the build time menu of the software and the run time menu triggers the A/D board to fetch the data from the instrument. The value of the each block in the setup is written to the diskette in an ASCII format.

3.3   EXPERIMENTAL PROCEDURE

The sample is pretreated by increasing the temperature of environmental chamber up to 200 ^{0}C and for 12 hrs to remove the moisture content. The procedure and thermal protocol adapted for the measurement of the charging/discharging current and conduction current is explained in sections below

3.3.1   Charging/Discharging current

Fig 3.2 shows the schematic arrangement of the study of the charging and discharging currents. After the preparation of the dielectric film, it is placed between two electrodes and kept in the environmental chamber. The currents are measured using a keithley 617 C electrometer that is connected to the low voltage electrode and data acquisition system. The frequency of the sampling can be adjusted up to 4 KHz but most of the data are taken at 1 Hz. A thermocouple is also attached to the holder to monitor the temperature .The thermocouple is attached to the DT series board and voltage values are logged in the data files. Sawa [35] introduced thermal protocol and Govinda Raju [36] introduced a variation of this technique, which is adapted in this study. Fig 3.4 shows the thermal protocol that the dielectric material goes through during the course of the experiments. The thermal protocol consists of the following.

T and V

B   C

E   F   G

D

VOLTAGE APPLIED

A

| 3Hr | 1Hr | 4Hr | 4 Hr |
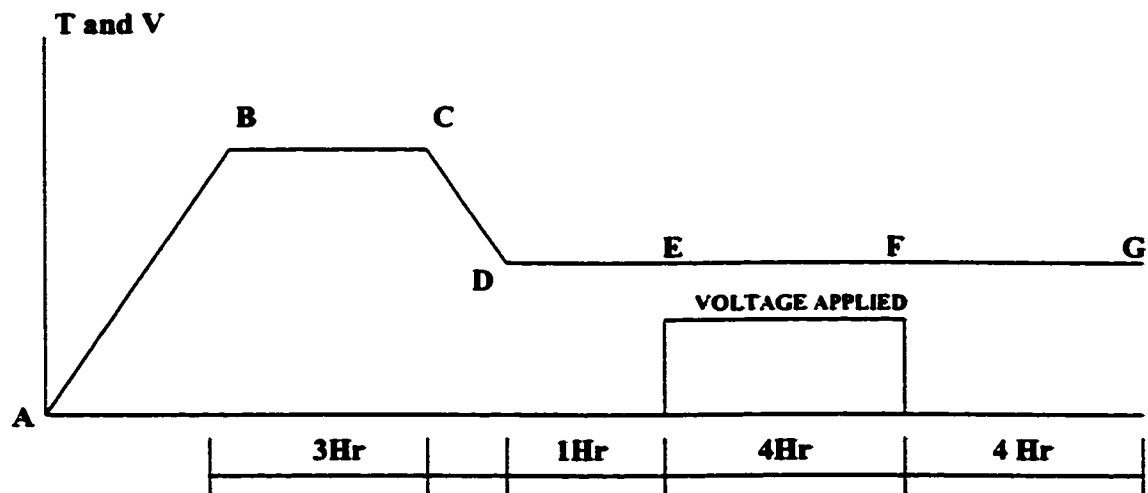
Fig.3.4   Thermal Protocol Adapted for study of charging and discharging currents.

T and V

B   C

E   F

D

16

5

5

5

3Hr   1Hr   Voltage applied

t
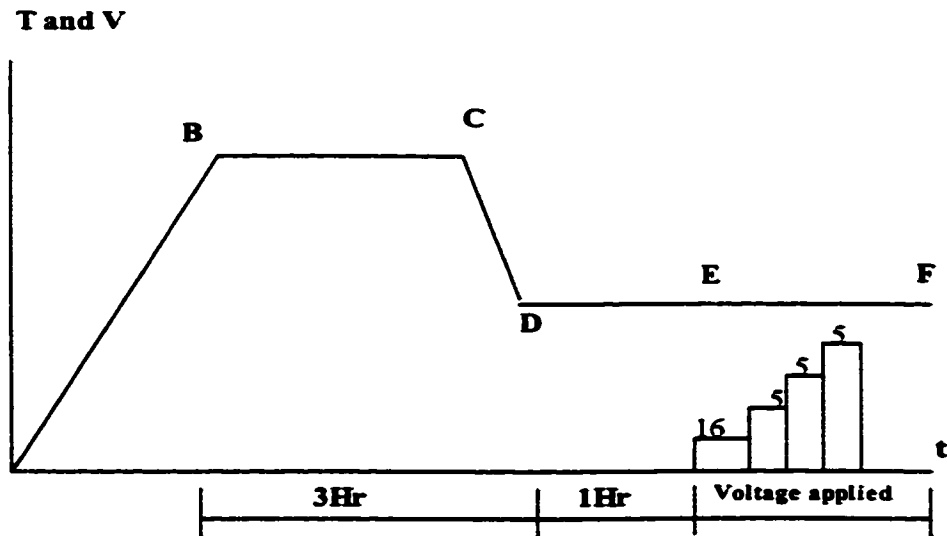
Fig. 3.5   Thermal Protocol adapted for the study of Conduction currents.

A-B   Increase the environmental chamber temperature from the room to 200 ^{0}C

B-C   Hold the temperature constant at 200 ^{0}C for 3 hours

C-D   Lower the temperature to the desired value

D-E-F Maintain the desired temperature for 2 hours

E-F   Apply the desired DC voltage for 4 hours and record the charging current

F-G   Remove the DC voltage, short circuit the electrode for 4 hours and record the discharging currents.

The electrodes are short circuited through out the protocol which starts at A and ends at E Before each measurement a blank run was performed in order to free the sample from the extraneous charge. This run consisted of raising the temperature the sample at constant rate to 200°C with the electrodes short-circuited for a period of 6 hours.

3.3.2 Conduction current

Fig 3.3 shows the schematic diagram of the study for the conduction current .The currents are measured using Keithley 617C electrometer and is programmed to record the reading after every 1000 seconds .The currents are retrieved using the front panel. The sample were heat treated at 200 ^{0}C under short circuit for 3 hrs and then cooled slowly to room temperature prior to measurement After 1hr the lowest electric field temperature is applied and the current is observed after 1000 second after allowing it to settle down. Thereafter the field is increased in short steps and at each step a time of 300 second is allowed for the dark current to settle down. Figure 3.5 shows the thermal protocol adapted for the conduction current and following steps describe the protocol

A-B   Increase the environmental chamber temperature from the room to 200 ^{0}C

B-C   Hold the temperature constant at 200 ^{0}C for 3 hrs

C-D   Lower the temperature to the desired value

D-E-F Maintain the desired temperature for 1hr

E-F   Apply the desired voltage and take the measurement of conduction current after 1000s,increase the field in short steps allowing a time of 300s between measurements
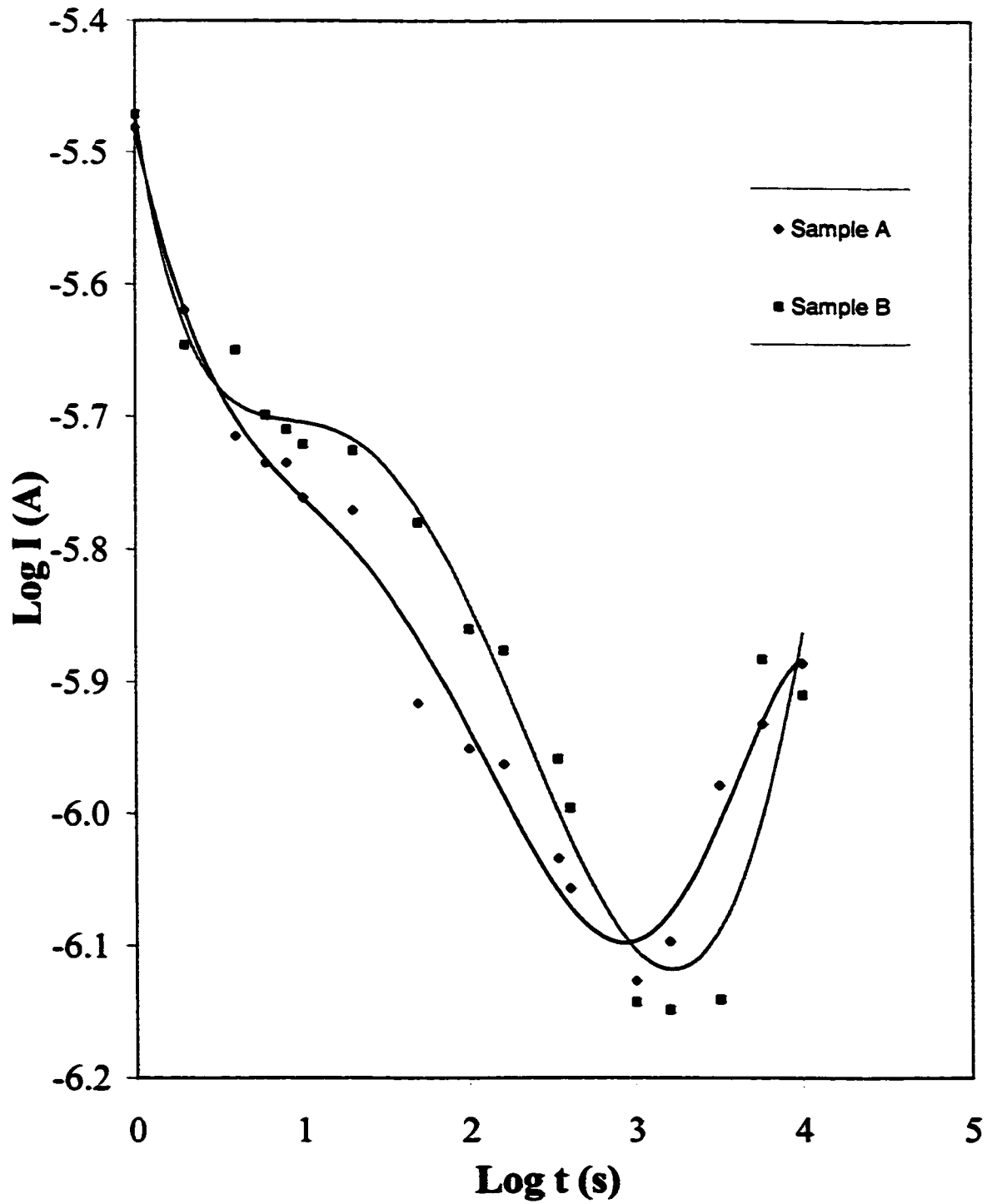
Fig. 3.6 Comparison of charging current for two samples at 200 ^{0}C and 6MV/m field subjected to similar heat treatment.
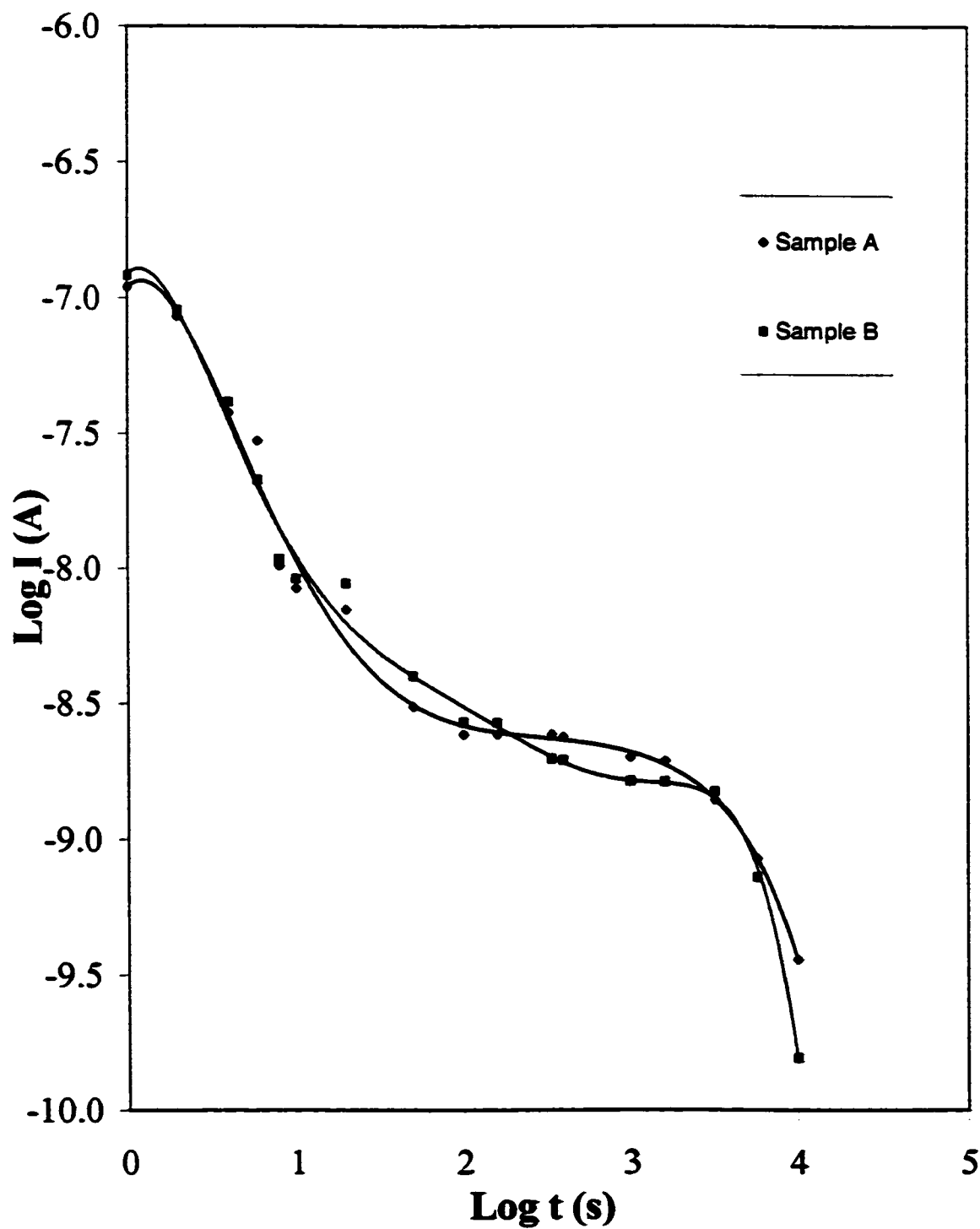
Fig. 3.7 Comparison of Discharging current at 200 °C and 6 MV/m field for two samples subjected to similar heat treatment,Electrode Material -Al.

and take the readings after every 600 seconds.

3.4 PRECISION OF EXPERIMENTAL ANALYSIS

Most of the experiments detailed in the work were limited to a single sample because of the time involved in the pre-heat treatment and the volume of the data. Since the sample were all taken from the single roll it was deduced that the chemical properties and the morphology remain the same.

In order to determine the precision of the experiments two samples of (HN500) films were subjected to the same heat treatment and the charging and discharging currents were measured. The results are shown in the figures 3.6 and 3.7, which show that there is a difference of approximately 1.5% between the measured values. This can be attributed to the different ambient conditions or moisture adsorption.

The currents are generally measured to an accuracy of ±2%. The voltages are measured to an accuracy is ±1%. The overall accuracy is estimated as ±3%.

<div align="right">

Chapter 4

</div>

CHARGING AND DISCHARGING CURRENTS IN POLYIMIDE (HN500 FILM)

In this chapter the procedure and the results of the charging/discharging currents on polyimide commercially referred as (Kapton® HN500 Film) supplied by DuPont are investigated and the effect of the various parameters are studied. The low frequency dielectric loss (ε'') is obtained from the discharging currents using Hamon's approximation.

4.1 EXPERIMENTAL TECHNIQUES

The charging and discharging current are measured in polyimide (HN500 Film) under the influence of varying parameters. Fig 3.2 shows the experimental setup. Before the commencement of the experiments the sample were heat treated for 12 hours at 200 ^{0}C to remove any moisture content. The samples were subjected to a thermal protocol cycle, which has been described in chapter 3. The experiments for a set of parameter have been conducted on the same film. The results have been reported for temperature range 50- 200^0 C in which the temperature is increased in short steps while the field is maintained at 6 MVm^{-1}, which corresponds to 750 volts. The results are also reported for a constant temperature of 200 ^{0}C and various fields in the range of 4-12 MVm^{-1}. A three terminal electrode is used to reduce the effects of the stray fields. The currents are measured with the Keithley 617C electrometer. Before each measurement a blank run is performed in order to free the sample of extraneous charges. This run consisted of raising the temperature to 200^0 C and holding it up to 5 hrs to reduce the effect of space charge build up.

4.2 RESULTS AND DISCUSSION

4.2.1. Charging and discharging current
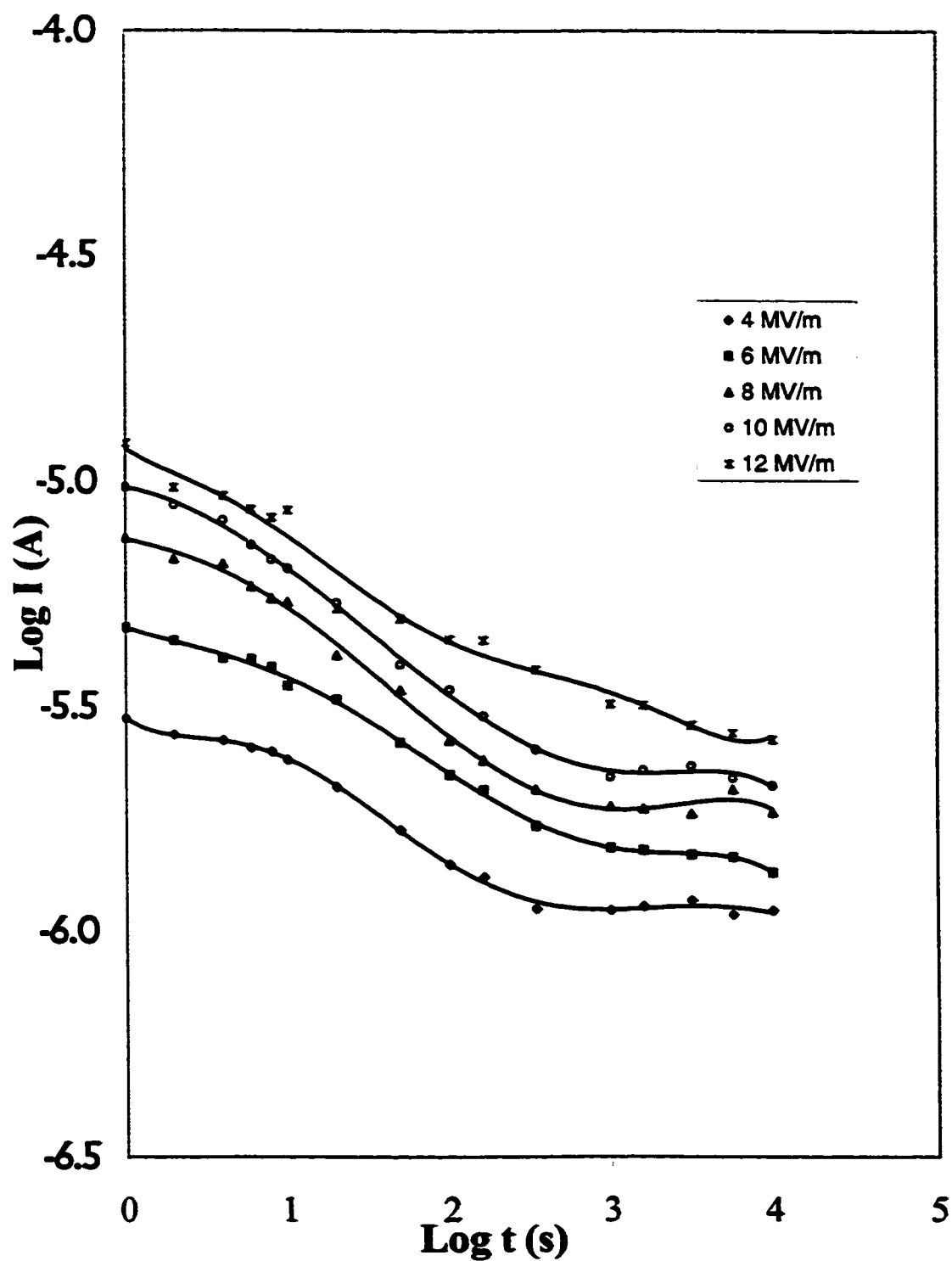
Fig. 4.1 Charging current at various field and constant temperature of 200 ^{0}C, Electrode material-Al for HN500 Film.
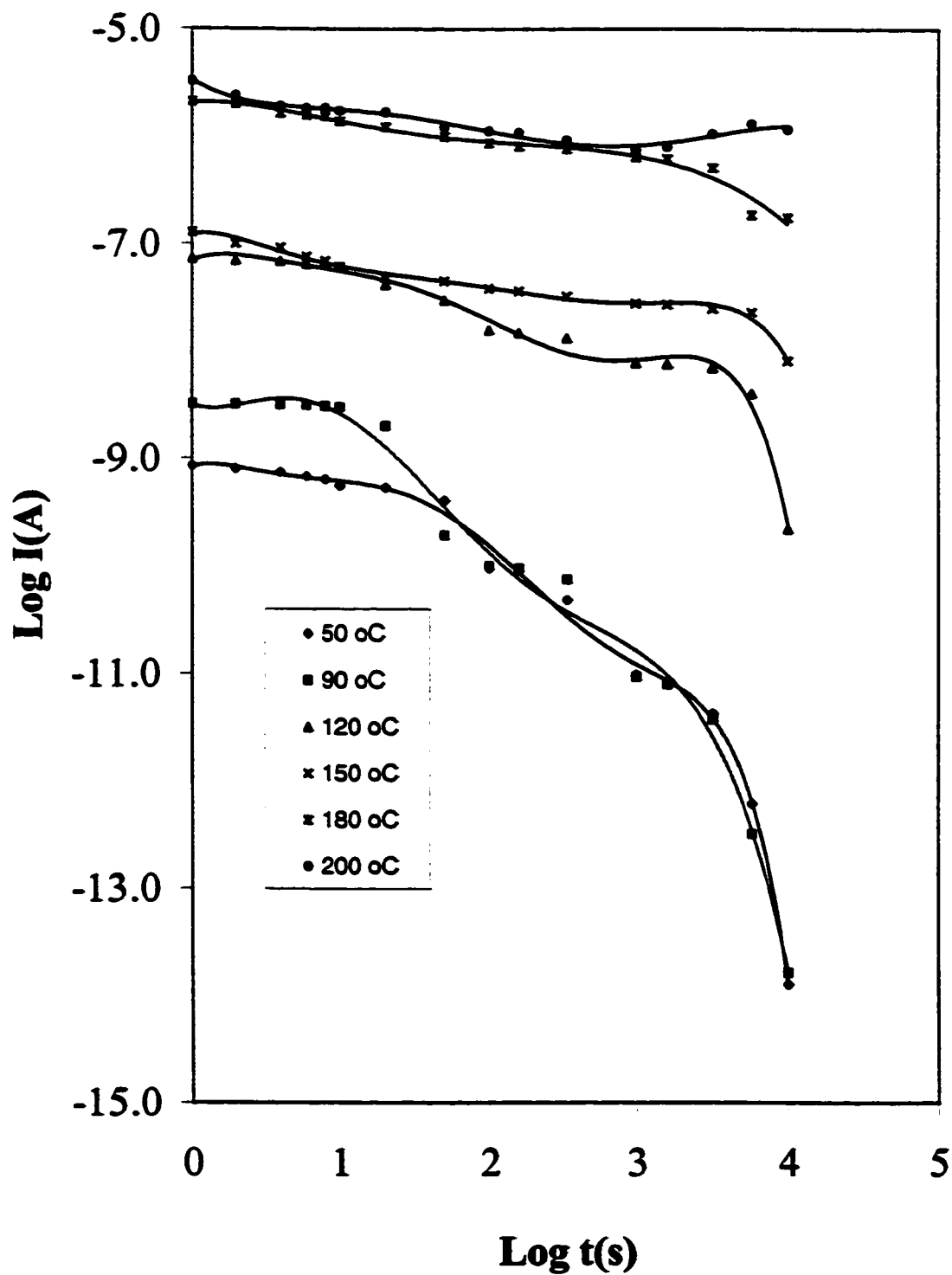
Fig 4.2 Charging current for various temperature and constant   6 MVm^{-1} field for HN500 film, Electrode Material -Al
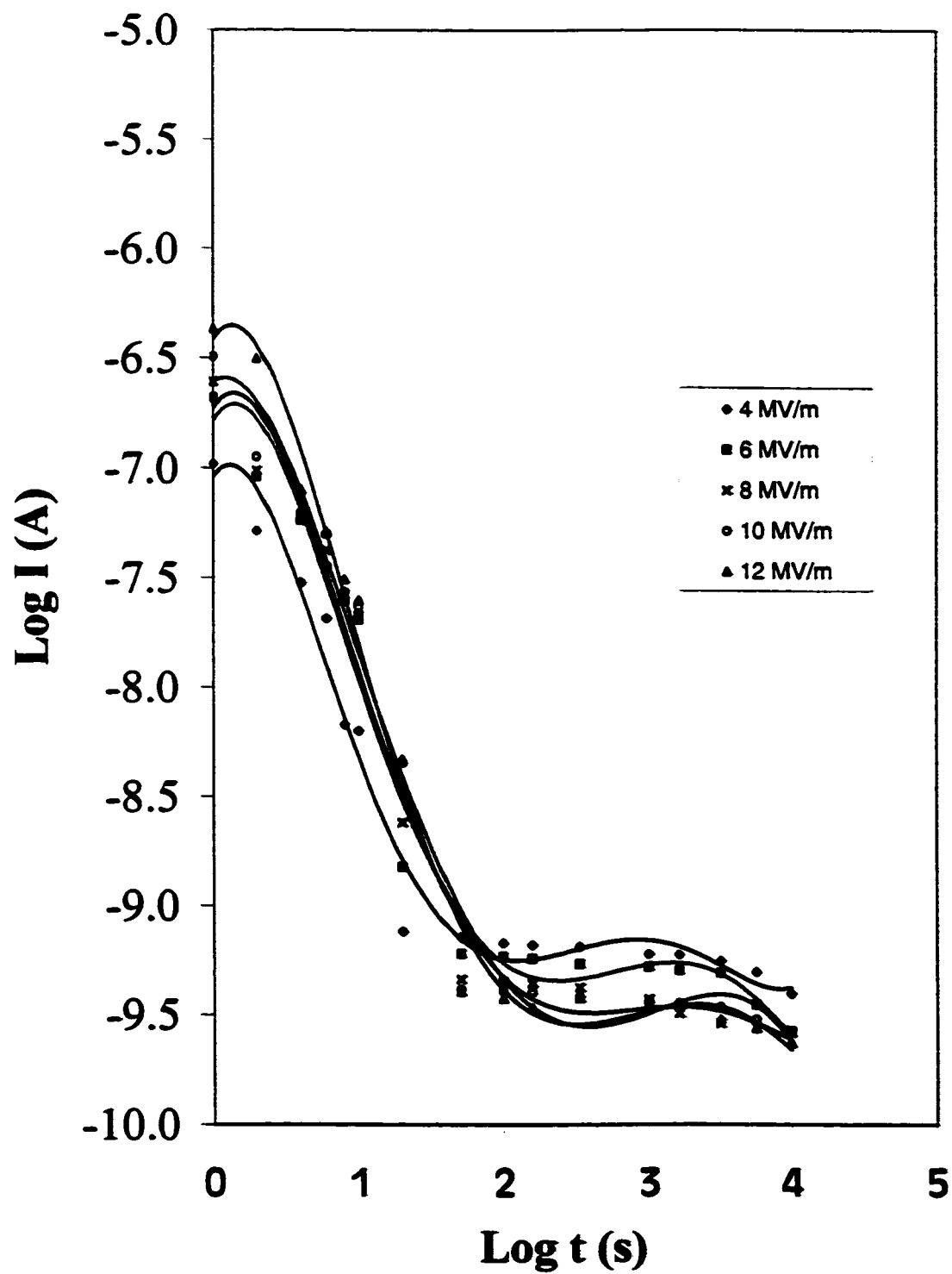
Fig. 4.3 Discharging current at various electric fields and constant temperature of 200 °C for HN500 Film, Electrode Material-Al.
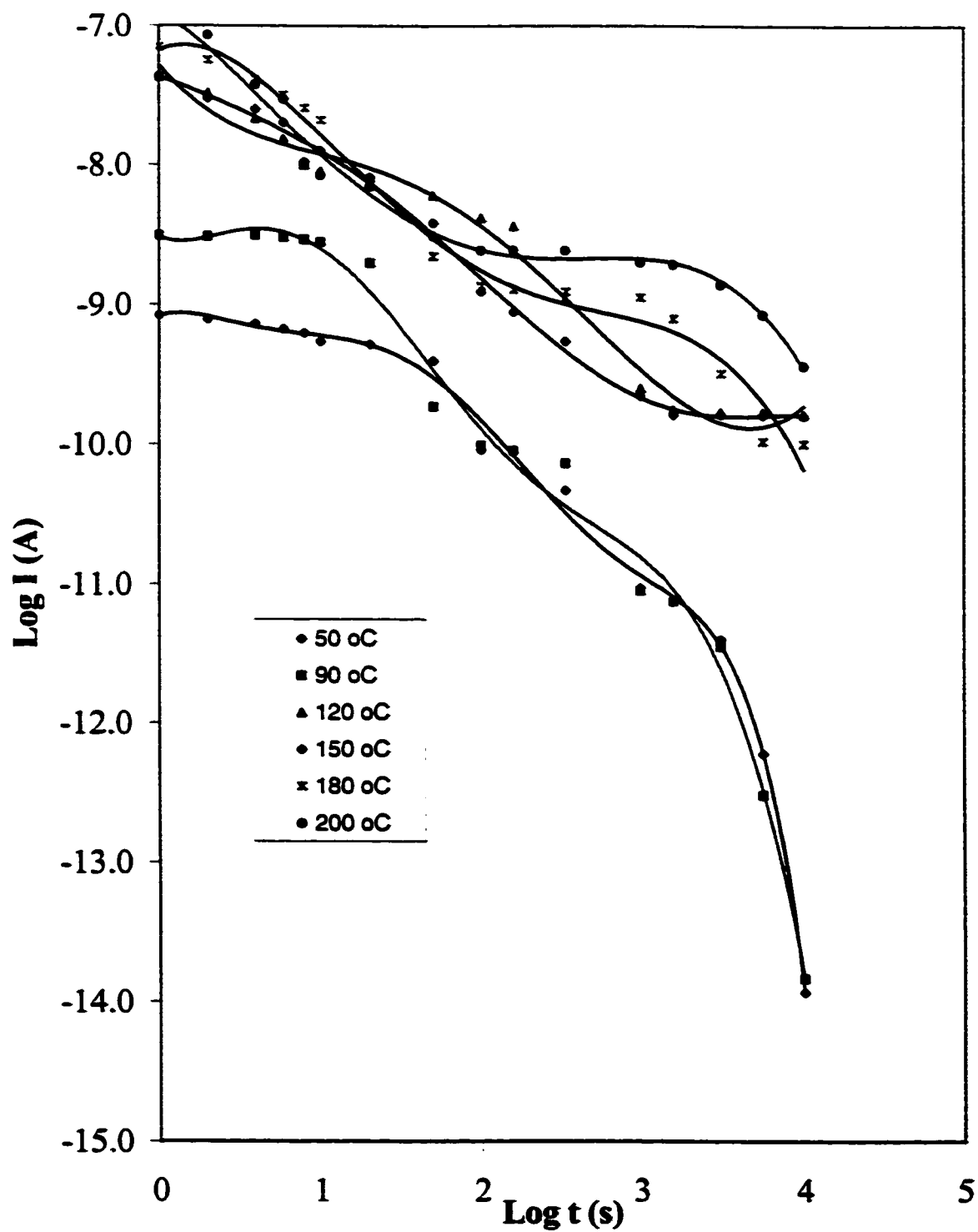
Fig. 4.4 Discharging current at various temperatures and 6 MVm⁻¹field, Electrode Material -Al for HN500 Film.

a) Time dependence

Figure 4.1 shows the charging currents for 127μm sample respectively with aluminum electrodes at constant temperature and various poling fields for duration of 5 hrs. The charging current decays slowly with time with the value of index n in the range 0.10 to 0.16. It is to be noted that the currents tend to flatten out to a steady state value. The current decay is appreciable for up to 100 seconds during which the polarization current forms the major component and for times greater than 100 seconds the transport currents tend to dominate. Raju [37] reported similar behavior for polyamide material Aramid paper for silver electrode material. Linkens[9] also found similar behavior for polycarbonate above 150 ^{0}C. Sawa [35] reported a constant current up to 10 MVm^{-1} while for fields between 10 -50MVm^{-1} decay in the value of the current. It was attributed the time variation of current to the space charge formation. The slow decay of the current has also been attributed to the slow filling of traps by charge carriers in conjunction with a space charge effect [7].

Figure 4.2 shows the charging current 127μm sample respectively with aluminum electrode at various temperatures and constant poling field at 6MV/m field. At temperatures 50–90 ^{0}C the current decays with a slope of 1.21 to 1.33 while for temperature slope 120- 180 ^{0}C the current tends to flatten out. The value of n lies in the range of 0.60 to 0.11.The decay is unusual in that at the higher temperature i.e. at 200 ^{0}C the current is seen to increase with time. Sawa [35] did not report a time variation of current with temperature for Kapton while Chohan [38] found similar behavior of current decay with the temperature.

Figure 4.3 shows the discharging currents as a function of time at constant temperature 200^0 C and various poling fields of 4 –10MV/m for aluminum electrodes. The current decays very fast up to 100seconds where the power law holds good for a value of 1.57 to 1.63 while at times greater the value of n lies between 0.09 to 0.12. Figure 4.4 shows the discharging current as a function of time at constant field and various temperatures from 90 to 120 ^{0}C. At temperatures 50-90 ^{0}C, the value of n is in the range of 1.2 to 1.23 while at higher temperatures the current decay is less pronounced with a value of n in range of 0.60 to 0.71. The polarization current appears to intersect at one point in time approximately 10 seconds. The charging currents and the discharging currents follow a mirror image of each other for low temperatures. The discharging current is of the opposite sign from the charging current and is composed only of polarization current. The data for the charging
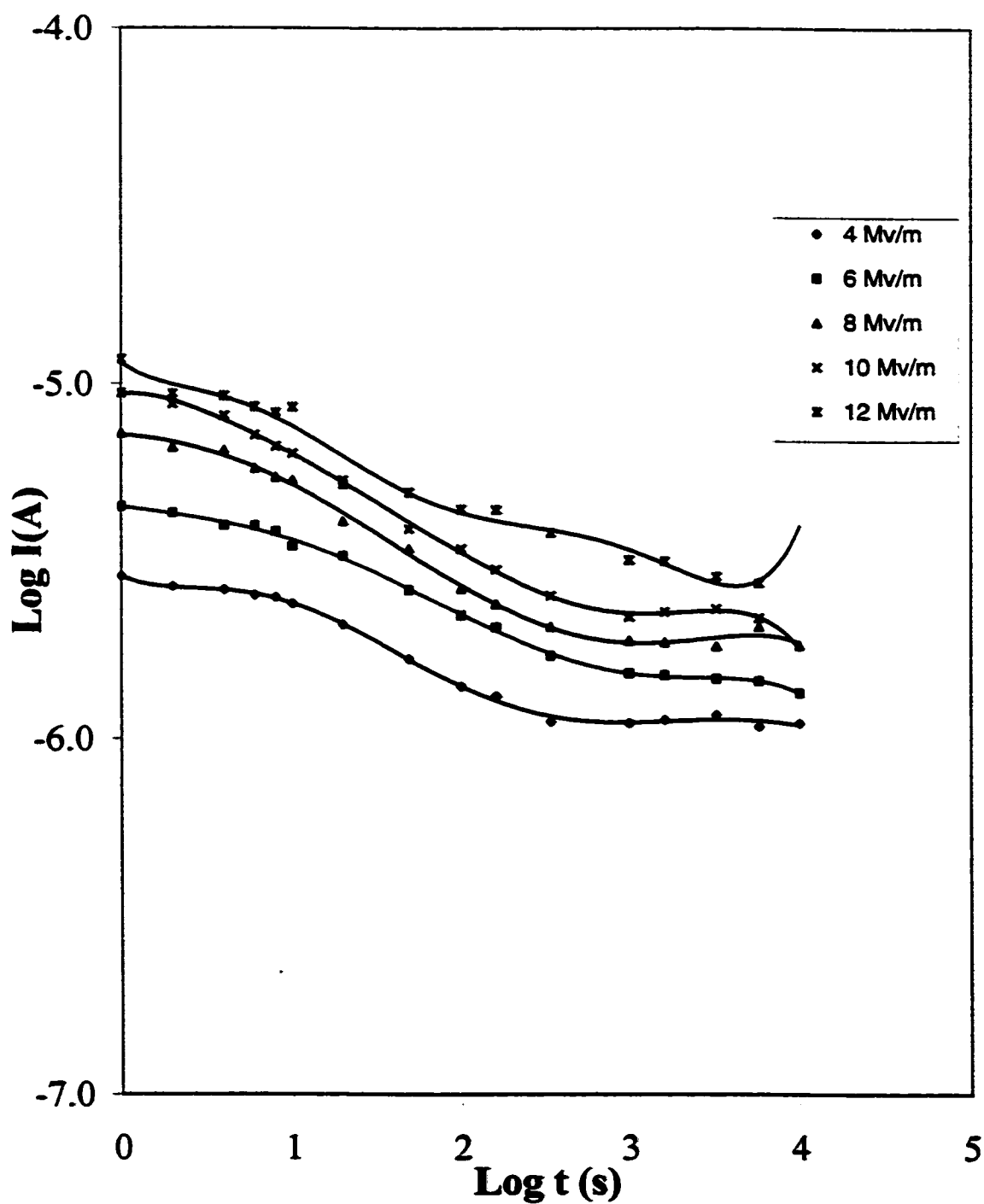
Fig. 4.5 Transport current at various fields and constant temperature of 200 ^{0}C for HN500 film, Electrode Material-AL
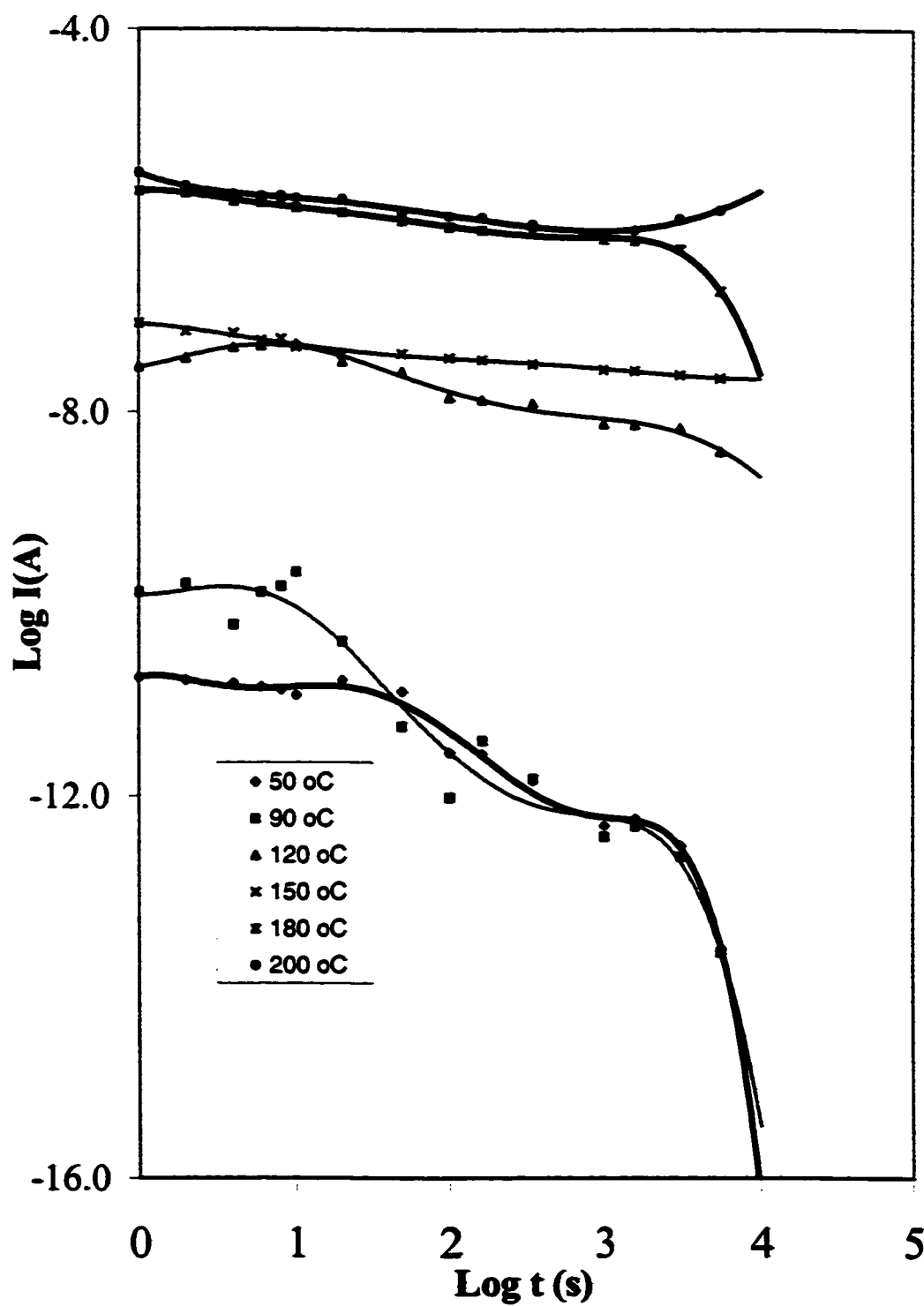
Fig. 4.6 Transport current at various temperatures and 6 MVm⁻¹ field for HN500 film, Electrode Material -Al

and current shows that they are dissimilar for temperatures greater than 120 ^{0}C.Such dissimilarities have been reported in previous studies [7,9] for polymers. Lindmayer [7] has discussed these dissimilarities and has shown that the transient of the current is due to the empty traps. The currents reduce to the space charge limited current once the traps are filled. During the discharging only some of the trapped carriers drift towards both the electrodes and hence a small current is recorded in the external circuit.

The difference between the charging and discharging is called the transport current [39] The analysis suggests that these transport current should be constant. Fig 4.5 shows the transport currents for 127 µm with silver electrodes at constant temperature and various electric fields. The transport current decreases for a time up to 100 seconds and then tends to flatten out. This is due to the fact that the discharging current decreases fast up to time for 100 seconds and then transport current becomes almost similar to the charging current as the difference between the two current becomes appreciable. Similar behavior has been reported in polyimide (PMDA-ODA) by Smith. [39].

Fig 4.6shows the transport currents for the 127 µm sample with aluminum electrodes at a constant field and the various temperatures 50-200 ^{0}C. At higher temperatures the transport current almost seems to be constant. It is seen that the currents tend to increase after about 10 ^{4} seconds. This is expected as the charging currents are found to be increasing at 200 ^{0}C.

b) Temperature dependence

Figure 4.7 shows the discharging currents at prescribed times over a temperature range of 50 to 200 ^{0}C and applied voltage of 1500 V. These values are plotted from the discharge currents of figure 5.3. The curves show a peak at about 120 ^{0}C. A peak is observed at about 120 ^{0}C, which shows that there is a change in the conduction process at 120 ^{0}C.

c) Field dependence

Figure 4.8 show the field dependence of the charging currents at a constant temperature of 200 ^{0}C with a thickness of 125µm The charging currents are plotted at times 10 to 1000 seconds and it can be seen that the time dependence has only a marginal effect as the currents tend to decay slowly. The observed relationship can be approximated to

$$I(t) = K(t) \ E^P$$

Where K is a constant independent of E and p $\cong$ 1. Similar linear relationship has been observed by Govinda Raju [40] in Aramid paper and in PET by DasGupta [10] for
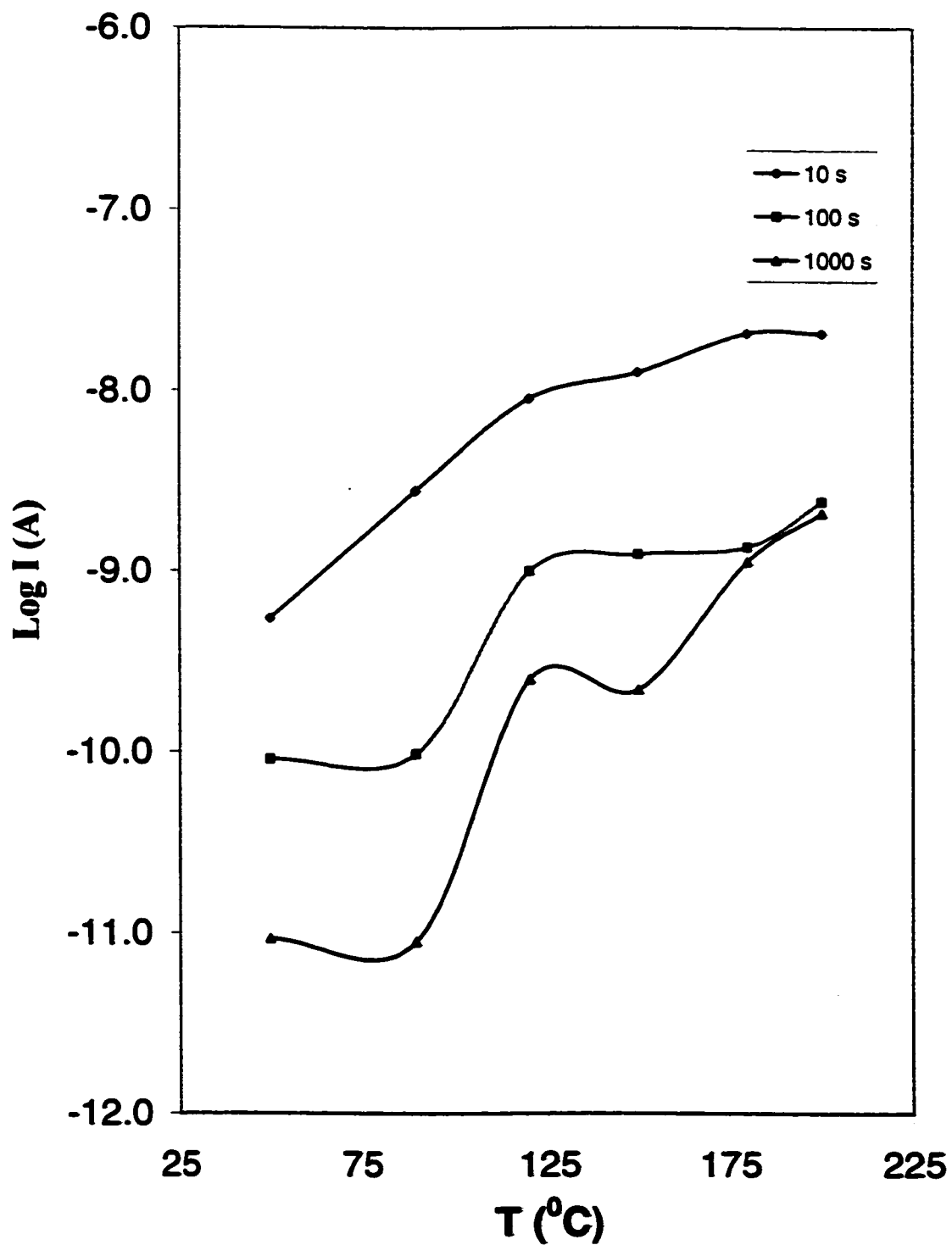
Fig. 4.7 Temperature dependence of discharging currents at prescribed times for HN500 film.Preapplied field 6 MVm^{-1},Electrode Material-Al.
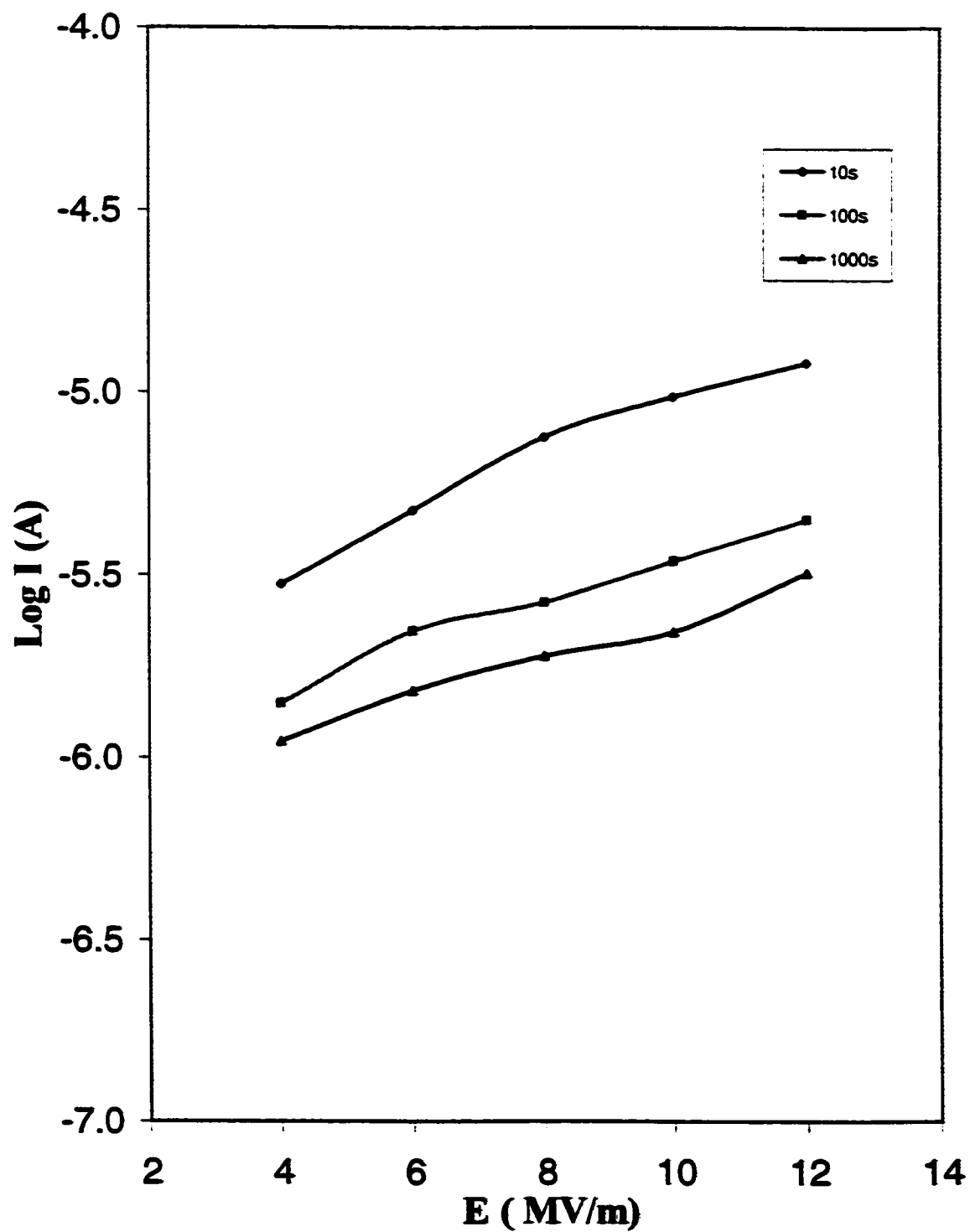
Fig. 4.8 Field dependence of charging current at prescribed times and constant temprature of 200 °C, Preapplied field 6 MVm⁻¹, Electrode Material -Al
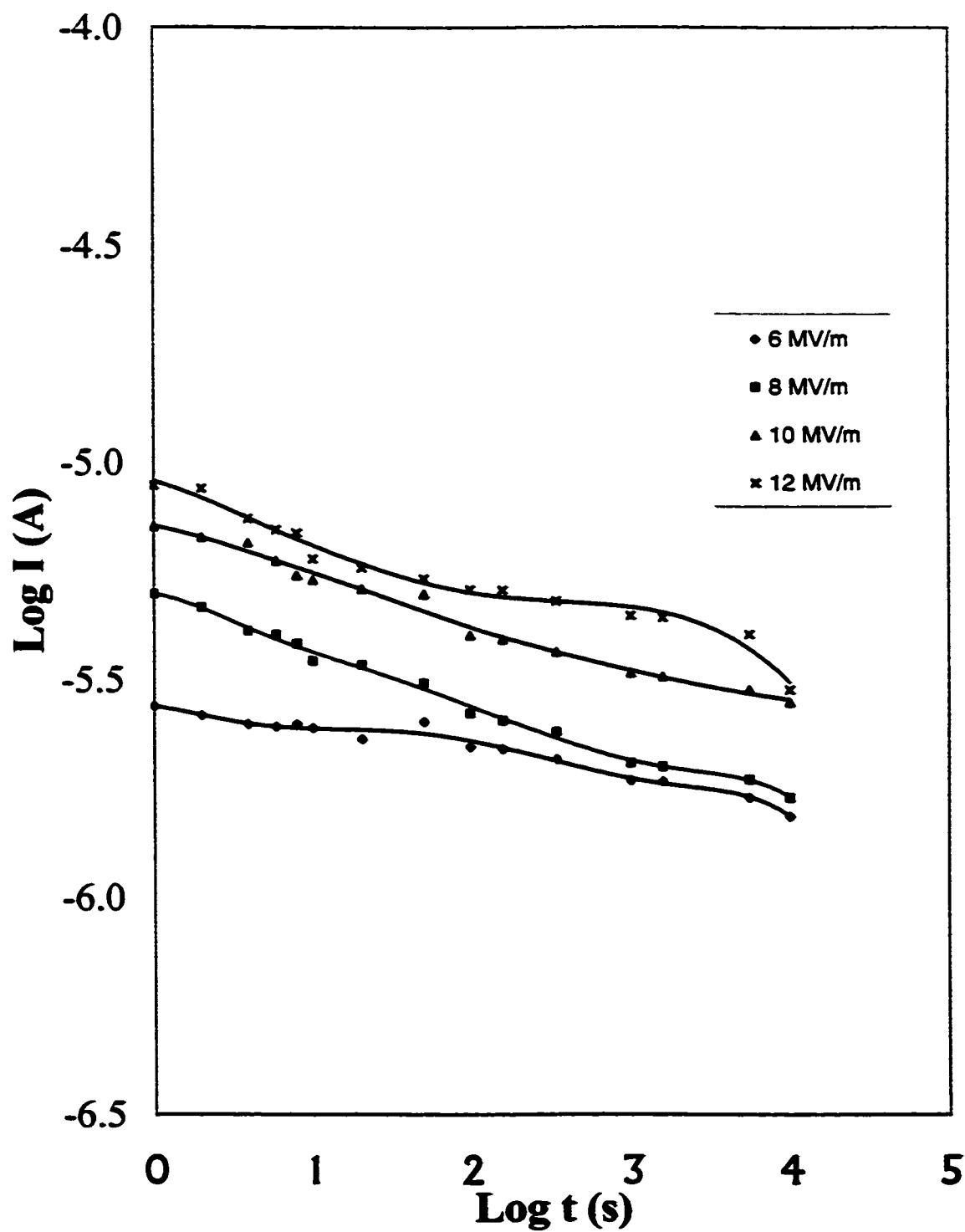
Fig. 4.9 Charging current for various electric fields and constant temperature of 200 ^{0}C for HN500 Film, Electrode Material -Ag.

temperature up to 350K. DasGupta [10] did not found this relationships to hold good for times greater than 10^5 seconds and higher temperature. DasGupta [10] attributed this to the onset of the quasi –steady state conduction that is superimposed on the charging transient.

d) Effect of Electrode Material

The effect of electrode materials is investigated using aluminum and silver electrode material at temperature of 200 ^{0}C and electric fields up to 8 Mv/m.

The charging and discharging currents for a constant temperature of 200 ^{0}C at various electric fields for silver electrodes are shown in the figure 4.9 and 4.10.

Comparing the charging currents of fig 4.1 and 4.9 it can be seen that they do not show a significant dependence on the electrode material except that there is a slight increase in the current magnitude at times higher than 10^3 seconds with the silver electrodes.

The discharging current of 4.3 and 4.10 does not show very significant dependence on the electrode material except that the current reduces at a faster rate for silver electrode material than that for the aluminum electrode material. If the currents show significant dependence and decay shows a marked dependence on time for the sliver electrode then the mechanism of electrode polarization can be inferred which caused by the surface oxidation of silver electrodes [41,42]

4.2.2 Low Frequency Dielectric loss Factor (ε'')

The time dependence of the discharging current can be used to calculate the low frequency dielectric loss using Hamons approximation [29] if there is broad distribution of relaxation time [43,44]. The loss factor is calculated using the equation 2.23.

Fig 4.11 shows the calculated values of ε'' against f at different temperatures. These curves were obtained using the set of isochronal data in the high temperature region .A complete set of loss peaks is shown to move to higher frequencies as the temperature increases, possibly due to dipolar orientation. Also for the high temperatures the value of dielectric loss increases to a magnitude value possibly due to Maxwell-Wagner type of polarization where mobile carriers blocked either at some internal boundary separating different phases or at the electrodes.
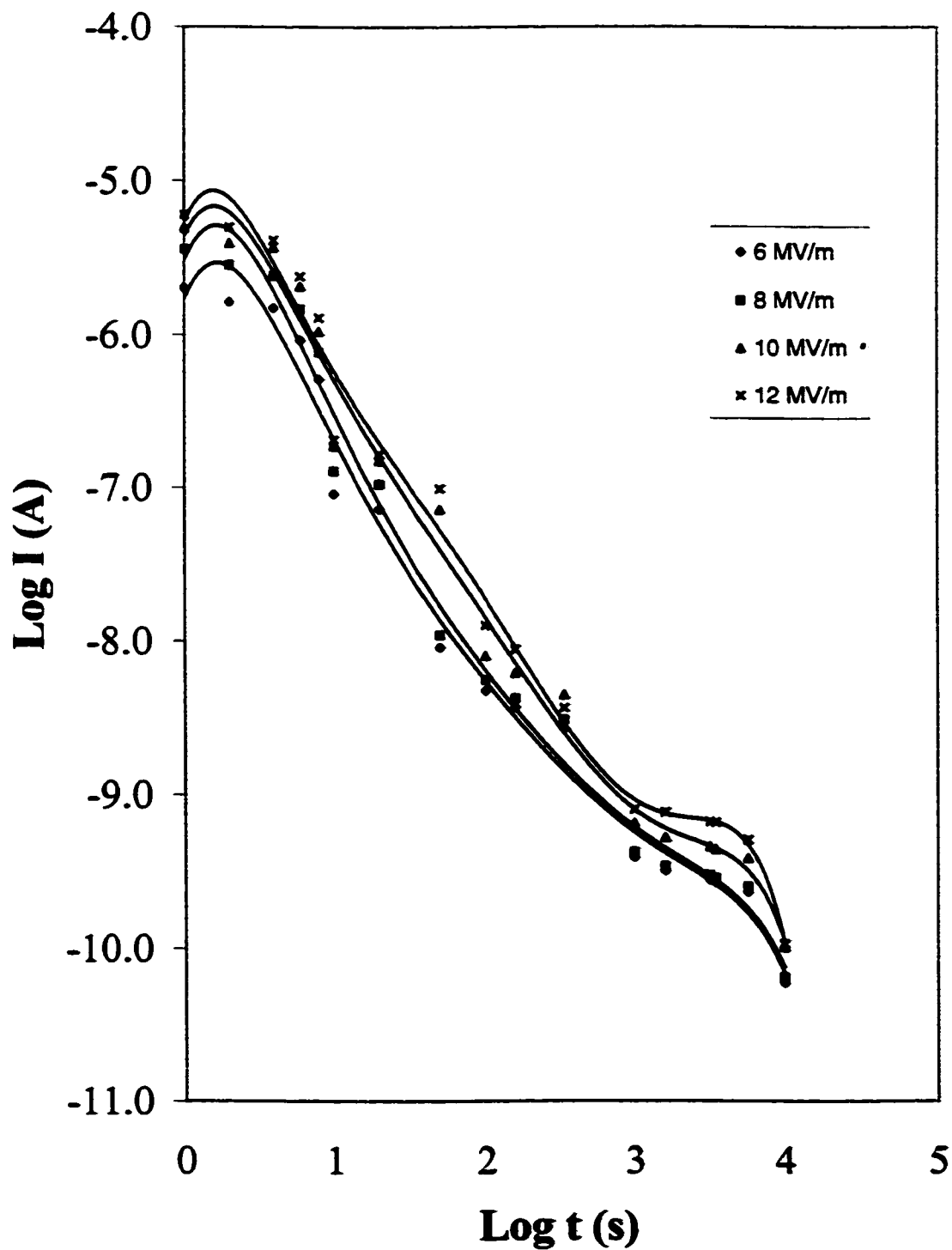
Fig. 4.10 Discharging current at various fields and constant temperature of 200 ^{0}C, Electrode Material-Ag for HN500 Film.
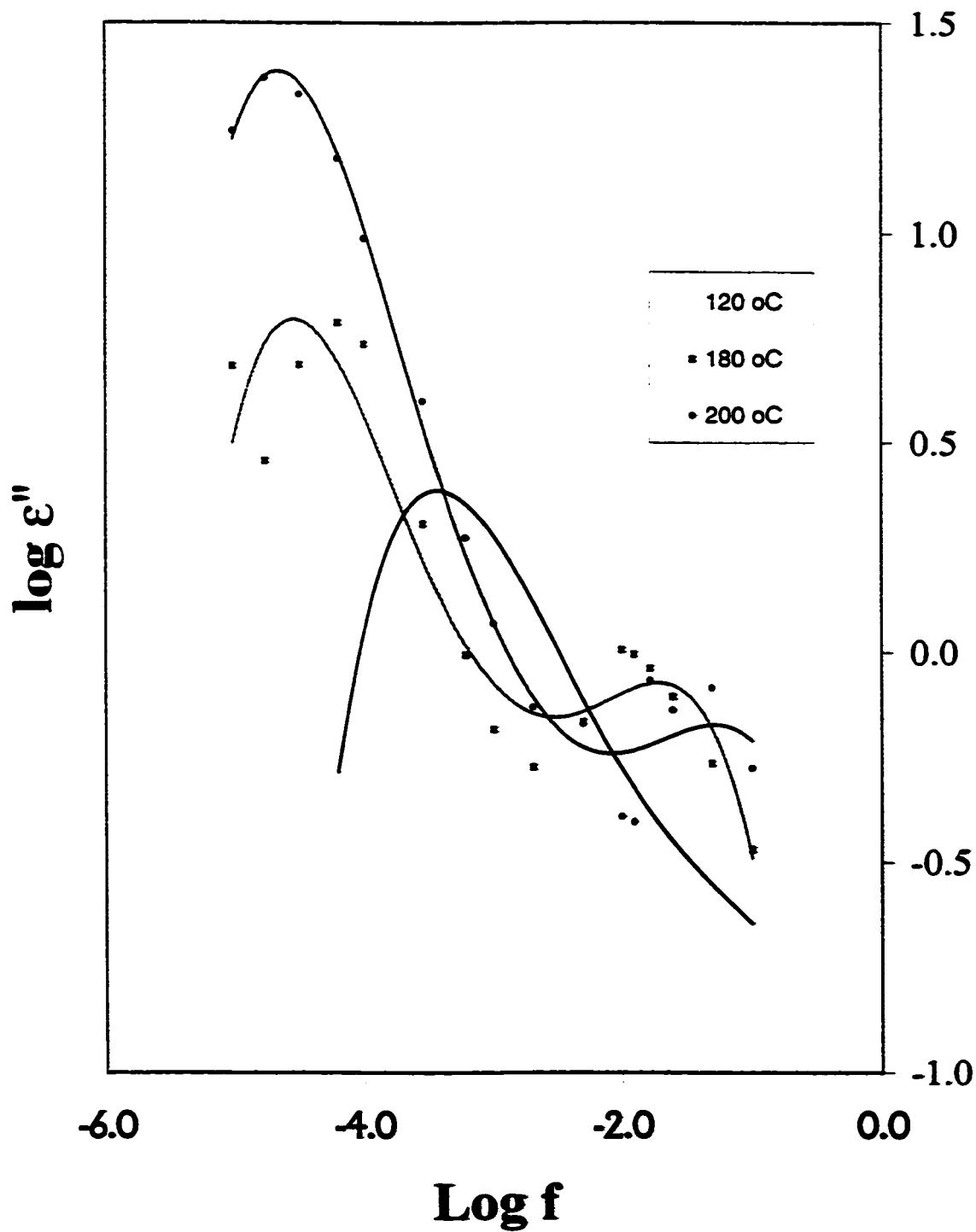
Fig. 4.11 Frequency dependence of dielectric loss ε" at various temperature ,Preapplied field 6MV/m, Electrode Material- Al for HN500 Film.

The temperature dependence of D.C conductivity (Log I vs. $E^{1/2}$) and loss peaks suggests that the same carriers are responsible for both the phenomena. The carriers that are trapped at the phase boundaries create a space charge and consequently polarization.

CONDUCTION CURRENTS IN POLYIMIDE (HN500 FILM)

5.1   INTRODUCTION

In this chapter the conduction currents are studied for Polyimide commercially available as (Kapton® HN500) and the results are evaluated against the available conduction current theories. Its chemical name is poly (4, 4' –diphenylene mellitimide) is a film-forming polymer manufactured by EI Dupont De Numerous Co USA. It is known as strongly heat resistant, and has excellent electrical and chemical properties. It has found applications as an insulator in motors, transformers, cables etc.

Hanscomb and Calderwood [45] studied the electrical conduction at high fields and for temperature range of 150 –175 °C and in polyimide film for both transient and steady state conduction. An exponential dependence of the current on the square root of the applied voltage is reported under the fast transient condition (80-100 ms). The currents are also found to be temperature and time dependent. The DC conduction is also field dependent. Both Poole –Frenkel and Schottky emission have been ruled to be the operative mechanisms; however Hanscomb [45] has put forward thermally assisted tunneling to be the operative mechanism, which was first suggested by Palanco [46]. Sharma [47] on the other hand has favored ionic conduction and has calculated the ionic jump distance of 5- 6 nm in the temperature range of 50-450 KVcm^{-1}.

Sussi [48] has observed two distinct regions in PTFE one at a field below 40 KVcm^{-1} and a lower temperature than 100 °C where the transport current is ohmic. For fields greater than 40 KV cm^{-1} the conduction currents deviate from the ohmic behavior and the plots could be fitted with a straight line with reasonable justification.

The objective of this work is to study the conduction current over the temperature range from 90 to 200 °C and electrical field strength up to 100 KVcm^{-1}. The measured conduction currents at various constant electric fields strengths and temperature are examined in the light of Schottky, Poole-Frenkel and Ionic conduction mechanisms.
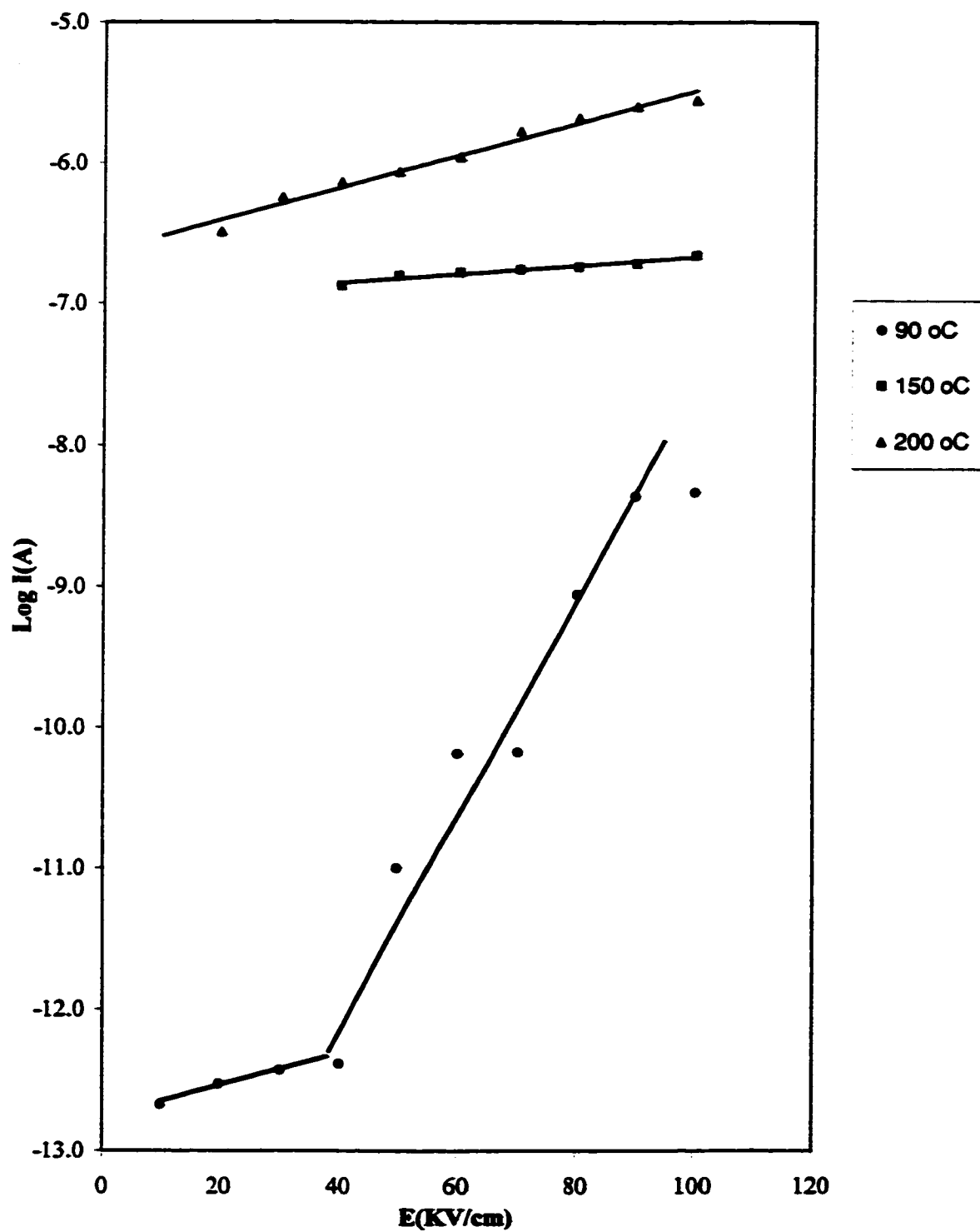
Fig. 5.1   Isochornal currents as a function of applied electric field at various constant temperature for HN500 Film.

5.2   EXPERIMENTAL PROCEDURE

The currents were measured on the specimen of Kapton® film with a thickness of 127 μm at various electric fields and constant temperatures in the range of 90 – 200 ^{0}C. The measuring electrodes were made of stainless steel with an outside diameter of 12 cm. The low voltage electrode had a diameter of 8.8 cm and a guard ring. It was connected to Keithley 617C electrometer .The temperature of the sample was controlled using an environmental chamber equipped with a microprocessor unit with the temperature control in the range of 0 to 300 ^{0}C.

The temperature control and measurement is accurate in the range of 0.1 ^{0}C. The voltage is applied using a Brandenburg stabilized DC power supply and the current is measured using Keithley 617C electrometer which is programmed to store the data which are retrieved from the front panel. The thermal protocol adapted during the study is reported in section 3.3.2. After keeping the temperature of the chamber constant for 1 hr the lowest value of electric field is applied and the current is recorded after 1000 seconds. Thereafter the field is increased in short steps and at each step a time of 600 second is allowed to settle down before the reading is taken. The settling times were chosen following the results of the charging and discharging currents.

5.3   RESULTS AND DISCUSSIONS

The conduction current results are analyzed and the results are interpreted on the conduction theories put forward. Four mechanisms have generally been put forward; they are Ionic conduction, Schottky emission, Pool-Frenkel effect and space charge effect.

From the slopes and intercepts of the curves the value of parameters like the Ionic jump distance, high frequency dielectric constant, etc can be found out and are summarized in table 5.1.

Fig 5.1 shows the conduction current as a function of electrical field at various temperatures for 127μm thick film and electrode material aluminum. For a temperature of 90 ^{0}C two slopes are observed while at higher temperatures the currents deviate from the ohmic plot and the graph can be fitted into straight lines.
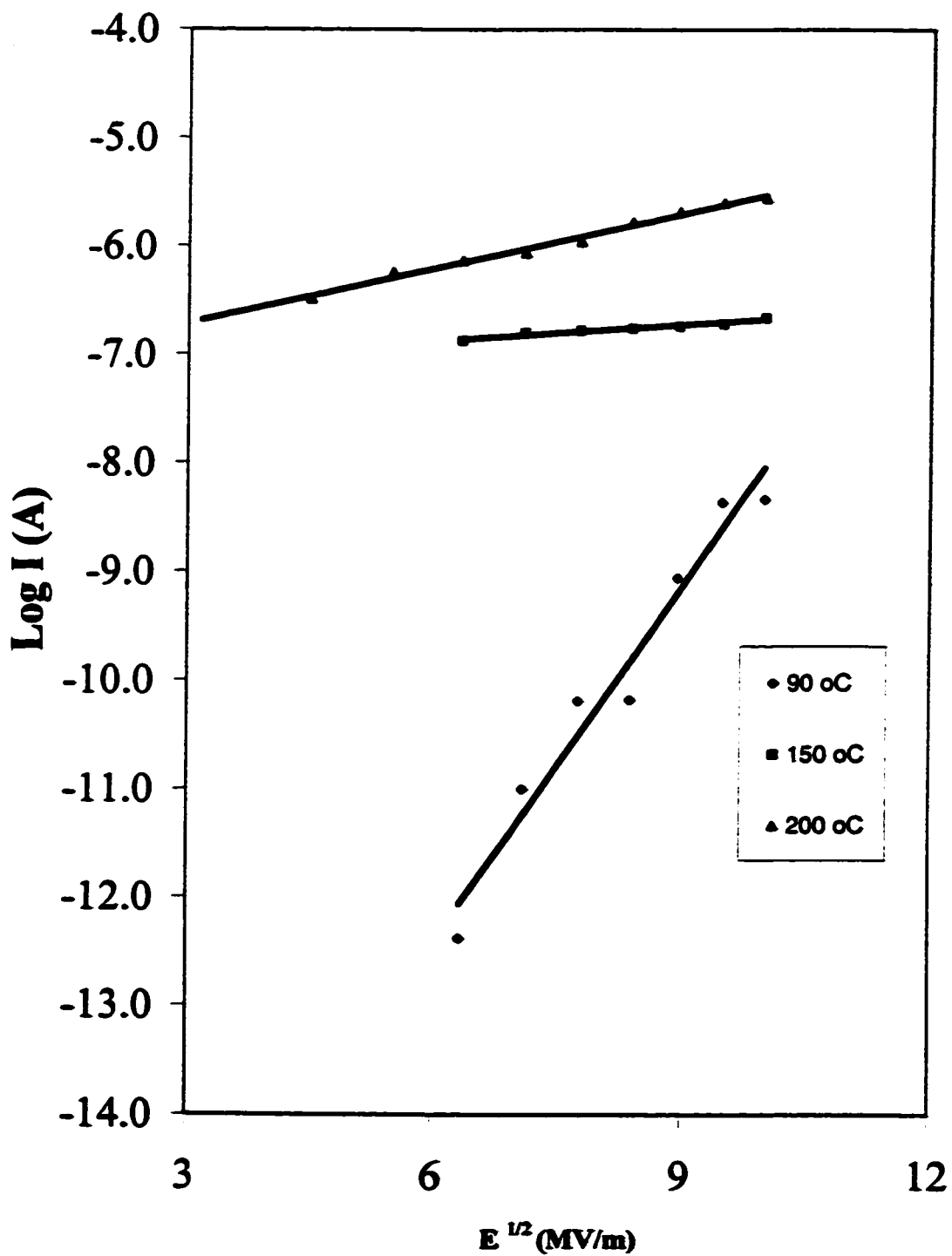
Fig. 5.2 Log I vs.E$^{1/2}$ at various constant temperatures for HN500 Film.

For mechanisms of ionic hopping the current density at high fields can be explained by the equation

$$J = 2 \, e \, N \, a \, v \, \exp(-\Phi/KT) \sinh eaE/2KT \qquad (5.1)$$

where e is the charge of the ion, v is the attempt to escape frequency, a is the separation distance between the traps, ϕ is the barrier height, E is the electric field, T is the absolute temperature, K is the Boltzman's constant.

The above equation can be reduced to

$$I = I_o \exp(eaE/2KT) \qquad (5.2)$$

I_o is the zero electric field emission current and is given

$$I_o = 2AeNa \, v \, \exp(-\phi/KT) \qquad (5.3)$$

where A is the surface area of the electrodes. From equation (5.2) it can be shown that the plot of I vs. E will yield a straight line having a slope of (ea/2KT) from which the separation distance between the traps can be calculated from the slope. The separation distances calculated from the fig 5.1 are shown in the table 5.1. From higher temperatures the jump distance is found to be increasing .The estimated values of the jump distance are 5.95 nm for 150 ^{0}C and 9.38nm for 200 ^{0}C. Values of ionic jump distance have been estimated by Sawa [37]. Sawa's values show a strong dependence on the temperature while the values obtained by Sharma [47] show only a moderate dependence on the temperature. Sawa [37] has reported that the different values of the ionic jump distance results from the different heat treatment of the samples adapted by different workers.

The nonlinear behavior of polymers at high fields may also be due to thermionic emisson either from the cathode or from donor like defect states in the sample (Poole-Frenkel effect). In the case of the field assisted thermionic emissions from the cathode the current density J is expressed for the Schottky equation as

$$J_s = A_c \, T^2 \exp(\phi_s - \beta s E^{1/2}/KT) \qquad (5.4)$$

Where A_c is the emission constant, T is the temperature, E is the electric field, βs is the Schottky coefficient given by

$$B_s = (e^3/4\pi\varepsilon_o\varepsilon_\alpha)^{1/2} \qquad (5.5)$$

Where e is the electronic charge, ε_o is the permitivity of free space, ε_α is the dielectric constant.

In the latter case the current density may be expressed according to the equation

$$J_{pf} = B \; E \; exp(\phi_{pf} - \beta_{pf} E^{1/2} / KT) \tag{5.6}$$

Where B is a constant, ϕ_{pf} is the zero field ionization energy of the donor, $\beta_{pf} E^{1/2}$ is the reduction in this energy due to application of electric field.

The plot of I vs. $E^{1/2}$ gives a reasonably straight line as shown in fig.5.2 and from the slopes the value of β_s and ϵ can be calculated. The agreement of the above-obtained values with the determined dielectric constant should give a reasonable indication of the process thought to be occurring.

The calculated values of the dielectric constant from the slopes of fig 5 .2 are found to be in the range of 0.069 to 1.8952 .For the Poole frenkel effect the values of ϵ_{pf} would be four times that obtained for the schottky dielectric constant. The dielectric constant as obtained for Poole-Frenkel gives a value of 0.207 at 90 ^{0}C, 1.292 for 200 ^{0}C and 5.6 for 150 ^{0}C. . The experimental value of the dielectric constant as obtained from [49] is 3.5. The values obtained for 150 ^{0}C are about 38% higher than the experimental values. Hence both schottky emission and Poole Frenkel may be ruled out as the possible mechanisms.

The zero electric field emission current density according to equation (5.4) is given by

$$J_o = A_c T^2 exp (\phi_s / KT) \tag{5.7}$$

where A_c is the emission constant and ϕ_s is the Schottky barrier height.

It is obtained from the y-axis of the intercepts of fig (5.2) from which the emission constant A_c can be obtained. The values of the emission constant can be obtained as 9.6282×10^{-5} to 2.42×10^{-3} Acm^{-2}K^{-2} They are about 5 and 3 orders of magnitudes lower than the expected values of 120 Acm^{-2}K^{-2}. Hence this further rules out the Schottky emission as a possible conduction mechanism.

The activation energy for the steady state conduction can be found out by plotting the extrapolated zero field emission current I_o that is obtained from the figure 5.1 against reciprocal temperature. A plot is shown in the figure 5.3. Equations 5.4 and 5.6 suggest that these should be a straight line. This is seen to be holding reasonably well. From the slope the effective work function between the Fermi level of the metal cathode and conduction band of the insulator can be calculated and is obtained as 1.20 eV. Calderwood [45] has estimated the values in the range of 1.5 to 1.53 for Kapton® H-Film.
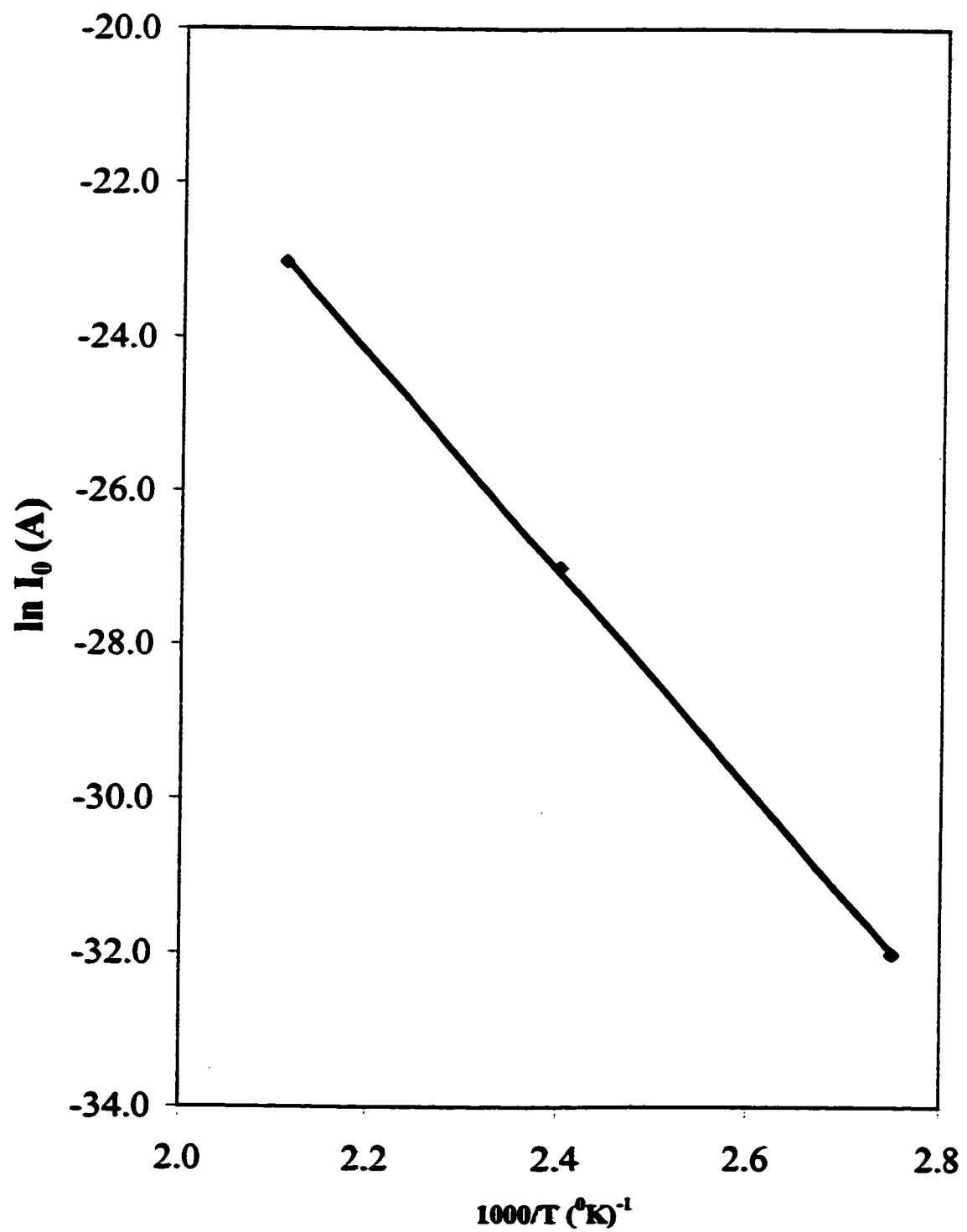
Fig. 5.3   Plot of I_0 as a function of 1000/T for HN500 Film.

The plot of I vs. $E^{1/2}$ does not show a linear variation with the reciprocal temperature hence this not only goes against the Poole Frenkel but also against the thermally assisted tunneling. Although on the basis of the present data alone it is not possible exclusively whether the conduction at high fields in kapton is ionic, Poole Frenkel or due to the thermally assisted tunneling, yet when these reports are evaluated and also seen in the background of other investigators it appears to more due to Ionic conduction.

Table 5.1   SUMMARY OF CONDUCTION CURRENT RESULTS IN HN500 FILM

T ^{0}C	Ionic Jump Distance	ε_s	ε_{pf}	A cm^{-2}K^{-2}
90	5.95	0.069	0.207	9.682 x10^{-5}
150	7.38	0.124	0.596	1.38 x10^{-3}
200	9.38	0.322	1.29	2.42 x10^{-3}

CHARGING/DISCHARGING CURRENTS IN POLYIMIDE-FEP FLUOROPOLYMER FILM (150FN019 FILM)

In this chapter the procedure and the results of the charging/discharging currents on Kapton®150FN019 Film (Teflon coated on one side) supplied by Dupont are investigated and the effect of the various parameters are studied. The low frequency dielectric loss (ε'') is obtained from the absorption currents using Hamon's approximation.

6.1   EXPERIMENTAL TECHNIQUES

The charging and discharging currents are measured in kapton™ 150FN019 film under the influence of varying parameters. Fig 3.2 shows the experimental setup. Before the commencement of the experiments the sample were heat treated for 12 hrs at 200 ^{0}C to remove any moisture content. The samples were subjected to a thermal protocol cycle, which has been described in section 3.3. The results on a given set of parameter have been conducted on the same film. The results have been reported for temperature range 50-200 ^{0}C in which the temperature is increased in short steps while the field is maintained at 6 MVm^{-1} that corresponds to 190 volts. The results are also reported for a constant temperature of 200 ^{0}C and various fields in the range of 4-12 MVm^{-1}. A three terminal electrode is used to reduce the effects of the stray fields. The currents are measured with the Keithley 617C electrometer. Infrared spectroscopy analysis is carried out on the sample to determine the Teflon coating and the results are shown in the figure 6.1 and 6.2. In Fig 6.2 a peak of fluoride is observed while in fig. 6.1 only carbon peak is observed which confirms that side of figure 6.2 has a Teflon coating. These results are required to study the cathode effects in the films.

Before each measurement a blank run is performed in order to free the sample of extraneous charges. This run consisted of raising the temperature to 200 ^{0}C and holding it up to 5 hrs to reduce the effect of space charge build up.
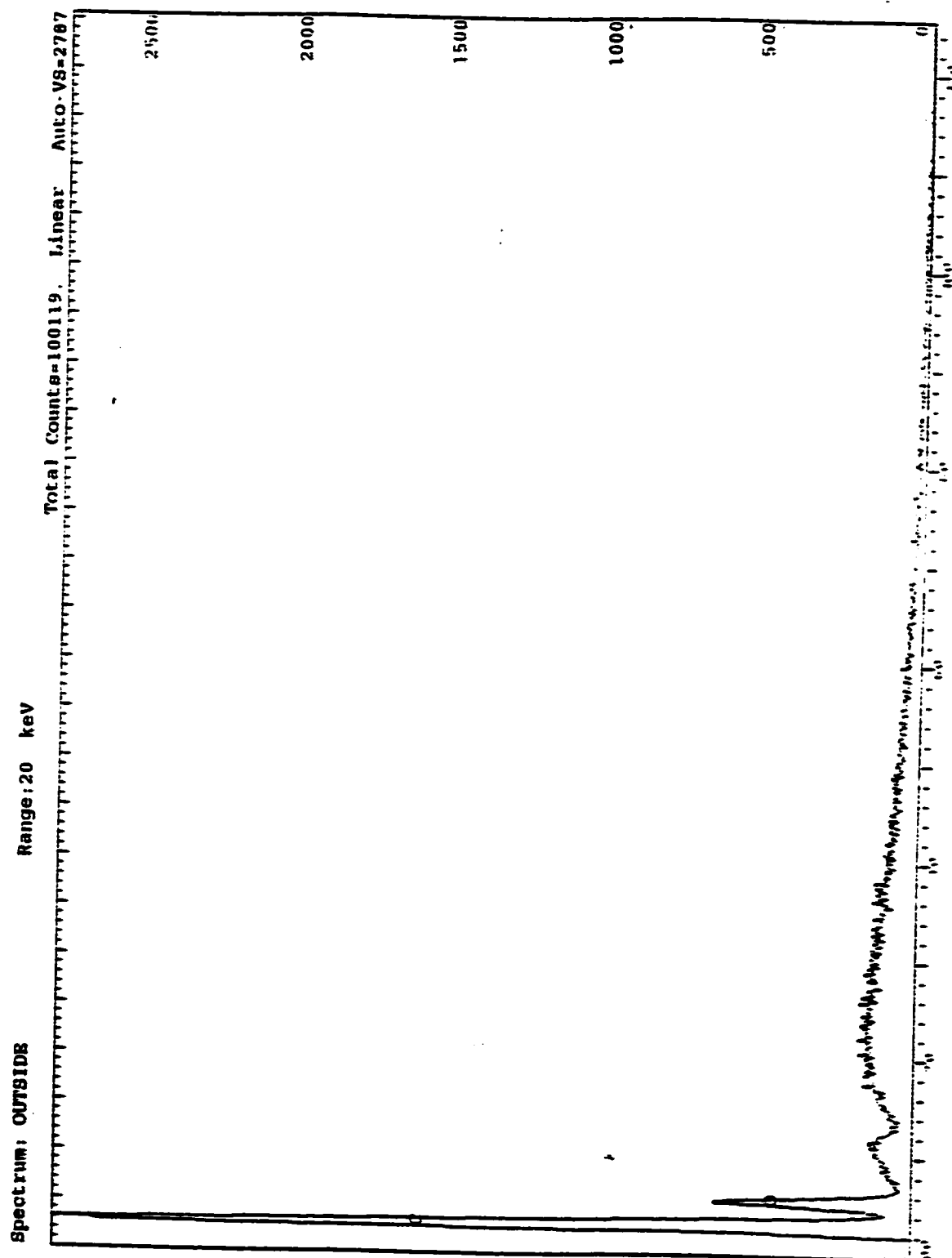
Fig. 6.1   **Infrared spectroscopy analysis for 150FN019 Film (outside)**
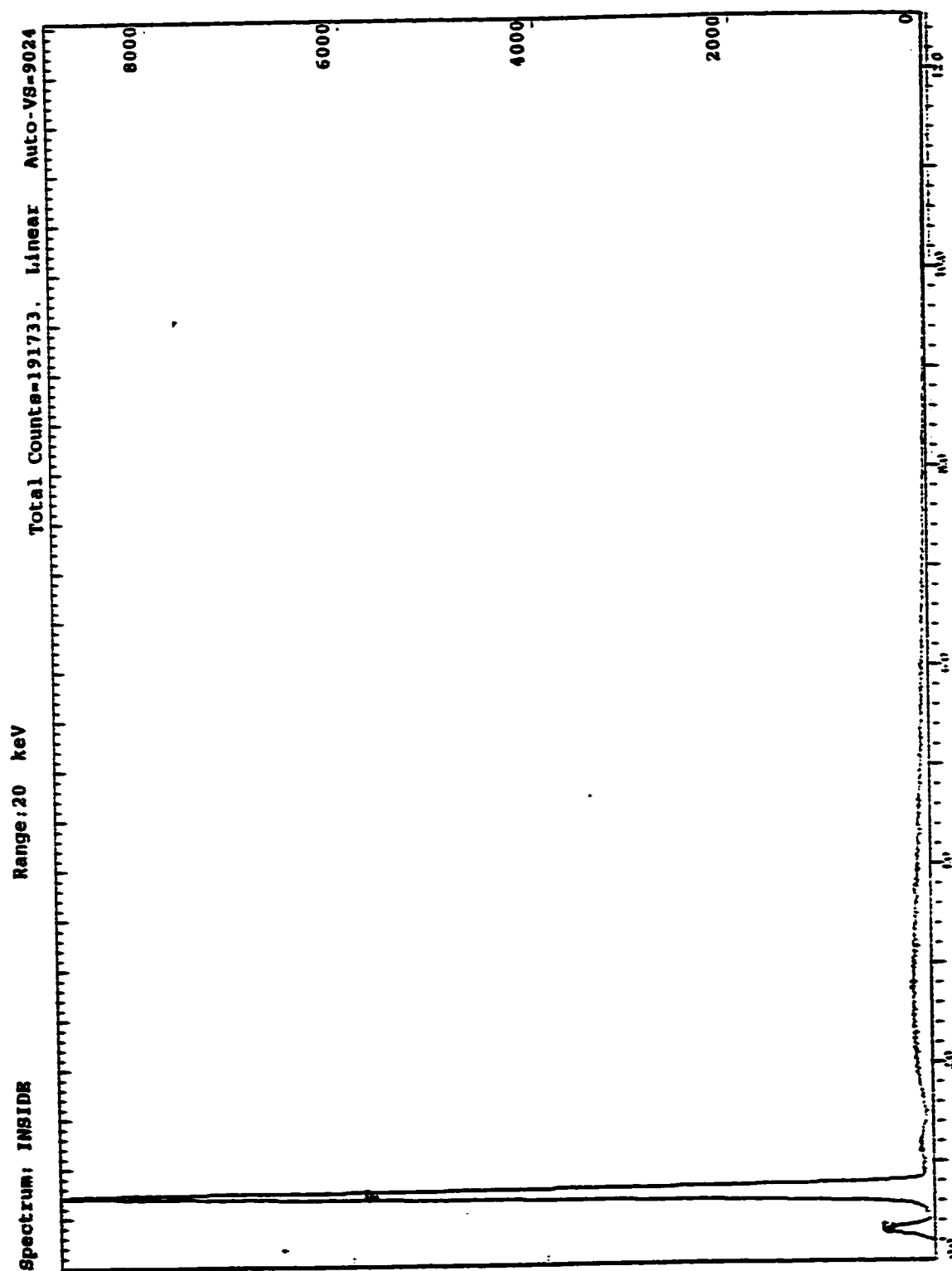
Fig.6.2 **Infrared spectroscopy analysis for 150FN019 Film (inside)**

Spectrum: INSIDE   Range:20 keV   Total Counts=191733. Linear   Auto-VS=9024
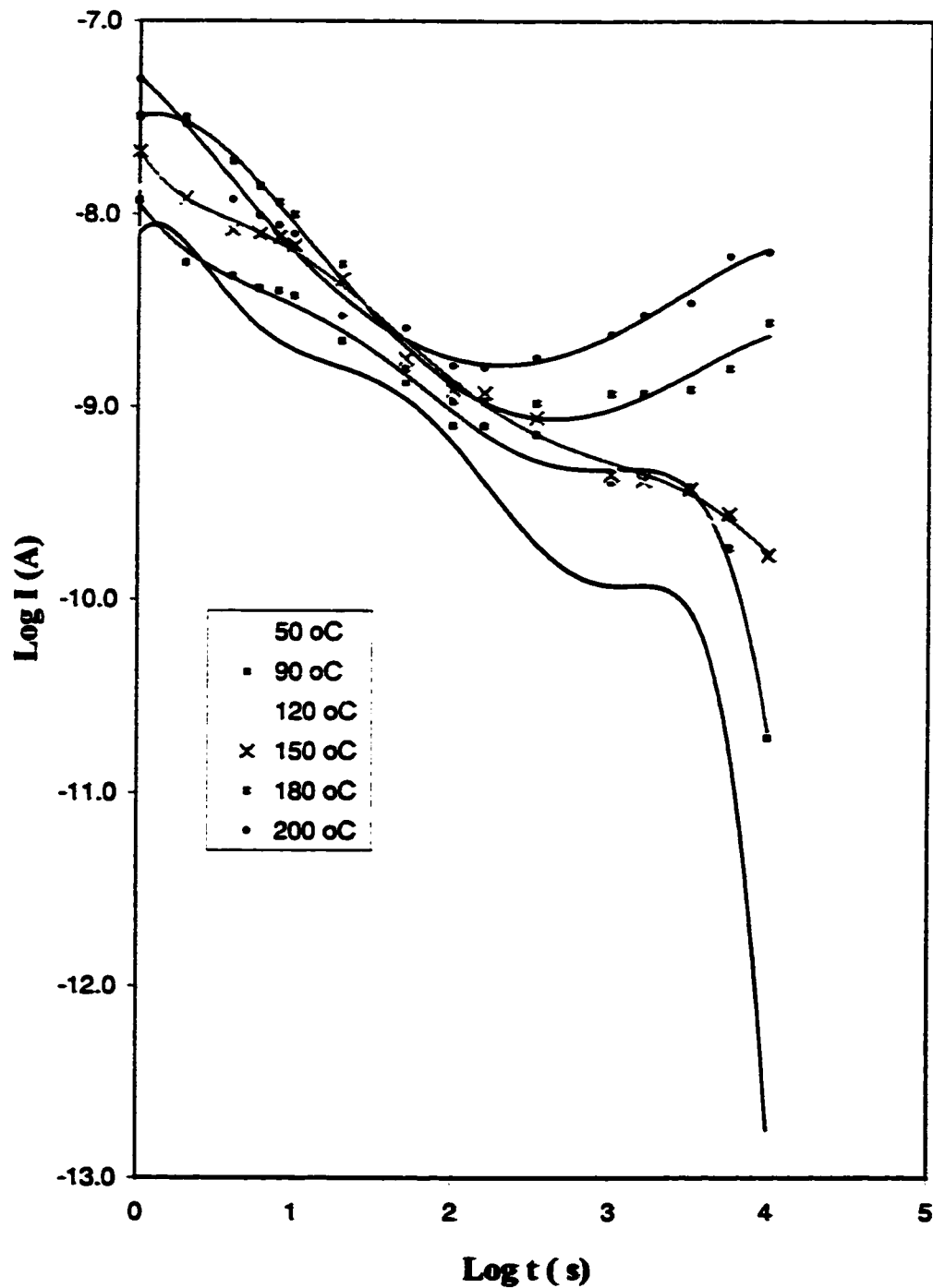
Fig 6.3 Time dependence of charging current for various temperatures and constant field of 6 MV/m for 150FN019 Film, Electrode Material -Al
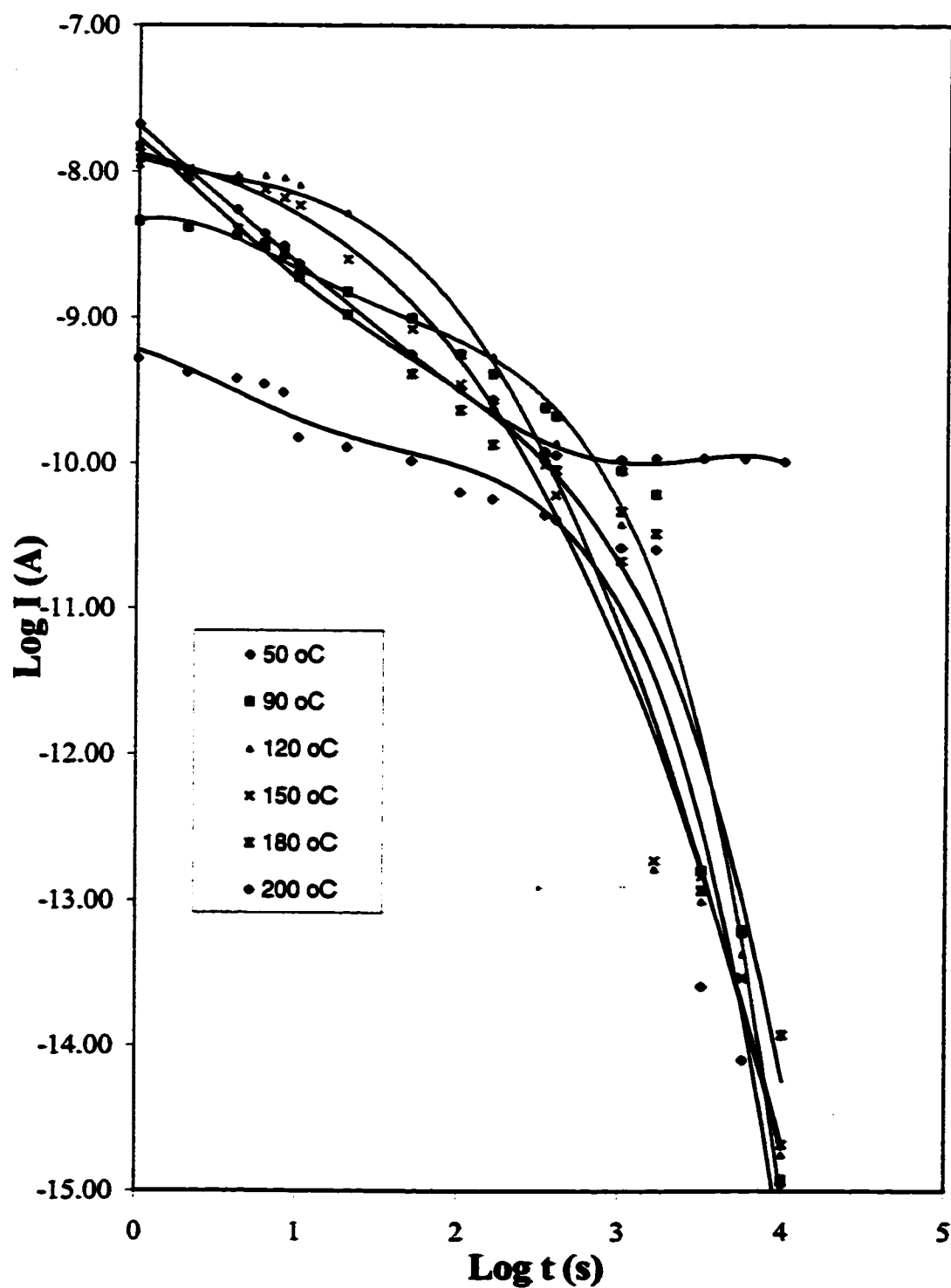
Fig. 6.4 Time dependence of discharging current for various temperatures and constant field of 6 MVm⁻¹, Electrode material -Al for 150FN019 Film.
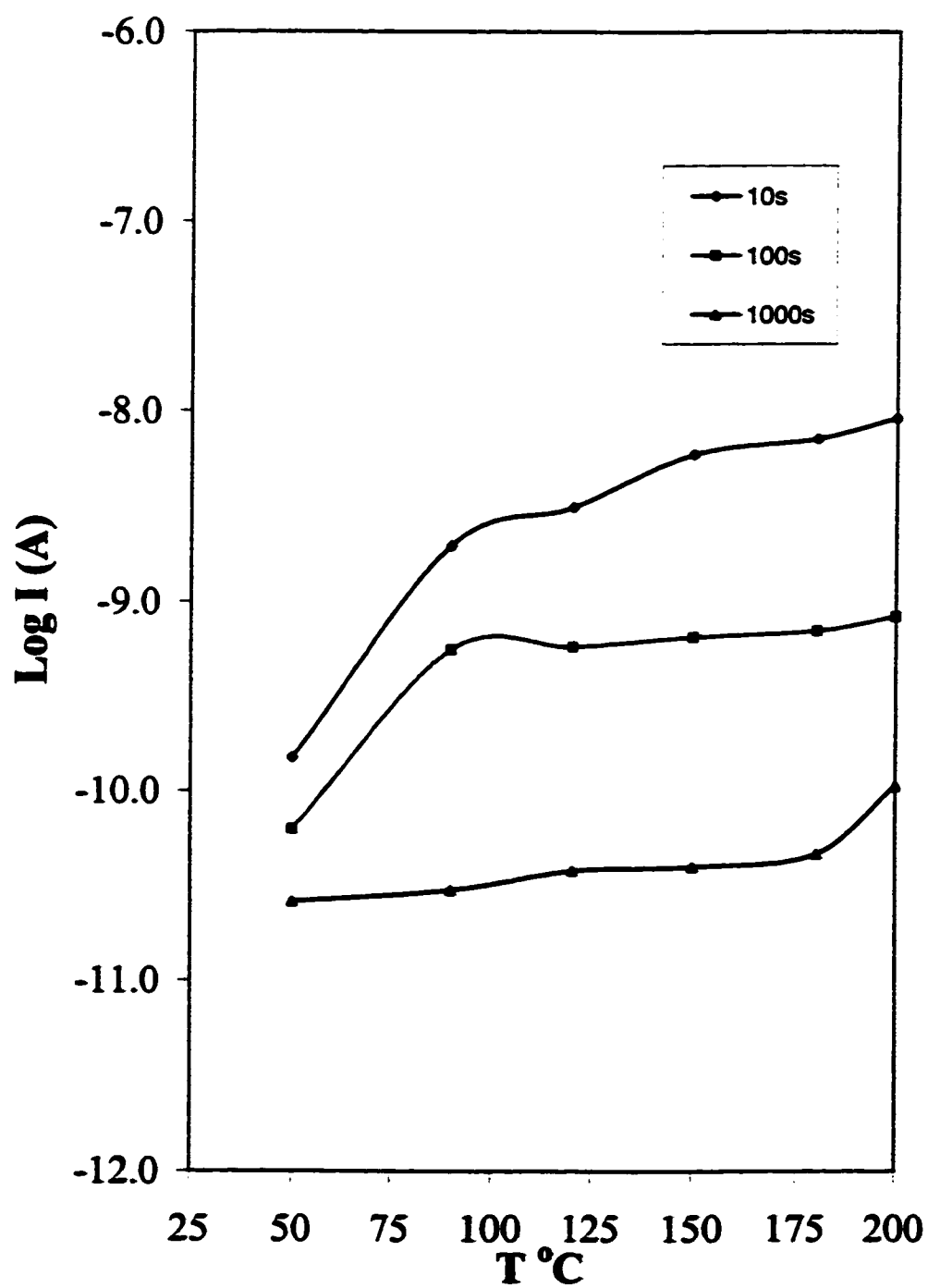
Fig. 6.5 Temperature dependence of discharging current at prescribed times and 6 MVm⁻¹ field,Electrode Material-Al for 150FN019 Film

6.2   RESULTS AND DISCUSSION

6.2.1. Charging and discharging current

a)   Time dependence

Figure 6.3 shows the charging currents in Kapton®(150FN019 Film) for $31.5\mu m$ sample respectively with aluminum electrodes at constant field and various poling temperatures for duration of 4 hrs. The charging current decay slowly with time with the value of index n in the range of 0.52 to 1.39 for temperatures up to 150 °C. For temperatures greater than 150 °C, the current is seen to decrease with value of n varying between 0.61 to 0.74 for times up to 100 second and for longer times the current increases. The slow decrease of the current in the initial stages can be attributed to the slow filling of the traps The observed behavior has also been interpreted due to the arrival of the space charge front following transport from the source electrode [50].

Fig 6.4 shows the plot of discharging current at constant field of 6 MVm⁻¹ and various temperatures of 50 –200 °C. For temperatures 50 to 180 °C the current decreases with the value of n in the range of 1.47 to 1.69. For temperature of 200 °C the value of n is found to be 0.57. The decay of the discharging currents can be interpreted in terms of superposition principle explained by Lewis [51]. Lewis showed that grounding of the sample be considered as a superposition of a previous applied voltage. When the sample is grounded then the total discharging current can be considered as the sum of the original current plus the charging current that flows upon application of the superimposed voltage. The more convincing model can be in terms of Jonscher universal dielectric theory [52] which states that the time domain response of the current has two value of n. An increase in the value at longer periods is due to dipolar mechanisms while the decrease in the value of n at longer period is due to interfacial polarization.

b)   Temperature dependence

Figure 6.5 shows the discharging currents at prescribed times over a temperature range of 50 to 200 °C and applied voltage of 190V. These values are plotted from the discharge currents of figure 6.4. The curves show no significant peaks and increases smoothly.

Fig. 6.6 Charging current at various fields and constant temperature of 200 °C, Electrode
Material- Al for 150FN019 Film.

Fig. 6.7 Discharging current for various fields and constant temperature of 200 °C,Electrode Material -Al for 150FN019 Film.
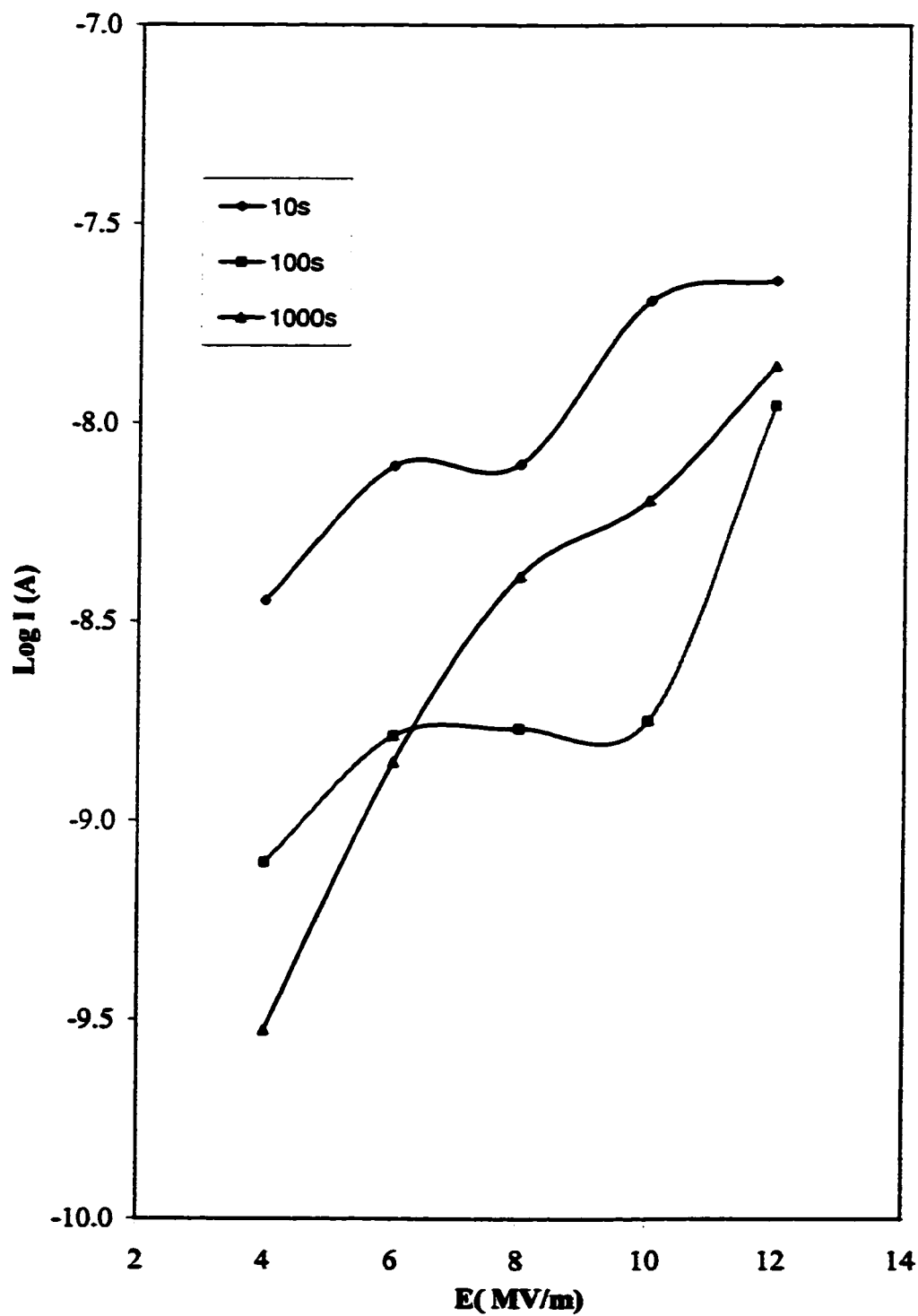
Fig. 6.8 Field dependence of Isochornal charging current at 200 °C at prescribed times,Electrode Material -Al for 150FN019 Film.

c) Field dependence

Figure 6.6 shows the charging currents at 200 ^{0}C and various field strength of 4 to 12 MVm^{-1}. At 4 MVm^{-1} field, the current decreases and the value of n is 0.62 where as for the fields 6 MVm^{-1} and higher the current decreases with a value of n in the range of 0.50 to 0.82 for up to 100 seconds. At times higher than 10^2 seconds the current increases to reach steady state conduction current. Chouhan [38] has found similar increase of current for Kapton®H film for temperatures 200 ^{0}C and field 8 MVm^{-1}. Figure 6.7 shows the discharging current at 200^0 C and various fields .The current decreases with a value of n in range of 0.56 to 0.60. The current decays fast for times up to 10^3 seconds where the power law holds good with a value of n in the range of 0.74 to 0.81 and for times greater than 10^3 and the current decay is much less pronounced with n ranging from 0.02 to 0.05. The charging and discharging currents show mirror images for low temperatures and are dissimilar for all other temperatures and fields. This behavior has been observed in other polymers [9,53]. The slopes of discharging current shows two values of n one at t < 10^3 sec and other at>10^3. This suggests that dipolar processes are operative mechanism at temperatures up to 90 ^{0}C and interfacial polarization is the operative mechanism at longer times and higher temperatures.

Figure 6.8 show the field dependence of the charging currents at a constant temperature of 200 ^{0}C .The charging currents are plotted at times 10 to 1000 seconds and it seen from fig 6.6 the current decrease at 100 seconds and then an increase is observed at 1000 seconds.

d) Effect of Electrode Material

The effect of electrode materials is investigated using aluminum and silver electrode material at temperature of 200 ^{0}C and electric fields up to 8 MVm^{-1}.

Figure 6.9 shows the charging current for silver electrodes at 200 ^{0}C and electric fields up to 12 MVm^{-1}. The currents decrease for up to 100 seconds with a value for n in the range of 0.51 to 0.68 which is approximately the same power law as followed for the aluminum electrode except that the magnitude of current for silver electrodes is more than that of aluminum electrode.

Figure 6.10 shows the discharging current at 200 ^{0}C and field up to 12 MVm^{-1} for silver electrode material. The currents decay with value of n ranging from 0.60 to 0.82.The discharging current comparison of figure 6.10 and 6.7 also does not show very significant
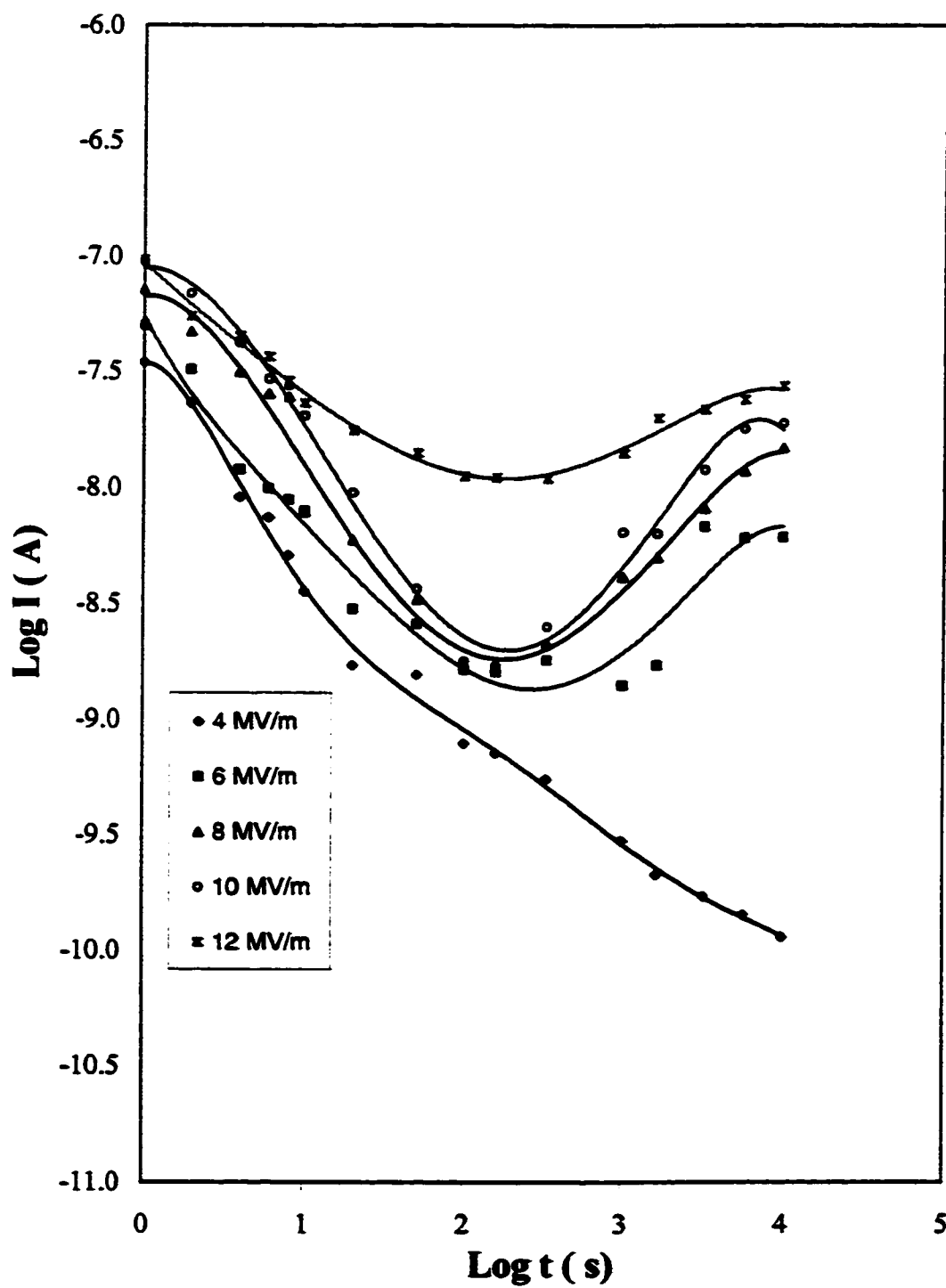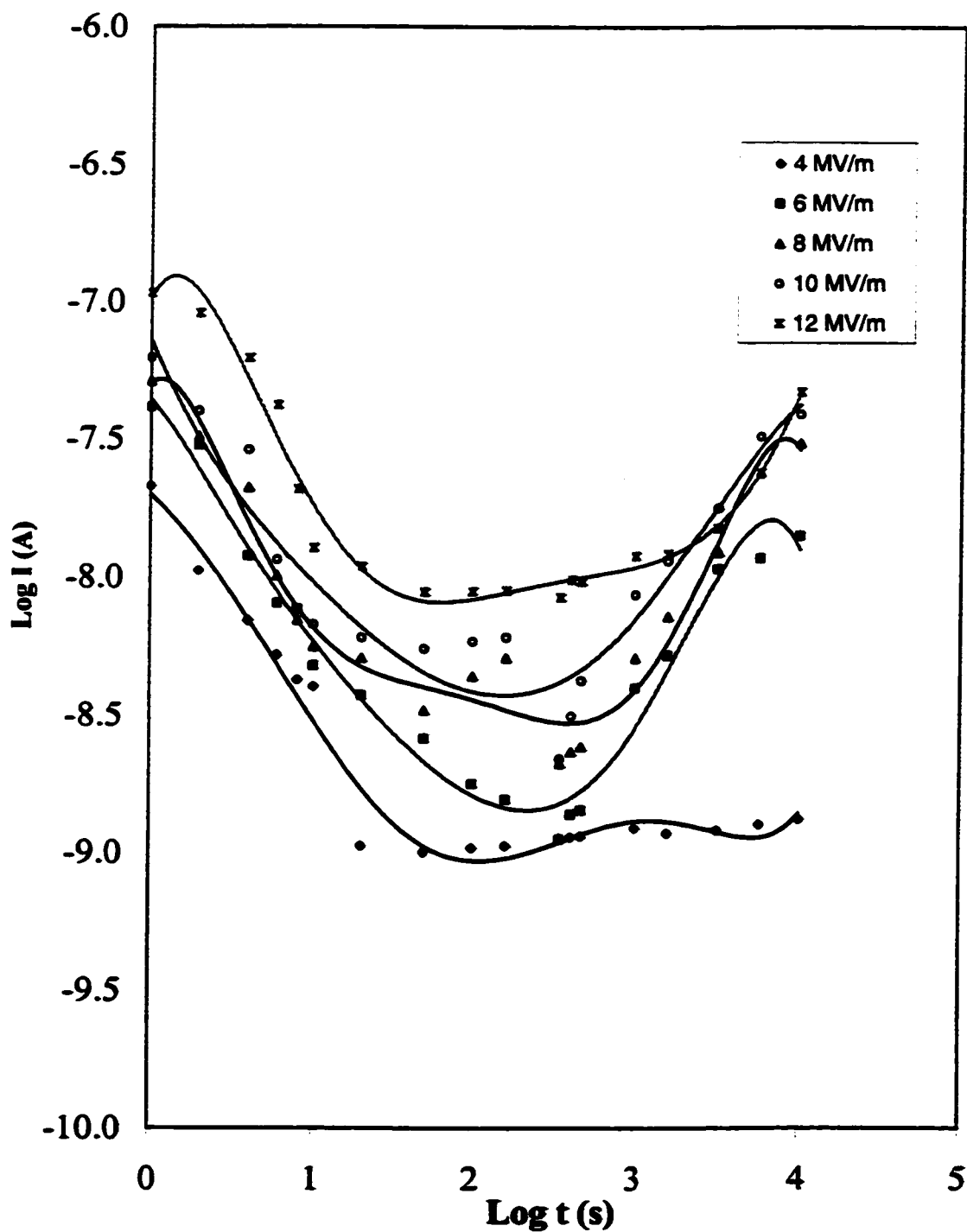
Fig. 6.9 Charging current at various electric fields and constant temperature of 200 °C,Electrode Material-Ag for 150FN019 Film.
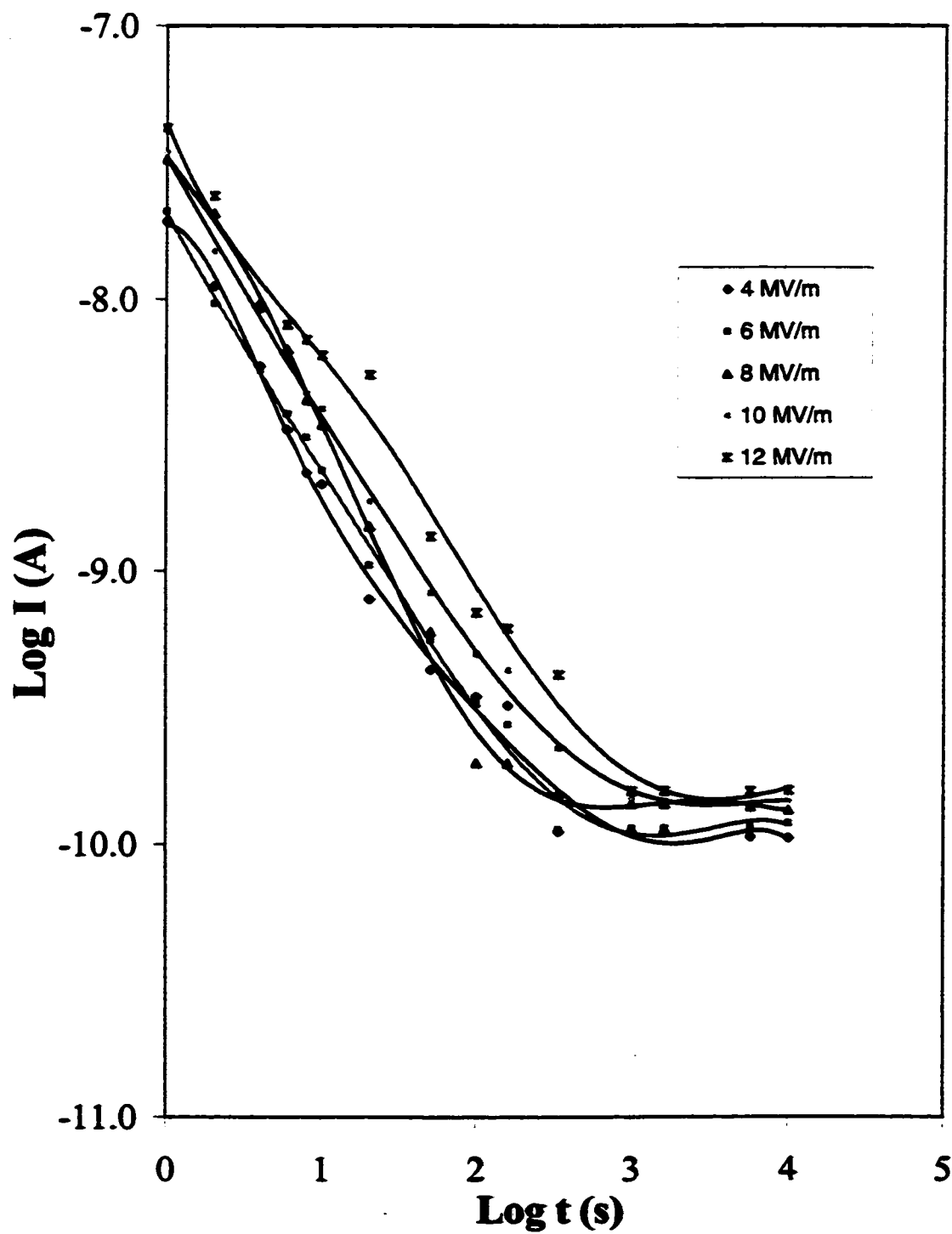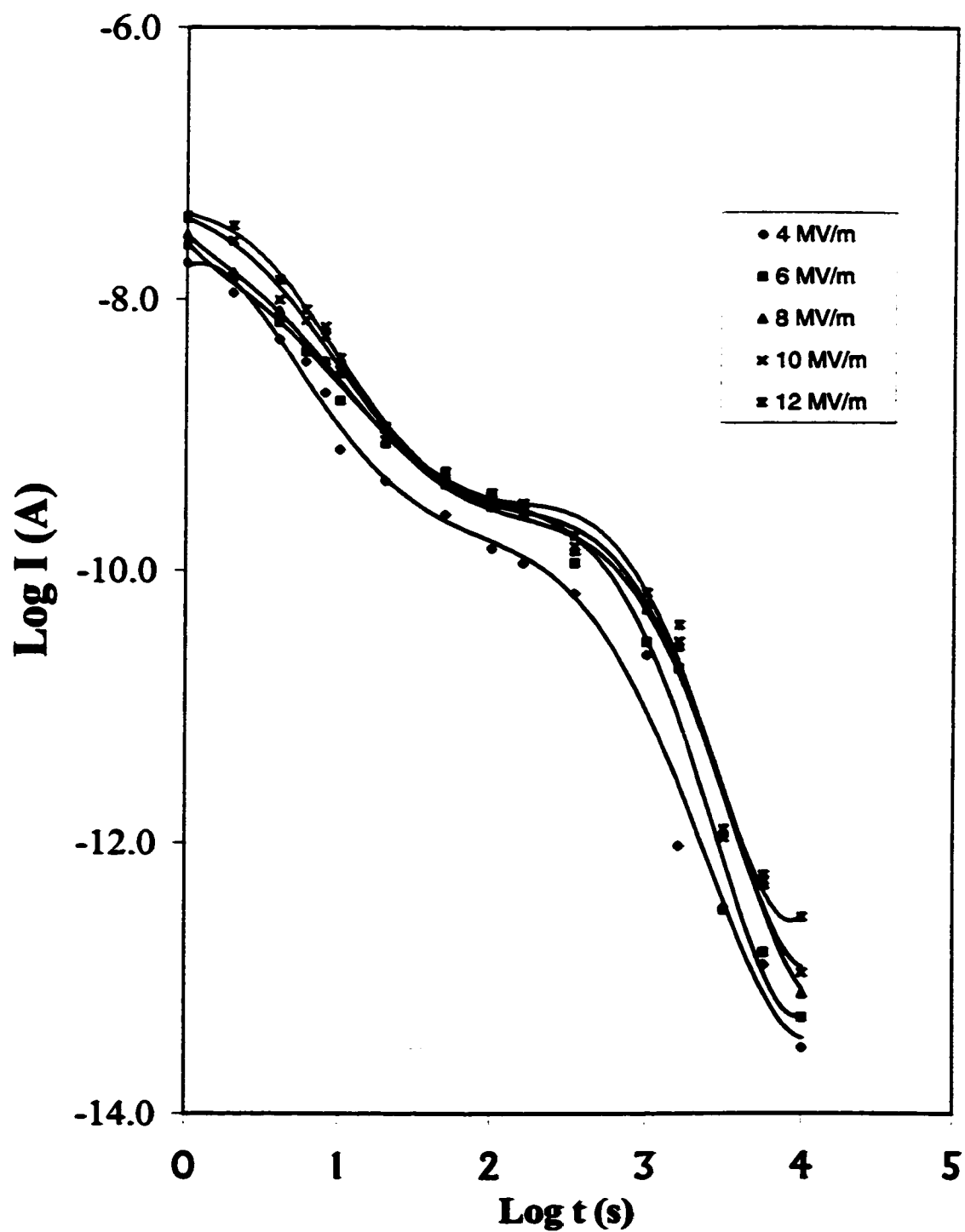
Fig. 6.10 Discharging current at various electric fields and constant temperature of 200 °C, Electrode Material- Ag for 150FN019 Film.
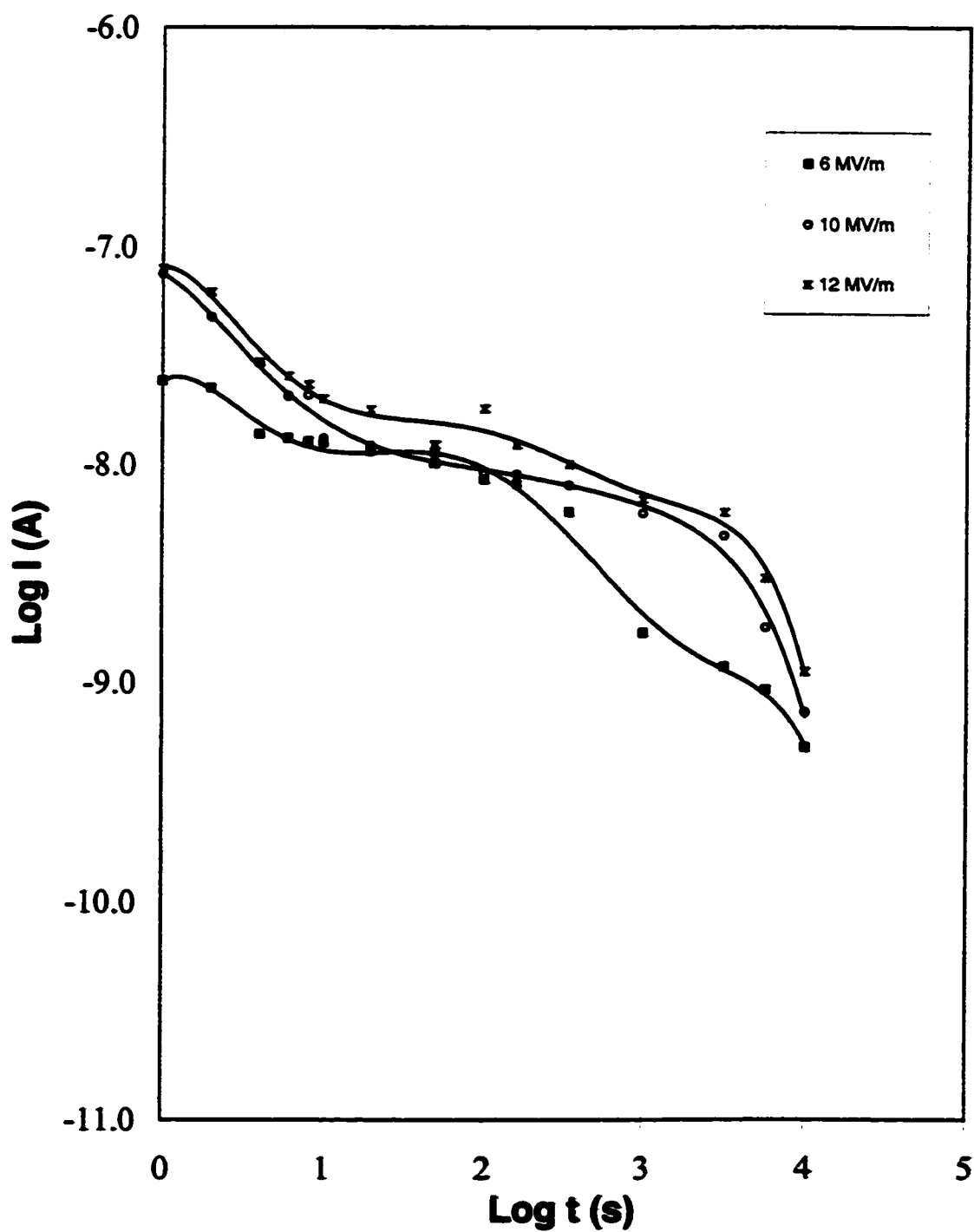
Fig. 6.11 Charging current at 200 °C and various fields ,Teflon coated surface as cathode, Electrode Material -Al for 150FN019 Film.
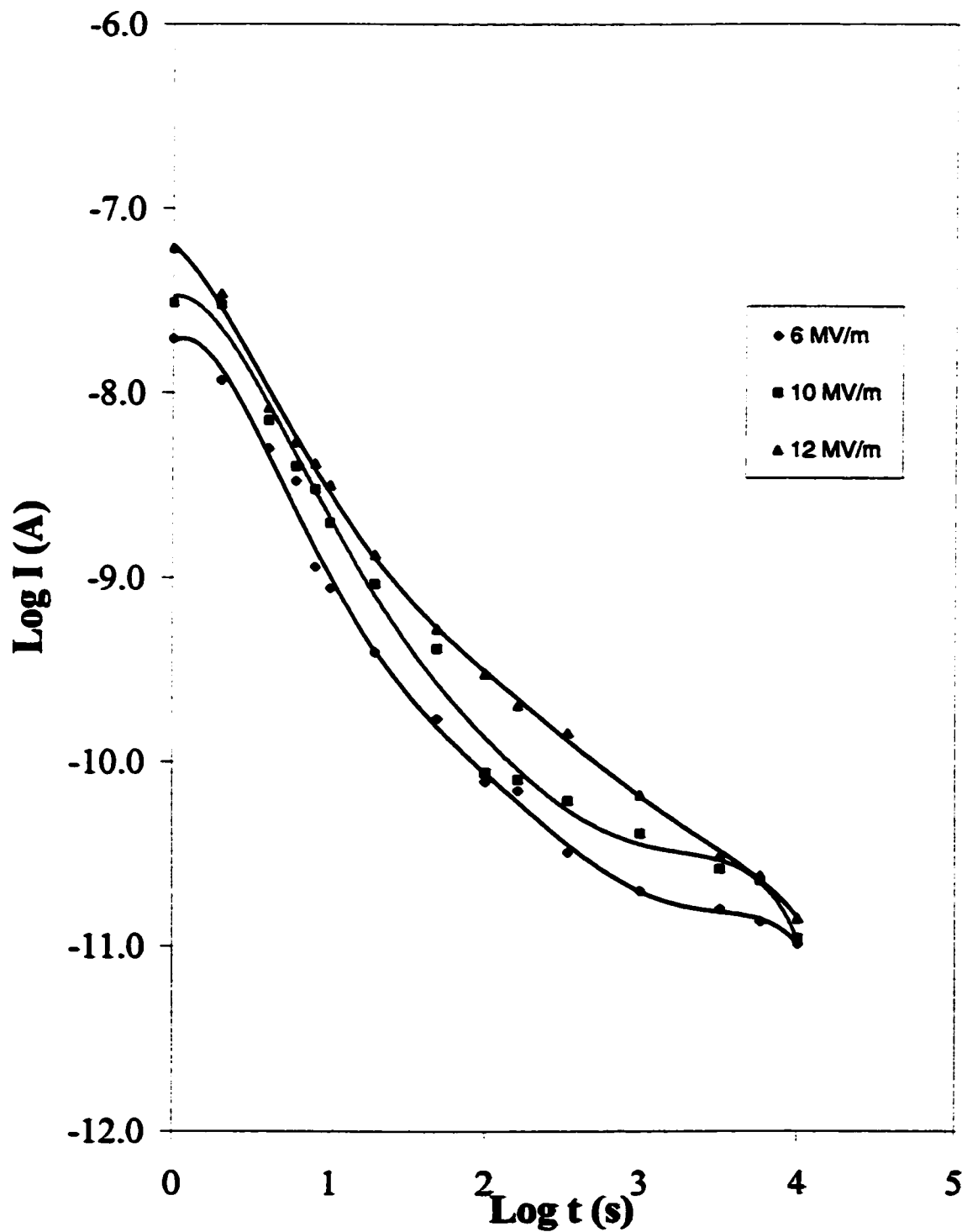
Fig. 6.12 Discharging currents for 200 ^{0}C and various fields,Teflon coated surface as cathode,Electrode Material -Al for 150FN019 Film.

dependence on the electrode material except that the current reduces at a faster rate for silver electrode material than that for the aluminum.

e) Cathode effects

Figures 7.11 and 7.12 show the charging/discharging current at 200 °C and various fields with Teflon coated side as cathode .The charging current decreases with a value of index n in the range of 0.44 to 0.49 and no increase in current is observed at any time. The discharging current decreases with a value of n in the range of 0.82 to 0.92. Comparing the charging currents of figure 6.11 and figure6.6 (showing the charging current with Kapton® side surface as anode), it is seen that there is no increase of charging current after 10^2 seconds. Also no electrode material dependence is found, therefore it can be deduced that there is no current injection from the cathode and that the carriers are generated in the bulk of the materials. The ions generated in the bulk of the dielectric film drift towards the cathode. They are blocked at the polyimide –FEP interface creating a decrease in the local field that leads to a decrease of current as seen in the figure 7.6. In the latter case the ions generated in the bulk of the material move towards the cathode and the local field is increased leading to increase in the current. If currents are observed at longer times ($>10^5$ seconds) the currents would be seen flatten out to a constant value.

6.2.2 Low frequency dielectric loss (ε")

The absorption current, which flows in the dielectric when a step a DC voltage may be used to obtain the information on the frequency dependence of loss factor (ε"). Hamons transform [29] described in the section 2.3 is used and the loss factor is given

$$\varepsilon'' = I(t)/2\pi f C_0 V$$

where I (t) = current at time t, C_0= geometric capacitance when the assembly replaced with vacuum, V is the step voltage, f is frequency given by 0.1/t.

Fig 6.13 and fig 6.14 shows the results of the calculated value of (ε") at low frequencies for two temperature regimes $0 \leq T \leq 120$ °C and $120 \leq T \leq 200$ °C. Fig 6.13 shows one broad peak for temperature up to 90 °C. It is seen that the maximum frequencies shift to higher value with the temperature from 50 to 90 °C indicating the presence of dipolar polarization. Figure 7.14 shows that the magnitude of the loss factor increasing by on order of magnitude and no peaks
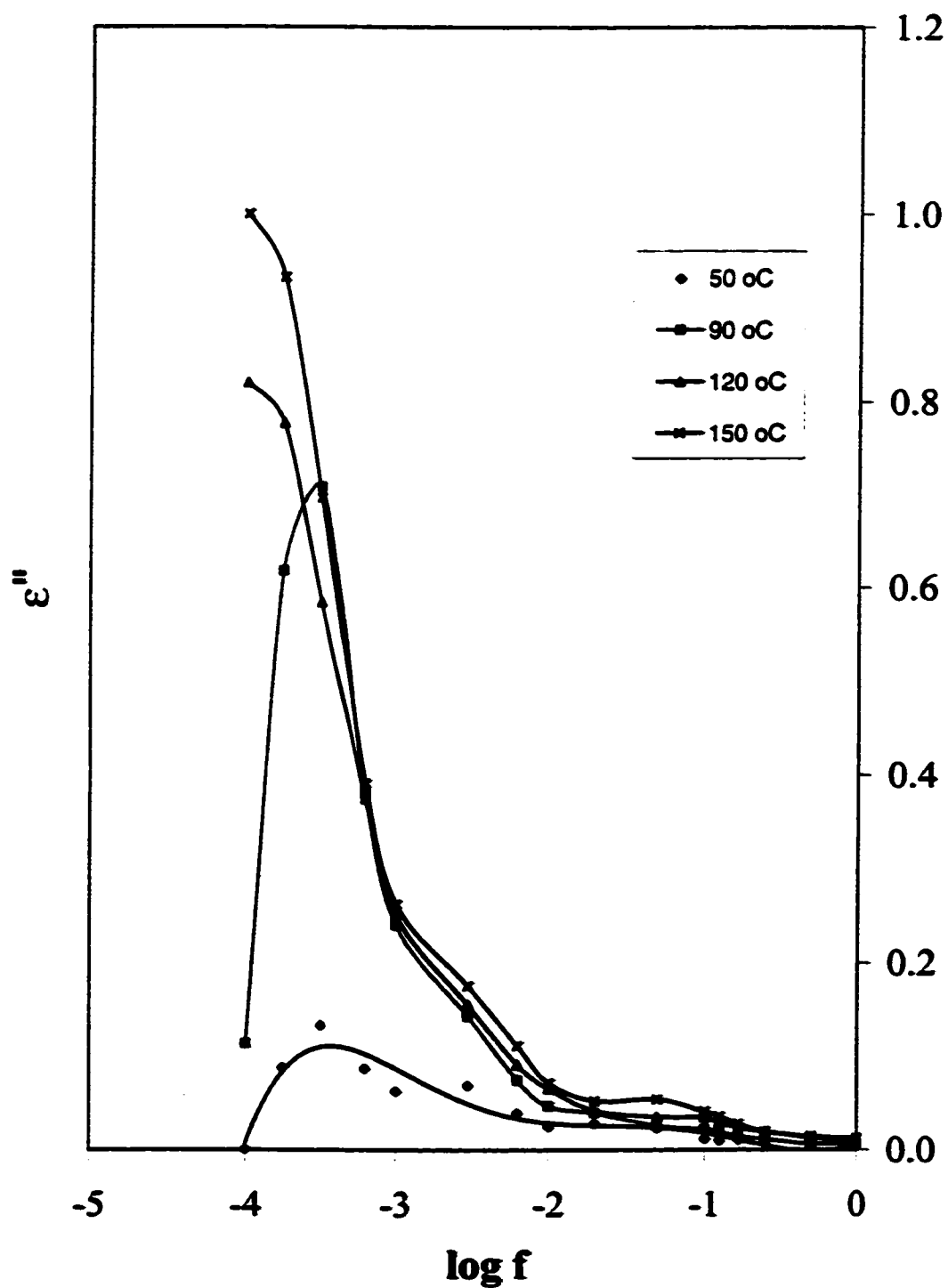
Fig. 6.13 Frequency dependence of dielectric loss ε'' at 50 -150 $^{\circ}$C temperature,Preapplied field 6 MVm^{-1},Electrode Material-Al for 150FN019 Film.
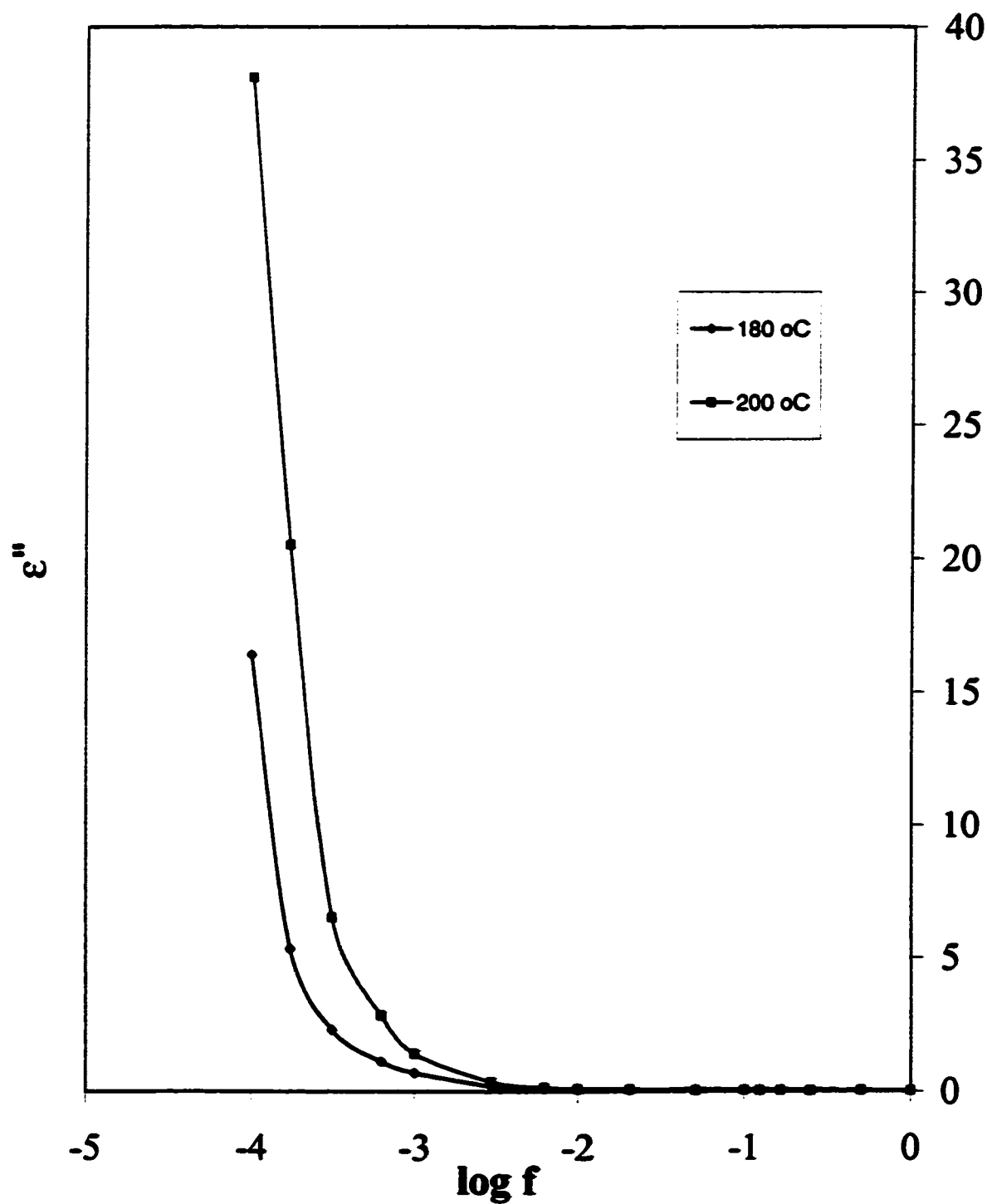
Fig. 6.14 Frequency dependence of dielectric loss ε" at 180-200 °C temperature ,Preapplied Field 6 Mvm⁻¹, Electrode Material -Al for 150FN019 Film.

are observed for higher temperatures which show that the presence of Interfacial polarization. The FN film has a coating of Teflon and it can be inferred that the carriers are trapped at the interface between the two layers confirming the process of Interfacial polarization.

<div align="right">Chapter 7</div>

CONDUCTION CURRENTS IN POLYIMIDE-FEP FLUOROPOLYMER (150FN019 FILM)

7.1 INTRODUCTION

In this chapter conduction currents are studied for 150FN019 Film which has a coating of Teflon®FEP fluoropolymer over a base of Kapton® polyimide Film. It is a non polar thermoplastic polymer and has excellent dielectric properties such as low dielectric constant of 2.0 and 2.1 at 60 Hz and 1 kHz respectively and lossfactor 0.0002 [2]. It is one of the most inert substances known. Film under study has a base of 25.4 μm kapton® and a coating of 12.7 μm of Teflon® on one side of the film.

There are a few papers published on the conduction currents on the PTFE. Govinda Raju and Sussi [35] have eliminated the Schottky and the Poole Frenkel effect as the explanation for the conduction process in PTFE. However they have favored electronic and ionic space charge to be dominant at different temperature levels. Ionic space charge was found to be dominant at T < 120 ^{0}C and electric fields less than 246 KVcm^{-1}. At T >120 ^{0}C and electric field greater than 100kVcm^{-1} electronic space charge was the dominant one. The ionic separation distance between the traps increased with the decreasing temperature from 200 – 80 ^{0}C.

Conduction current in PTFE at high fields ranging from 78.7 –118.1KVcm^{-1} and temperatures from 162 to 200 ^{0}C has been studied by Lilly [54]. It was concluded that the conduction mechanism was ionic and electronic each dominant at different field level and both influenced by space charge.

In this work the conduction current in 150FN019 film are examined for temperature ranging from 90 to 200 ^{0}C and electrical field strength up to 100 KVcm^{-1}. The measured conduction currents at various electric fields strengths and temperatures are examined in the light of Schottky, Poole-Frenkel and Ionic conduction mechanisms.

7.2   EXPERIMENTAL PROCEDURE

The conduction current were measured on a specimen of 150FN019 film with a thickness of 31.5 μm at various electric fields and constant temperatures ranging from 90-200 ^{0}C. The electrodes are made of stainless steel having outside diameter of 12 cm. The low voltage electrode is 8.8 cm in diameter and has a guard ring. The voltage electrode is connected to Keithley 617C electrometer. The temperature of the sample was controlled using an environmental chamber consisting of microprocessor unit with the temperature control in the range of 0 to 300 ^{0}C.

The temperature control and measurement is accurate in the range of 0.1 ^{0}C. The voltage is applied using a Brandenburg stabilized DC power supply and the current is measured using Keithley 617 C electrometer. The electrometer is programmed to store the readings that can be retrieved from the front panel. The thermal protocol adapted during the study is reported in chapter 3. After keeping the temperature of the chamber constant for 1 hour the lowest value of electric field is applied and the current is recorded after 1000 seconds. Thereafter the field is increased in short steps and at each step a time of 600seconds is allowed to settle down before the reading is taken. The settling times were chosen following the results of the charging and discharging currents.

7.3   RESULTS AND DISCUSSIONS

The conduction current results are analyzed and the results are interpreted on the basis of the available conduction theories. Four mechanism have generally been put forward; they are ionic conduction, Schottky emission, Pool-Frenkel effect and space charge effect.

From the slopes and intercepts of the curves the value of parameters like the ionic jump distance, high frequency dielectric constant, etc can be found out and are summarized in table 7.1.

Figure 7.1 shows the transport current obtained from the charging and discharging current at 200 ^{0}C and various electric fields. It is seen for long times (approaching 10^4 seconds) the transport current is nearly constant however at short times it decreases with time.
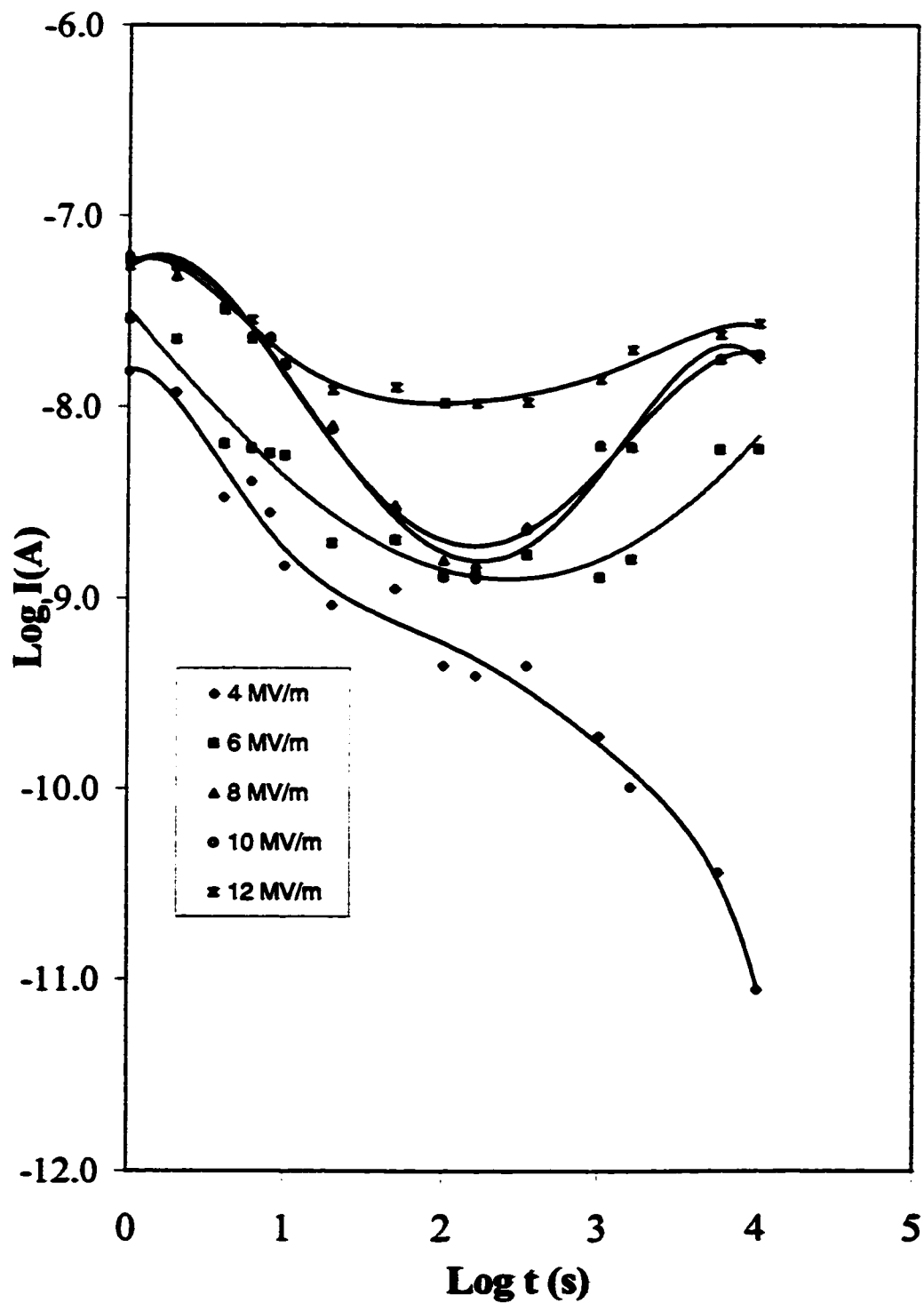
Fig. 7.1 Transport current at 200 °C and various field for 150FN019 Film.
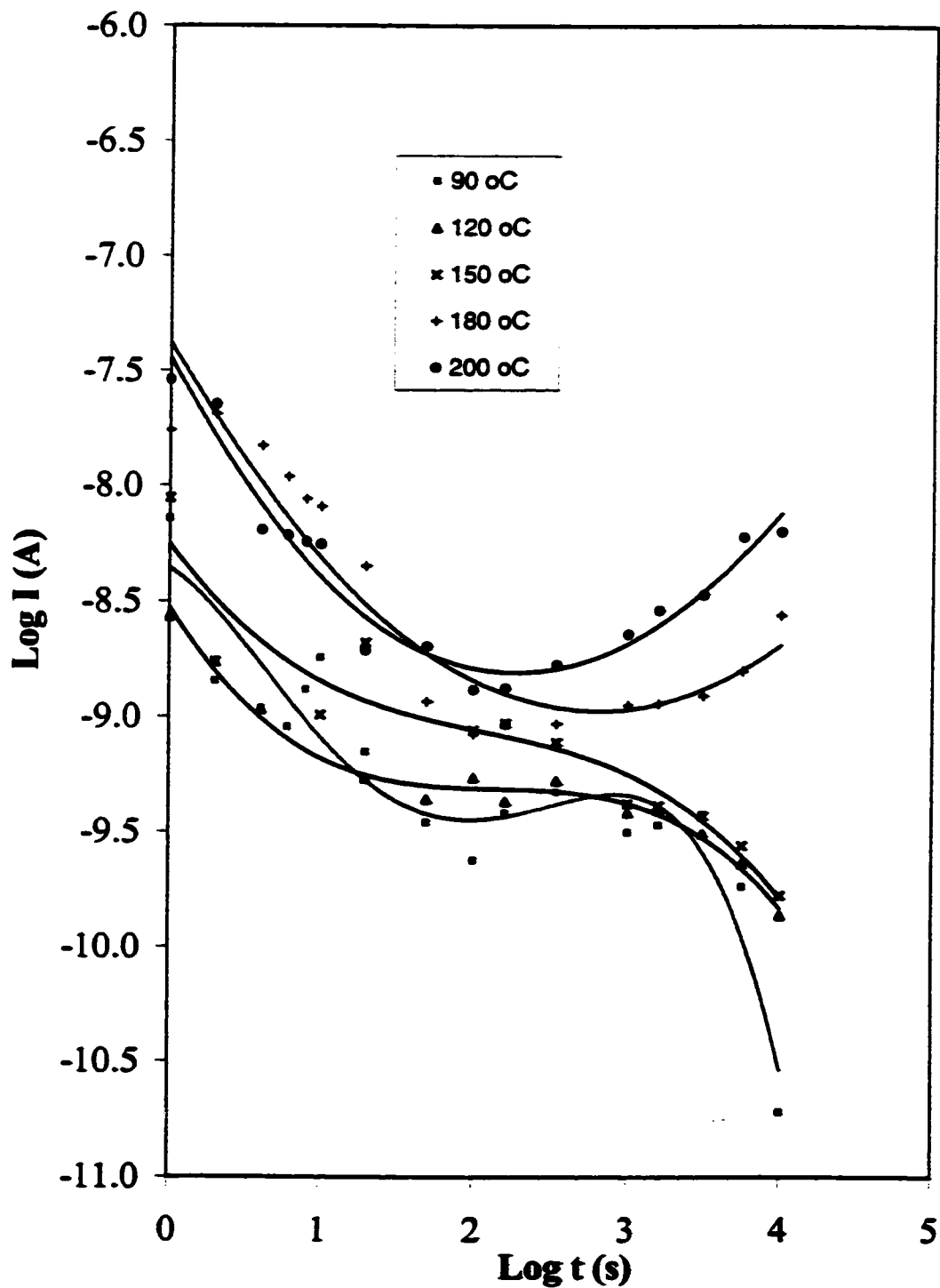
Fig 7.2 Transport current at various temperatures and pre applied field of 6 Mvm⁻¹ for 150FN019 film

Figure 7.2 shows the conduction current as a function of electrical field at various temperatures. For lower temperatures the current is seen to decrease with time while it tends to flatten out at higher temperatures and longer times. The plots follow ohmic behavior at low temperature and field, while at higher temperatures there is a progressive reduction of the slopes.

For mechanisms of ionic hopping the current density at high fields can be explained by the equation (5.1).

From equation (5.2) it can be shown that the plot of I vs. E as shown in figure7.3 will yield a straight line having a slope of (ea/2KT) from which the separation distance between the traps can be calculated from the slope. The separation distance calculated is shown in the table 7.1.

From higher temperatures the jump distance is found to be increasing. The estimated values of the jump distance are 19.41 nm for 90 ^{0}C and 38.64nm for value of 200 ^{0}C.

Sussi [35] has reported conduction current results in Teflon with the values of ionic jump distance ranging from 1.78 to 3.42nm for field less than 100KVcm^{-1} and temperature up to 120 ^{0}C. For field higher than 100KVcm^{-1} and the temperature greater than 120 ^{0}C the separation distance decreases with increasing temperatures. The calculated values of the separation distance were found to be temperature dependent.

Sussi [48] has reported the value of ionic jump distance of 18.8 nm to 37.2 nm in Nomex-Polyster-Nomex and found that the jump distances were increasing with temperature. Govinda Raju [40] has reported results for Aramid paper (Nomex 410) where the separation distance between the traps are in the range of 4.4 to 10nm,are temperature dependent, increasing temperatures yielding higher values. Sussi [16] has attributed the large ionic jump distance found in N-P-N due to the presence of different layers. The ionic jump distances were found to be about 4 times higher than found in (Nomex 410) alone.

The nonlinear behavior of polymers at high fields may also be due to thermionic emission either from the cathode or from donor like defect states in the sample (Poole-Frenkel effect). In the case of the field assisted thermionic emissions from the cathode the current density J is expressed for the Schottky equation as (5.4) and hence from the slopes of I vs. E$^{1/2}$ plot the value of B$_s$ and ε can be calculated. The values of the parameters obtained when compared with the determined dielectric constant should give a reasonable indication of the process though to be occurring. The calculated value of the dielectric constant ε$_s$ is found to be in
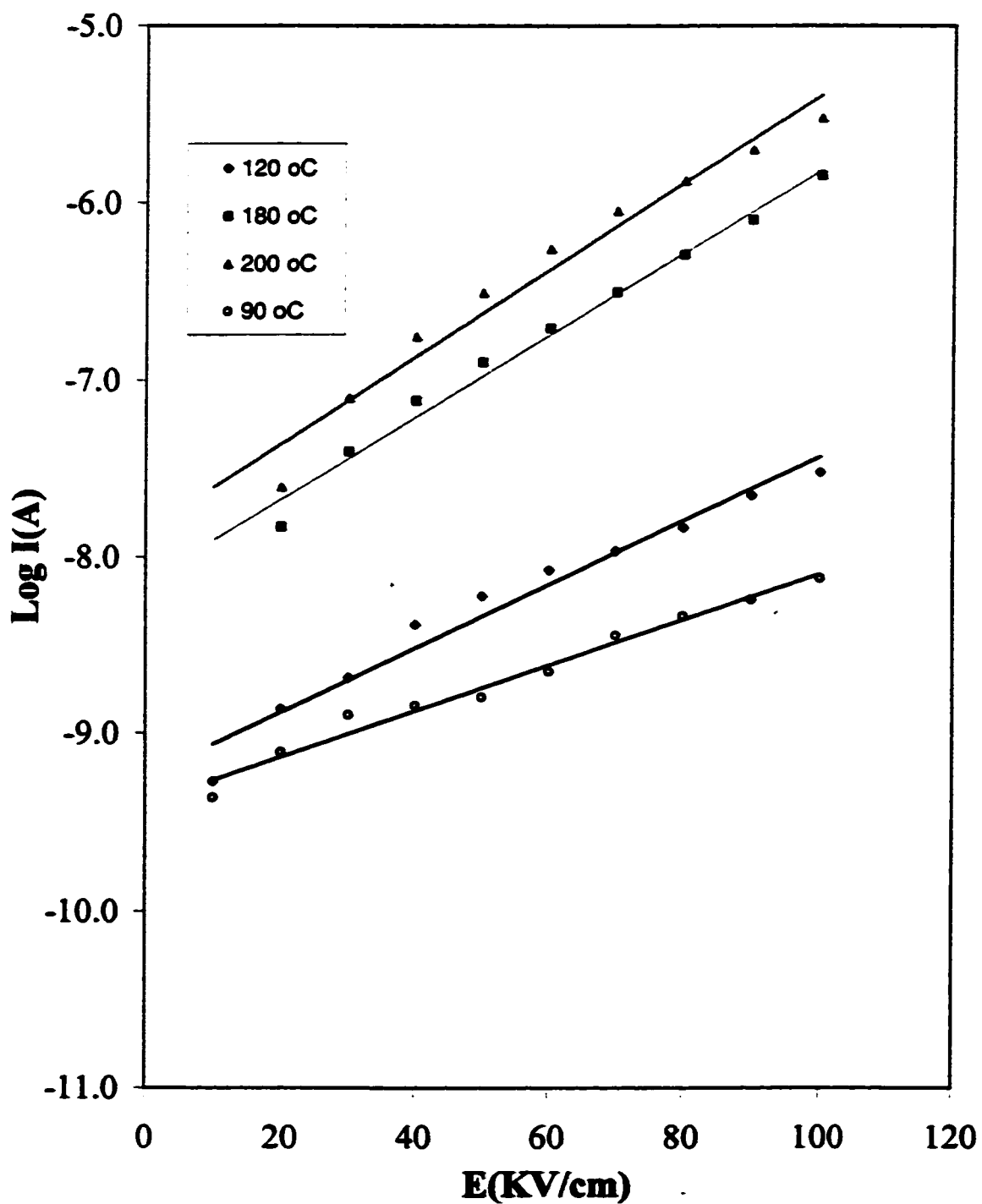
Fig. 7.3 Isochornal current as a function of applied electric field at various constant temperature for 150FN019 Film.
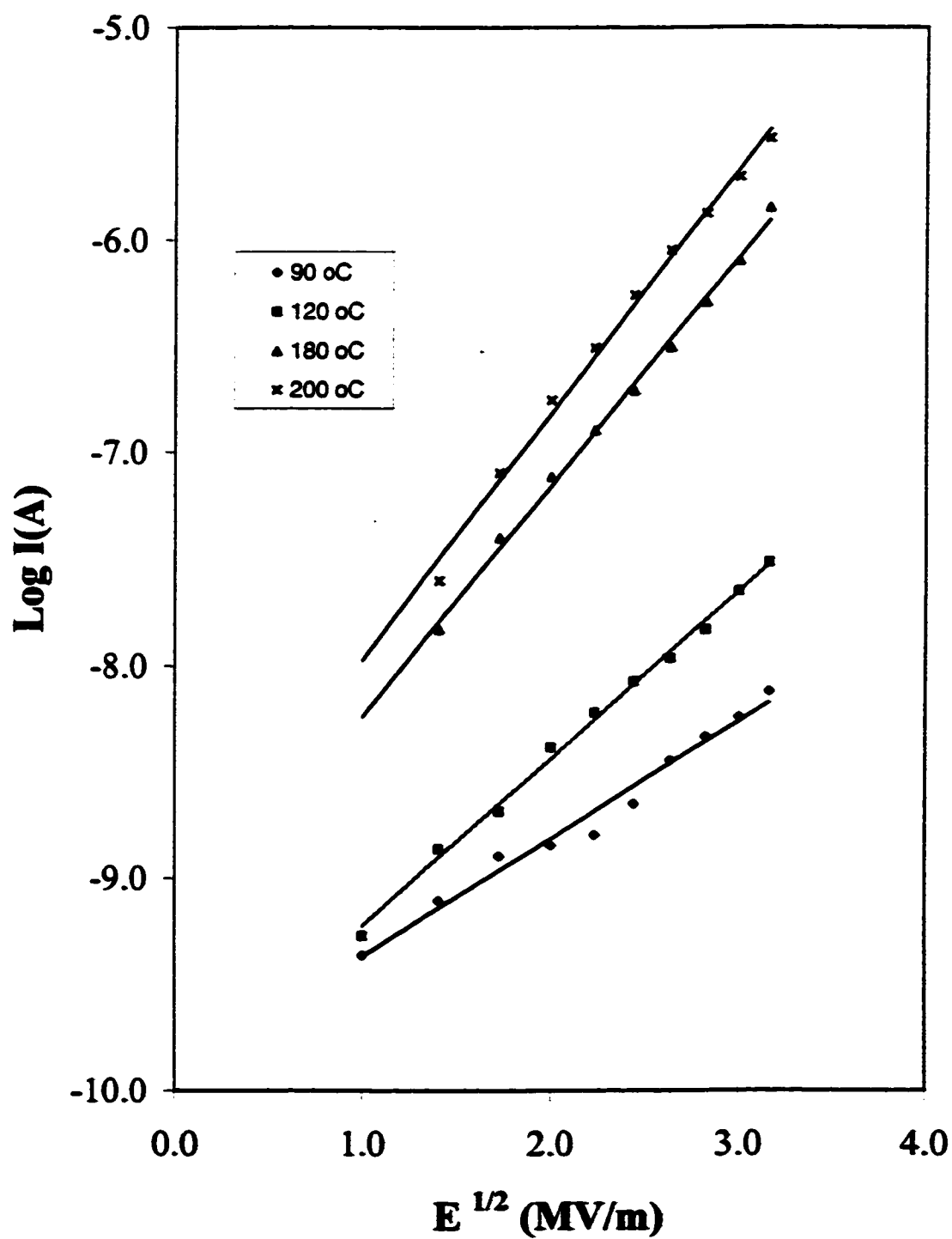
Fig. 7.4 Log I vs. E$^{1/2}$ at various constant temperatures, Electrode material-Al for 150FN019 Film
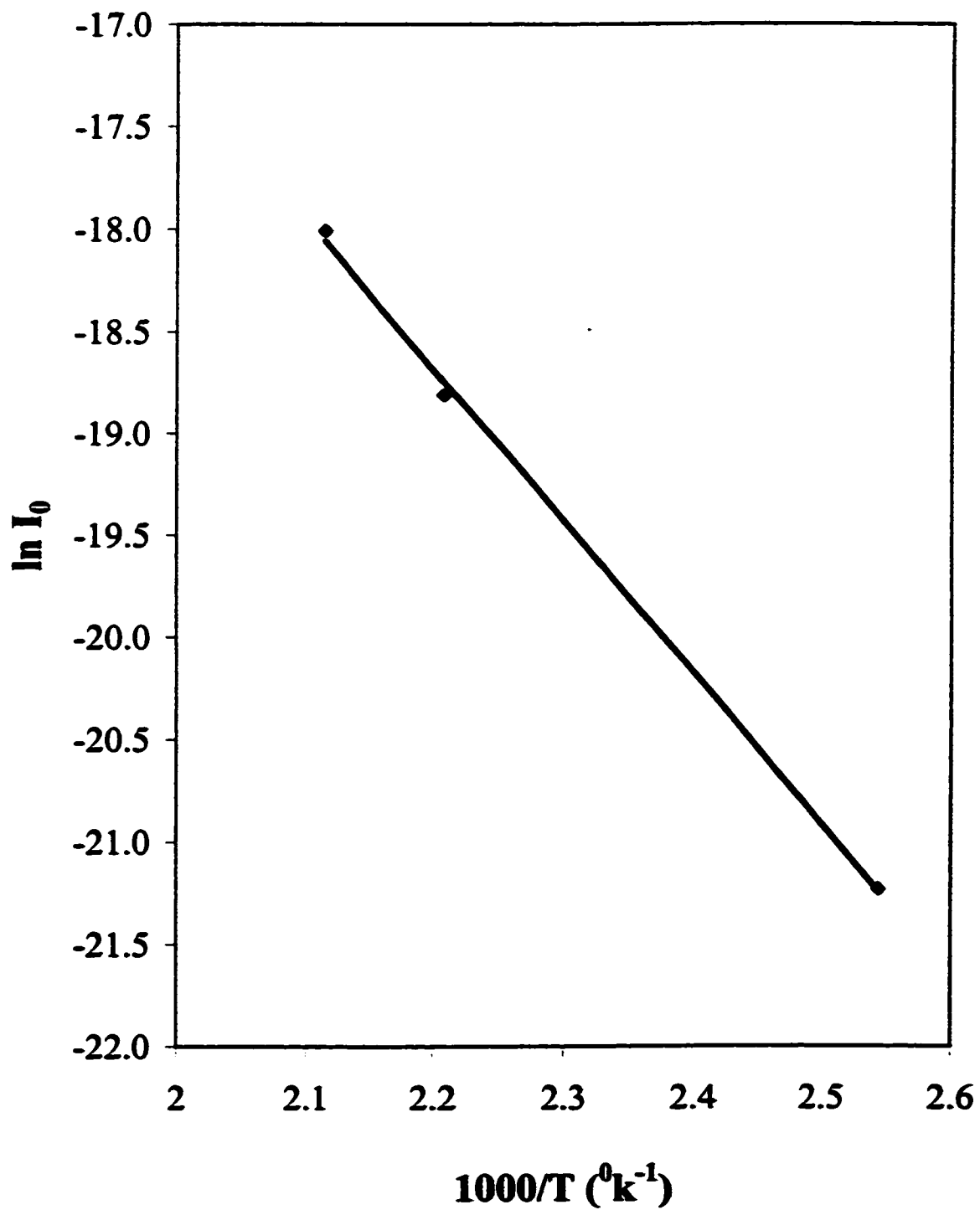
Fig 7.5   Plot of I_0 vs. 1000/T for 150FN019 Film.

the range of 0.12 to 0.012. For the Poole Frenkel effect the values of ε_{pf} would be four times that obtained for the Schottky dielectric constant. The dielectric constant as obtained for Poole-Frenkel gives a value of 0.46 at 90 ^{0}C, 0.05 for 200 ^{0}C. The experimental value of the dielectric constant as obtained from [49] is 2.7. The values are very low as compared with the obtained experimental values. Hence both Schottky emission and Poole Frenkel may be ruled out as the possible mechanisms.

The zero electric field emission current density according to equation (5.6) is given by the y-axis of the intercepts of fig (7.4) from which the emission constant A_c can be obtained. The values of the emission constant can be obtained as 8.17×10^{-8} to 3.16×10^{-8} $Acm^{-2}K^{-2}$. These are about 7 order of magnitudes lower than the expected values of 120 $Acm^{-2}K^{-2}$. Hence this further rules out the Schottky emission as a possible conduction mechanism.

The activation energy for the steady state conduction can be found out by plotting the extrapolated zero field emission current I_o, obtained from the figure 7.3 against reciprocal temperatures. A plot is shown in the figure 7.5. Equation 5.4 and 5.6 suggest that it should be a straight line. This is seen to be holding reasonably well. From the slope the effective work function between the Fermi level of the metal cathode and conduction band of the insulator can be calculated and is obtained as 0.70 eV.

Thermally assisted tunneling corresponds to the thermal activation of the electrons over the metal –dielectric interface barrier with the presence of applied field to reduce the barrier height.

Although on the basis of the present data alone it is not possible exclusively whether the conduction at high fields in 150FN019 film is ionic, Poole Frenkel or due to the thermally assisted tunneling yet when these reports are evaluated and seen in the background of other investigators, it appears that the conduction is due to drift of ions under the influence of applied field.

Table 7.1 **SUMMARY OF CONDUCTION CURRENTS RESULTS IN 150FN019 FILM**

T ^{0}C	Ionic Jump Distance	ε_s	ε_{pf}	A cm^{-2}K^{-2}
90	19.41	0.12	0.46	8.816×10^{-8}
120	21.01	0.04	0.17	6.07×10^{-8}
180	38.06	0.015	0.06	3.32×10^{-8}
200	38.64	0.012	0.05	3.16×10^{-8}

Chapter 8

CONCLUSIONS AND SUGGESTIONS
FOR FUTURE WORK

8.1   CONCLUSIONS

The concluding remarks and suggestions for future work are summarized in this Chapter.

In Chapter 5 the charging and discharging currents are investigated over the temperature range of 50 to 200 ^{0}C and field ranging up to 12 MVm^{-1} for HN500 Film. The effect of the various parameters such as electrode material, poling electric fields and temperatures were studied. The results show that the charging and discharging current were mirror images for temperatures up to 90^0 C and dissimilar for the other temperature range investigated. The charging/discharging currents show no appreciable dependence on the electrode material investigated. The mechanism responsible for the charge decay is due to dipolar process with the shift to interfacial polarization at about 200 ^{0}C along with ionic hopping. The transport currents were evaluated from the charging and discharging current and the resistivity was found to be decreasing from 5.59 x 10^{16}Ω cm at 90 ^{0}C to 3.31x 10^{12} Ω cm at 200 ^{0}C. The low frequency dielectric loss were obtained from the discharging current and the loss peaks were found to be moving to higher frequencies with temperature while for 200 ^{0}C the loss factor increases by about an order of magnitude.

In Chapter 6 the conduction current results in HN500 film were investigated over the temperature range of 200 ^{0}C and fields up to 100KVcm^{-1}. The results were examined in the light of the available conduction theories. For temperature of 90 ^{0}C and fields up to 40KVcm^{-1} the conduction currents are ohmic and for higher fields and temperatures significantly depart from the ohmic behavior. The ionic jump distance was found to be increasing with the temperature and found in the range of 3.48 to 9.42 nm.

In Chapter 7 the charging and discharging currents for 150FN019 film were investigated for the temperature up to 200 ^{0}C and fields up to 12MVm^{-1} under the influence of various parameters of field, poling temperature and electrode material. The currents are dissimilar at all the temperatures investigated. The resitivity decreases from 1.29 x10^{17}Ω cm at 90 ^{0}C to

5.25 x 10^{12} Ω cm at 200 ^{0}C. The low frequency dielectric loss factor are obtained with the absorption current and two sets of curves are obtained for temperature regimes $0 \le T \le 90$ ^{0}C and $0 \le T \le 200$ ^{0}C. For temperatures up to 90^0 C one relaxation peak is observed at about 3 $x10^{-4}$ Hz while for the higher temperatures the loss factor increases very rapidly and no peak is observed.

In Chapter 8, the results of the conduction currents for 150FN019 film are discussed for fields up to 100KVcm^{-1} and the temperatures up to 200 ^{0}C. The results did not reveal that either Schottky or the Poole Frenkel mechanism was operative mechanisms. The ionic jump distance were found to be in the range of 19-38 nm following a increasing trend with the temperature

8.2   SUGGESTIONS FOR FUTURE RESEARCH

Thermally Simulated Polarization and Depolarization currents should be studied to provide better insight in the charging and the relaxation process in the polyimides.

Corona charging techniques should be employed to study the mechanism of charge storage and release from the bulk of the materials.

The charging/discharging current should be investigated under vacuum to eliminate the effect of air humidity.

Other electrode material such as gold or colloidal graphite should be employed

Laplace transforms methods should be employed to study the low frequency dielectric loss factor.

FTIR analysis should be carried out to study in detail the data of polyimide cure and the trace amounts of hydrogen-bounded water.

DIELECTRIC MATERIAL USED FOR INVESTIGATION

The purpose of this chapter is to give an overview of the dielectric material understudy and their applications. Over the years, the more traditional involvement of polymers in electrical applications has been electrical insulation. Only in the recent times the emphasis has been placed on study of electrical properties in which polymers are being used.

Polymer consists of long chain macromolecules with the repeating manomer units. A polymer is usually named by putting prefix "Poly-" in front of the name of the monomer from which it has been derived [55], [59] Polymeric material are unique because of the range of the structural forms that can be synthesized and the way in which changes can be made in the structure in the local or general way. They can exist as amorphous materials, as crystalline materials, or a mixture of crystalline and amorphous materials

The polymer selected belongs to class polyimides. Polyimides as a class of compounds have been available since 1926[55][59]. They offer inherent dielectric strength, low dielectric constant, mechanical flexibility and resilience. The data on the electrical and mechanical properties of the materials have been obtained from publications, handbook and the website [49] [58]

Applications of Polyimide Films

Insulator in motors, transformers, capacitors, electronic devices, wire and Cables because of its outstanding combination of thermal, mechanical and electrical properties

Microelectronics application

Housing of components, packaging of IC and intermetallic dielectric layers and resists in microlithography because of its properties as comparable to the inorganic materials such as SiO_2 and its good planarization capability

Other applications

Include automotive, space and safety devices

Polyimide film (500HN film)

Polyimides are cyclic chain polymers. They are characterized by the presence of imide functionality, a cyclic secondary amine bound to two carbonyl groups. The chemical structure of Kapton is as shown in the figure 3.1
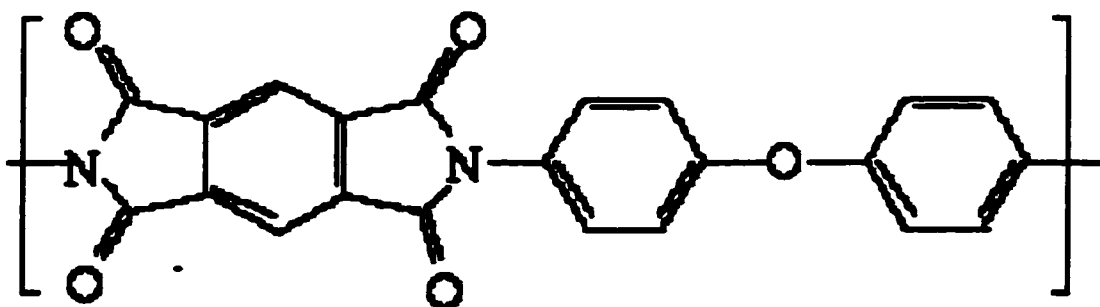
Chemical structure of Polyimide film

Polyimide (500HN Film) has excellent physical, mechanical and electrical range over the temperature range from -269 to 400°c. It has the highest UL flammability rating V-0, the char beginning above 800 °C. It also exhibits excellent chemical properties and has no known organic solvent for the film.

Typical Properties of Polyimide (500HN Film)
Film thickness, 5 mil (127 μm)
Electrical properties
Dielectric Strength   3000
AC KV/mil (KV/mm), min.   (118)
Method: ASTM –D-149-94 (Average of ten specimens). Flat sheets in air placed between 0.25" (6mm) diameter brass electrodes with 0.03125" (0.8 mm) edge radius subjected to 60 cycles AC voltage at 500 V/sec rate of rise to the breakdown voltage.

Volume resistivity, 10^{12}
Ohm –cm at 200°C min
Method: ASTM D –257-93

Dielectric Constant at   3.9
1 kHz, max
Method: ASTM D-150-94. Use conducting silver paint electrodes, two terminal system of measurement at standard conditions; Results are based on an average of five tests using measured thickness of specimens

Dissipation factor   0.0036
Method Same as above

Mechanical properties

Tensile strength,   24,000
Psi (Mpa) at 23°C
Method: ASTM –882-91

Elongation, % MD   50
And TD at 400°C

Shrinkage % MD and   2.5
TD at 400 °C
Moisture Absorption % max   4.0
Method: ASTM S-570-92

Polyimide –FEP fluoropolymer film (150FN019 Film)

Moisture absorption of polyimide is a long-standing reliability issue due to the possibility of metal corrosion of devices, affects polarization and dielectric properties. Small amounts of absorbed water in polyamic acid solutions decrease the heat resistance of polyimide. Kapton polyimide film is coated with Teflon FEP fluoropolymer resin as it imparts heat seal ability, moisture barrier and enhanced chemical stability.FEP fluoropolymer is reputedly one of the most inert substances known to man. The water absorption for 150FN019 film is 1.7% max as compared to 4% max for HN500 film at 23°C and 98% relative humidity [49]

The film under study has a 25.4µm base Kapton® film with a coating of 12.7 µm Teflon FEP fluoropolymer film on one side

Typical properties of Polyimide –FEP Fluoropolymer (150FN019 Film)
38.1 mm(1 mil)
Electrical Properties
Dielectric strength   197 (5000)
V/µm (V/mil)
Method: ASTM D-149-91
60 Hz ¼ in electrode 500V/rise

Dielectric Constant at 1 KHz   3.4
Method: ASTM D-150-92

Dissipation factor at 1 KHz   0.0018
Method: ASTM –D-150-92

Volume Resistivity Ohm-cm
At 23 °C   2.3 x 10^{17}
AT 200°c   3.6 x 10^{14}
Method: ASTM D-257-91

3.2.1 Mechanical Properties

Tensile strength Mpa (Psi)	162(23,500)
Yield Point at 3 % Mpa (Psi)	
200oC	43(6000)
Stress at 5 % Elongation	
Mpa (Psi) 200 oC	41(6000)
Moisture absorption % 23 °C	
50 % RH	0.8
98 % RH	1.7
Method: ASTM D-570-81	

COMPARISON OF PROPERTIES OF HN500 AND 150FN019 FILM WITH SOME INORGANIC DIELECTRICS

COMPARISONS

The specific properties of the polyimide film (HN500 and 150FN019) which makes them suitable as an insulating materials and a substitute to the inorganic dielectric materials are listed in table 8.1.

A significant feature is the low dielectric constant (below 3.5) and the high volume resistivity which is obtained in the range of $10^{17}\Omega$ cm at about 90 ^{0}C which is more than the normal device operating temperatures.

The resistivity obtained for the HN500 film fall in the range of $10^{16}\Omega$ cm, which is comparable to PIQ polyimide manufactured by Hitachi.

The dielectric breakdown strength does not differ greatly from those of the inorganic insulators and closely resemble that of SiO_2 [55,56].

The melting point is 450-500 ^{0}C is significantly less than inorganic dielectric materials but this is not of specific concern since the process required (deposition, sputtering and bonding operations) are done below that temperature.

A high Young's modulus, elongation at break and high tensile strength indicates good mechanical stability, which is comparable to inorganic dielectric.

The crucial advantage of the polyimides over inorganic insulators as an intermetallic dielectric is the planarizing ability. It is very important to know the chemistry and the processing history as they affect many of the physical and the electrical properties.

TABLE OF COMPARISON [55-56]

Properties	HN500 FILM	150FN019 FILM	SiO$_2$	Si$_3$N$_4$	Al$_2$O$_3$
Volume Resitivity	10^{16}	10^{17}	10^{16}	10^{12}	10^{14}
Dielectric Constant	3.1	2.7	3.5-4.0	7-10	7-9
Breakdown Strength	10^7	10^7	10^6-10^7	10^6-10^7	10^5
Tensile Strength (x 10^6 gfcm^{-2})	1.8	1.7	1.4	6.4	28
Thermal Conductivity (m cal cm^{-1}s^{-10}C^{-1})	0.4	0.4	5	28	78
Melting point ^{0}C	400	400	1710	1900	2050

BIBLOGRAPHY

[1]   G.Samuelson, Reprints Org.Coat Plastics Chem. 43, 446.1980.

[2]   L.B.Rothman, J Electro. Chem.Soc. Solid State Sci.Technology 127:10, 2219,1980

[3]   F.W.Smith, M.I.T Thesis [1985].

[4]   G.A.Brown, "Polymer Materials for Electronics applications" ACS Symposium Series 184", American Chemical Society, Washington DC 1982 p151.

[5]   D.S.Soane and Zoya Martynenko,"Polymers in Microelectronics", 1989.

[6]   R.J.Munick, "Transient Electric currents from Plastic Insulators ", J.Appl.Phys. Vol. 27 No.10 pp 1114- 1118, 1956.

[7]   J. Lindmayer, "Current transients in Insulators" J.Appl. Phys. Vol36 No1 pp 196-201, 1965.

[8]   H.J.Wintle, "Absorption currents and steady currents in polymer dielectrics" J. Non-Crist. Solids, Vol. 15 pp.471-486, 1974.

[9]   J.Vanderschueren and A.Linkens, " Nature of Transient currents in Polymers", J.Appl. Phys.,Vol.49, No, 7 pp 4195 -4205, 1978.

[10]   D.K.DasGupta and K.Joyner, "On the nature of absorption currents in polyethylene terephthalate (PET) ", J.Phys.D: Appl. Phys. Vol.9 pp 2041- 2048, 1976.

[11]   C.A.Mead, "Electron Transport Mechanisms in thin Insulating films" Phys, Vol.7 pp 105-106, 1974.

[12]   D.K.DasGupta, K.Doughty and R.S.Brockley, " Charging and Discharging current in Polyvinyldine Fluoride", J.Phys. Vol13 pp 2101-2114, 1980.

[13]   A.VonHippel, " Dielectric Materials and Applications" The Technology press MIT, John Wiley and Sons N.Y.1958.

[14]   C.F.J.Bottcher, "Theory of Electric Polarization "Second edition NY 1963.

[15]   S.Umera, J.Poly.Science, Polymer Phys. Vol.10, pp2155, 1972.

[16]   J.R.Macdonald, J.Chem. Phys. Vol54, pp2026, 1974.

[17]   R.Meaudre and G.Mesnard, Rev Phys.Appl. Vol7, pp213, 1972.

[18]   R.H.Walden, J.Appl. Phys. Vol43 pp1178, 1972.

[19]   H.J.Wintle, J. Non Cryst. Solids Vol15 pp 471 [1974].

[20]   H.J.Wintle, IEEE Trans. Electrical Insulation EI 120 pp424, 77.

[21]   Miyoshi and Chino, Jan. J.Appl. Phys. Vol6 pp191, 1967.

[22] M.Kryzewshi and A. Zyamaski, J.Polymer Science Vol14 pp 245, 1970

[23] M.Lampert and P. Mark, " Current Injection in Solids" Academic press NY.

[24] L.E.Ambroski, J.Polymer Science Vol62 pp 331, 1962.

[25] R.A.Foss and W.Dannhauser, J.Appl.Polymer Science Vol 7 pp 1015, 1963.

[26] R.E.Barker and C.R.Thomas, J.Appl. Physics Vol34, pp 3403, 1964.

[27] B.Gross, "On the Theory of dielectric loss "Physical review vol59 p748, 1941

[28] H.Frohlick, " Theory of dielectrics", Oxford Press.

[29] B.V.Hamon, "An approximate method to deducing dielectric loss factor from direct
      current measurement", Proc IEE (London) Vol99 pp 151-155, 1952.

[30] Govinda Raju, "Dielectrics in Electric fields" 2002 (to be published).

[31] Baird.M.E, " Determination of dielectric behavior at low frequencies from
      measurement of anomalous charging and discharging current", Review of Modern
      Physics, Vol40 pp 219-227, 1968.

[32] J.G. Kirkwood, J.Chem. Phys., 1939.

[33] Klein N Mortan, L. Adv Electronics and Electron Phys. Vol26, Academic Press N.Y
      (1969).

[34] Technical Specification guide Keithley 617C, URL: http://www.keithley.com.

[35] M.A.Sussi and G.R.Govinda Raju, "Electrical conduction in Polytetrafluoroethylene",
      1990 Annual Report, Conference on Electrical Insulation and Dielectric phenomena
      CEIDP, Pacano Manor, IEE Insulation society pp28-31 Oct 4 1990.

[36] M.A.Sussi and G.R.Govinda Raju, "Absorption and Thermally Stimulated
      Polarization current in Aramid Paper", SAMPE Journal, Vol.28, No.4, 1992.

[37] G.Sawa, S.Nakamura, K.Iida, and M.Ieda, " Electrical Conduction of
      Polypyromellitimide films at temperature of 120- 180° C", Jap. J.Appl. Phys.Vol 19,
      No3 pp 453- 458, 1980.

[38] M.H.Chohan, H.Mahmood, Farhana Shah, "Absorption-Desorption currents in
      polyimide film", J. Material Science Vol.14, 1995 pp552.

[39] F.W.Smith, H.J.Neuhaus, D.Senturia, Z.Feit, D.R.Day and T.J.Lewis, "Electrical
      Conduction in Polyimide between 20- 350°C" Electronic Mat.Vol6 pp 93-106, 1987.

[40] G.R.Govinda Raju, "Conduction and thermally Simulated Discharge current in
      Aramid paper ", IEEE Trans.Electr.Insul., Vol 27, No1 pp 162 –173, 1992.

[41]   H.J.Wintle, "Engineering Dielectrics" Volume II A, Edited by R. Barkitas Chap6, pp
        588 –600, 1983.

[42]   M.M.Perlman, " Thermally simulated current and voltages and dielectric properties,",
        J.Electrochem. Soc., Solid State Science and Tech. Vol.119 No.7 pp 892-898, 1972.

[43]   D.K.DasGupta and K.Joyner, " On the nature of absorption current in PET", J.Phys.D
        Appl. Phys.Vol9, pp 824-840, 1976.

[44]   M.E.Baird, G.J.Goldsworthy and C.J.Creasey, " Low frequency Dielectric behavior of
        Polyamides", Polymer Letters, Vol.6 pp 737-742,1968.

[45]   J.R.Hanscomb and J.H.Calderwood, "Thermally Assisted Tunelling in Polyimide film
        under steady state and transient conditions" J.Phys.D: Appl.Phys., Vol6, 973,pp 1093-
        1104.

[46]   Polanco J.I and Roberts G.G., 1970 Phys. Stat. Solid A 13 603-6.

[47]   B.L.Sharma and K.C.Pillai, "Electrical Conduction in kapton Polyimide film at high
        electrical fields", Polymer, 1982 Vol 23 pp 17-20.

[48]   M.A.Sussi,"Charge Storage and Decay in High Temperature Insulating Materials",
        PhD Thesis, 1992.

[49]   Dupont Films/Fibers, " Technical guide " World Wide Web, URL: http://
        www.dupont.com".

[52]   A.K.Jonscher, "The universal dielectric response " Conference on Electrical Insulation
        and dielectric phenomena Pocono Manor PA Oct 28 1990 pp 23-40.

[53]   I.E.Noble and D.M.Taylor, J.Phys. D.Appl. Phys. Vol13 No2 pp 2115 –2122,1980

[54]   A.C. Lilly and J.R. MacDowell, "High field Conduction in films of Mylar and
        Teflon", J Appl.D: Vol.39 No1, pp.141-147, 1968.

[55]   L.A.Dissado, J.C.Fothergill, "Electrical Degradation and Breakdown in Polymers",
        IEE Materials and Devices Series 9,1992.

[56]   V.B.Jipson and K.Y.Ahn, Solid Sate Technology 27:1 141,1984.

[57]   Technical guide, " Data Translation", http:// www.datatranslation.com.

[58]   W.T.Shugg,"Handbook of the Electrical and Electronic Materials", Second Edition,
        1995.

[59]   R.W.Sillar,"Electrical Insulating materials and their applications" 1993.

VITA AUCTORIS

Name:	Riaz R Shaikh
Place of Birth:	Ahmedabad, India
Date of Birth:	October 24,1972

Education:

1988-1990   A.G.Higher Secondary School
Ahmedabad, India
High School

1990-1994   North Gujarat University
Patan, India
Bachelor of Electrical Engineering

2000-2002   University of Windsor
Windsor, Ontario, Canada
Master of Applied Science

Work History:

1994-1996   Electric Control Gear (India) Ltd.
Ahmedabad, India
Electrical Engineer

1996-1998   Trumac Engineering Company Ltd.
Ahmedabad, India
Plant Engineer

1998-2000   Adwan Trading and Contracting Company.
Jeddah, Saudi Arabia
Application Engineer